Glutamine: fructose-6-phosphate aminotransferase 2 (*GFPT2)* is a novel NF-κB target that links cancer metabolism with metastatic phenotypes in non-small cell lung cancer

Szymon Jakub Szymura

Krakow, Poland

M.Sc. Biotechnology, Jagiellonian University, 2010
M.Sc. Biochemistry, University of Virginia, 2012

A Dissertation Presented to the Graduate Faculty of the University of Virginia
in Candidacy for the Degree of Doctor of Philosophy

Department of Biochemistry and Molecular Genetics

University of Virginia
May 2016

_____

_____

_____

_____

ABSTRACT

Lung cancer is one of the most prevalent cancer types and the leading cause of cancer related mortality in the world. Non-small cell lung cancer (NSCLC) constitutes the majority of lung cancers with the five-year survival rate at 17%. Poor survival rates are due to late-stage diagnosis and limited response to standard of care cisplatin-based chemotherapy. Recent efforts in targeted therapy in lung cancer yielded limited success due to the activation of compensatory survival mechanisms and acquisition of drug resistance. Metastasis in NSCLC is driven by the trans-differentiation process called epithelial to mesenchymal transition (EMT) that promotes migratory and invasive phenotypes in cancer cells. EMT is induced by cytokines secreted by cells present in tumor microenvironment. The Mayo laboratory has shown that transforming growth factor beta (TGFβ) and tumor necrosis factor (TNF) cooperate to induce EMT in NSCLC and that activation of the nuclear factor kappa B (NF-κB) pathway is essential for the transition. Cancer cells show elevated uptake and utilization of glucose and glutamine via aerobic glycolysis (Warburg effect) and anaplerotic TCA cycle respectively. Glucose and glutamine are both required for the synthesis of UDP-N-acetylglucosamine (UDP-GlcNAc) in the hexosamine biosynthesis pathway (HBP). UDP-GlcNAc is a precursor molecule for multiple processes including protein glycosylation, generation of glycosaminoglycans and O-GlcNAcylation of nucleocytoplasmic proteins. Aberrant elevation of glycans has been implicated in cancer progression, survival

and metastasis. Glutamine: fructose-6-phosphate (GFPT) is a first and rate-limiting enzyme in HBP. Here we show that neuronal-specific GFPT2 isoform is a novel NF-κB target, up-regulated during TNF/TGFβ-induced EMT in NSCLC and in response to MEK inhibition in *KRAS*-mutant NSCLC. GFPT2 induction elevates protein O-GlcNAcylation in mesenchymal cells and is required for the migration and invasion of mesenchymal NSCLC. Consistent with these observations high GFPT2 expression co-relates with poor clinical outcome of lung adenocarcinoma patients.

ACKNOWLEDGEMENTS

I would like to thank Dr. Marty Mayo for accepting me to his laboratory, helping me with my application to the UVA graduate school and being my mentor for the past years. I would like to thank him for his tremendous support and patience thorough my time in graduate school and for teaching me a great amount about cancer biology. I would like to thank Dr. Joel Hockensmith for accepting me into BMG program. I would like to thank Dr. Zygmunt Derewenda for leading a Polish student exchange program that gave me and others invaluable opportunity to study at the University of Virginia. I would like to thank my committee members: Dr. Stefan Bekiranov, Dr. David Kashatus and Dr. Patrick Grant for their constructive suggestions and encouragement. I would like to thank my former mentors Dr. Joanna Cichy and Dr. Derk Amsen for introducing me to the world of science and for being truly inspiring role models. I would like to thank Dr. David Allison for being my friend and mentor during my first years in the U.S. as well as Jackie D'Innocenzi for being a great friend, an inspiring human being and a brilliant labmate. I would also like to thank Jacob Zaemes for his great help and all present and former Mayo lab members including Sheena Clift, Lisa Gray, Brian McKenna, Jake Wamsley, Emily Glidden and others for their collaboration and help. Finally I would also like to thank Debbie Sites for her patience and help with all formalities of the graduate school.

I would like to especially thank Ewelina Zasadzińska, and my family and friends for their support and understanding.

TABLE OF CONTENTS

LIST OF FIGURES

LIST OF ABBREVIATIONS

ADC - adenocarcinoma

CIC – cancer initiating cells

ECM – extracellular matrix

EMT – epithelial to mesenchymal transition

GAG - glycosaminoglycan

GAPDH - glyceraldehyde-3-phosphate dehydrogenase

GFPT – glutamine fructose-6-phosphate aminotransferase

HA - hyaluronan

HAS – hyaluronan synthase

HBP – hexosamine biosynthesis pathway

HIF1a – hypoxia-inducible factor 1-alpha

IKK – IκB kinase

NF-kB – nuclear factor kappa B

NSCLC – non-small cell lung cancer

OGA – O-GlcNAcase

OGT – O-linked N-acetylglucosamine (GlcNAc) transferase

PG - proteoglycan

SCC – squamous cell carcinoma

SCLC – small cell lung cancer

TGFβ – transforming growth factor beta

TNF – tumor necrosis factor

UDP-GlcNAc – uridine diphosphate N-acetylglucosamine

UPR – unfolded protein response

CHAPTER I

General Introduction

Lung Cancer

Lung cancer is one of the most prevalent cancer types and the leading cause of cancer-related mortality in the world. This year in the U.S alone, a predicted 224,390 new lung cancer diagnoses will be accompanied by 158,080 lung cancer-associated deaths, which constitutes about 25% of total cancer-related mortality (1). The five-year survival rate for patients with lung cancer in the U.S is 17.8% (2). Despite efforts to reduce incidence of lung cancer in Western countries, the worldwide prevalence of lung cancer is on a rise due to increased incidence in China and developing countries, totaling an estimated 1.59 million deaths in 2012 globally (3).

Tobacco products consumption is the main etiological factor associated with development of lung cancer. About 85% of lung cancers occur in present or former cigarette smokers. Moreover smokers are 16 times more likely to develop lung cancer than never smokers (4). Cigarette smoke contains more than 60 known carcinogens including benzo(a)pyrene, tobacco-specific nitrosamines and aromatic amines, exposure to which cause a formation of DNA adducts resulting in errors in DNA replication and DNA mutations (4). Other environmental factors may contribute to the development of lung cancer in the remaining 15% of non-smoker population including asbestos, silica fibers, diesel fumes, air pollution, radon, arsenic, and nickel, among others (4).

Lung cancer can be categorized by cell type into small-cell lung cancer (SCLC) and non-small cell lung cancer (NSCLC) (2). SCLC constitutes about 15% of lung cancer cases and is limited almost entirely to the smoker population

(2, 4-5). SCLC is thought to originate from neuroendocrine cells near the bronchi and is highly aggressive with a five-year survival rate of 6% (2). NSCLC constitutes about 85% of lung cancer cases and with a five-year survival rate of 21% (2). NSCLC can be further subdivided into three types: adenocarcinoma (ADC), squamous cell carcinoma (SCC) and large cell carcinoma. ADC is the most frequent subtype of NSCLC, accounting for 40-50% of cases. ADC arises predominantly in distal airways from secretory glandular cells lining the alveoli (2, 5). ADC is the most frequently diagnosed NSCLC subtype in smokers and never-smokers, women, and the Asian population and tends to form slower than other NSCLC but shows more aggressive phenotype and metastasizes at an earlier stage (5-6). SCC is the second most prevalent NSCLC, accounting for 30-40% of cases. SCC arises in more proximal airways from squamous epidermal cells that line bronchial tubes and is more strongly associated with smoking and chronic inflammation than ADC (2, 5-6). Large cell carcinoma comprises the remaining 10-15% of NSCLC that could not be identified as ADC or SCC histologically; however, it is not clear whether it is a separate genetic entity. Large cell carcinomas can originate in any part of the lung, are less differentiated and often grow and metastasize rapidly (2, 5-6).

No single tumor-driver mutation common for all NSCLC has been identified, which reflects a high heterogeneity of this disease. However a general pattern of mutagenic activation of growth factor signaling pathways and inactivation of tumor-suppressor genes is observed. In adenocarcinomas activating mutation of epidermal growth factor receptor gene *EGFR* occurs in

10% of patients, predominantly in never-smokers (8, 11). Similarly alterations in human epidermal growth factor receptor 2 (HER2/neu) gene *ERBB2*, hepatocyte growth factor receptor *MET* gene and fusion of anaplastic lymphoma kinase (*ALK*) receptor tyrosine kinase (RTK) with echinoderm microtubule-associated protein-like 4 (*EML4*), ROS proto-oncogene 1 (*ROS1*) and Ret proto-oncogene (*RET*) are observed in 3%, 7% and 5%, 2% and less than 1% of ADC respectively (8). Amongst downstream components of growth factor signaling cascade most commonly altered in ADC are *KRAS*, mutated in 30% of patients, predominantly in the smoker population, and *BRAF* occurring in about 7% of patients. *NF1* gene, encoding negative regulator of RAS proteins is mutated in about 11% of ADC (8). Additionally *STK11* encoding tumor-suppressor liver kinase B1 (LKB1) that negatively regulates AMP-activated protein kinase (AMPK) and mammalian target of rapamycin (mTOR) pathway is mutated in 17% of ADC (8). Other pathways altered in ADC include DNA damage-response governed by p53, cell cycle progression and apoptosis machinery. *TP53* encoding p53 and ataxia-telangiectasia (*ATM*) genes are mutated in 46% and 9% of ADC respectively and are mutually exclusive (8). *MDM2* gene, encoding negative regulator of p53 is a known tumor promoter and its activating mutation occurs in about 8% of ADC (8). In the cell cycle machinery *CDKN2A* gene encoding $p16^{INK4A}$, a cyclin-dependent kinase (CDK) inhibitor is inactivated in 43% of ADC whereas its downstream effector retinoblastoma *RB1* is altered in 7% of cases (8). Within the apoptotic machinery, anti-apoptotic gene *BCL2* is activated in about 10% of ADC. A number of genetic changes present in ADC also occur in

squamous cell carcinoma with different frequencies (8). *TP53* mutations are present in 50-80%, *BCL2* in 25%, *CDKN2A* in 15% and *NF1* in 11% of SCC (9). SCC show similar rate of *RB1* mutations and carry less frequent changes in receptor tyrosine kinases (RTKs) *EGFR* (9%) and *FGFR1* (7%) (9) Additionally frequent activation of PI3K signaling is observed with *PTEN* inactivated in 15%, *PIK3CA* activated in 16% and *AKT3* activated in 16% of SCC (9). The majority of listed genetic alterations became a target of therapies with small molecule inhibitors with some success; however, despite a great advance in identification of mutations in cancer samples with the advent of next generation sequencing (NGS), more than 30% of NSCLC still lack an identified cancer driver mutation.

Surgical resection of primary tumor in combination with adjuvant chemotherapy remains the most effective treatment for patients with early stage disease in which tumor has not extended beyond the bronchopulmonary lymph nodes (4). The five-year survival rate for early stage NSCLC patients is 52.2% however locoregional recurrence after resection occurs in 20-25% of patients (4). For the late inoperable stage of disease a combination of cisplatin or carboplatin with paclitaxel, gemcitabine or docetaxel and radiotherapy were standard first-line treatment with limited efficacy yielding five-year survival rate of 3.7% (4). Identification of mutation in *EGFR* associated with good response to treatment with tyrosine kinase inhibitor (TKI) gefitinib was a fundamental discovery that led to the introduction of TKIs erlotinib, gefitinib and afatinib as a first-line treatment for *EGFR* positive NSCLC patients. Median progression-free survival (PFS) of patients receiving erlotinib was 9.7 and 13.1 months as compared to 5.2 and 4.6

months in patients receiving standard chemotherapy in two phase III clinical trials on European and Asian population respectively (12-13). Similarly crizotinib has been approved for patients with *ALK* translocation with PFS of 10.9 months as compared to 7.0 months for patients receiving standard chemotherapy (14). Despite good initial responses a drug resistance eventually develops in cancer cells. As *EGFR* and *ALK* mutant cancers constitute less than 20% of NSCLC, treatments directed against tumors with other cancer driver mutations are needed. Currently several phase I, II and III clinical trials aim at evaluating feasibility of targeting *KRAS* mutant NSCLC with combinatorial use of MEK inhibitors trematinib or PD-0325901 and standard chemotherapy, among others (15). Other targets of current clinical trials include ROS1, RET, HER2, MET, phosphatidylinositol-4, 5-biphosphate 3-kinase catalytic subunit (PIK3CA) and B-Raf proto-oncogene (BRAF) (15-16).

Inoperable late stage NSCLC is characterized by a varied degree of metastatic dissemination at the time of diagnosis and correlates with poor five-year survival rate of 3.7% (4). Invasion to proximal sites such as mediastinal pleura, diaphragm, chest wall, great vessels and heart can precede metastasis of local lymph nodes from where systemic cancer dissemination to bone, liver, adrenals and brain occur. Palliative surgery and radiotherapy may help manage the disease however metastatic NSCLC is terminal (4).

Metastasis and Epithelial to Mesenchymal Transition

Cancer metastasis is a complex phenomenon during which cells of a primary tumor invade surrounding tissues, enter lymphatic and blood vessels (intravasate) and travel to distant sites as circulating tumor cells (CTC), exit the circulatory system (extravasate) and begin to grow as macrometastases following variable time of latency (17-18). For NSCLC and other most common cancers that derive from epithelial tissue (carcinomas) acquisition of motile and invasive properties is an initial step in metastasis and requires a global change of the cell phenotype towards more fibroblast-like cells. A growing body of evidence indicates that this is achieved through an evolutionarily conserved process of epithelial to mesenchymal transition (EMT) (19-22).

EMT occurs during wound healing and at multiple stages of embryogenesis including gastrulation and neural tube formation in both vertebrates and invertebrates (21-25). During this process differentiated epithelial cells organized in layers with apical-basolateral polarity and extensive intercellular connections through tight junctions and adherens junctions composed of E-cadherin, re-differentiate and lose their polarity and E-cadherin expression. Instead they upregulate the expression of N-cadherin and replace their cytokeratin cytoskeleton with vimentin filaments (21-25). Additionally mesenchymal cells show elevated resistance to apoptosis and induce the expression of numerous matrix metalloproteinases (MMP) capable of digesting the extracellular matrix (ECM) which results in detachment from the basement

membrane without activation of a specialized form of apoptosis called anoikis (21-25). At the same time increased secretion of the components of ECM including fibronectin, collagens, laminins, proteoglycans and hyaluronan provides a substrate for cell movement (21-25). Together those changes enable epithelial tissue a temporal motility required for an enclosure of a wound or delamination of the neural tube (21-25). Physiological EMT is tightly controlled by gradients of signaling molecules in the environment and can be reverted in a process of mesenchymal to epithelial transition (MET) to restore the initial epithelial phenotype. Pathological EMT can be triggered in carcinoma cells by factors present in tumor microenvironment to generate highly invasive and migratory cancer capable of metastasis (21-25).

Multiple factors have been implicated in the induction of EMT. Among them tumor growth factor beta (TGFβ) superfamily is the best characterized (26-28). It comprises more than thirty structurally related proteins including three TGFβ (TGFβ1-3), Activins, Inhibins, Nodal, a number of bone morphogenic proteins (BMPs), growth and differentiation factors (GDFs) and anti-Müllerian hormone (AMH) (26-28). All members of TGFβ family have been implicated in the induction of EMT at different stages of embryogenesis whereas TGFβ1 is a predominant inducer of EMT in an adult organism during wound healing and in cancer (26-28). TGFβ1 is abundantly present in tumor microenvironment and is produced primarily by activated stromal fibroblast (26-28). All TGFβ family members act as homo- or heterodimers by binding to their concomitant receptors of type I and II, which upon ligand binding heterotetramerize (29-30). TGFβ

receptors have a dual specificity serine/threonine and tyrosine kinase activity and phosphorylate receptor Smad (R-Smad) proteins resulting in their translocation to the nucleus and activation of gene expression in addition to activating PI3K/Akt, ERK, p38 and JUN N-terminal kinase (JNK) pathways that all contribute to the induction of EMT (29-32). In a similar manner other growth factors signaling through receptor tyrosine kinases (TKRs) including fibroblast growth factor (FGF), hepatocyte growth factor (HGF), insulin-like growth factor 1 (IGF1), epidermal growth factor (EGF), platelet-derived growth factor (PDGF) and vascular endothelial growth factor (VEGF) are able to induce EMT in different cancers through activation of PI3K/Akt, ERK, p38 and JNK pathways (32). Three other evolutionarily conserved pathways essential in embryogenesis, WNT, Hedgehog (HH) and Notch were shown to induce EMT, however the mechanism of this induction is not as well understood (32). Additionally hypoxic condition in tumor tissue has been shown to induce EMT through canonical hypoxia-inducible factor 1 alpha (HIF-1α) pathway (32).

Pathways involved in regulation of EMT converge on the induction of a group of “master-switch” transcription factors; zinc-finger transcription factor SNAIL, zinc-finger E-box-binding (ZEB) and basic helix-loop-helix (bHLH) factor TWIST that can directly repress epithelial and induce mesenchymal gene expression (22, 32). Two SNAIL factors (SNAIL1 and SNAIL2) are known to activate EMT in development and cancer through direct binding to E-box DNA elements within proximal promoter regions of target genes. SNAIL is responsible for co-recruitment of Polycomb repressive complex 2 (PRC2) which contain

methyltransferases G9a, suppressor of variegation 3-9 homologue 1 (SUV38H1), enhancer of zeste homologue 2 (EZH2), histone deacetylases 1, 2 and 3, Lys-specific demethylase 1 (LSD1), and the co-repressor SIN3A. These complexes add activating (H3K4 methylation, H3K9 acetylation) or repressing (H3K9 and H3K27 methylation) histone marks to control gene expression (32). Similarly two ZEB factors (ZEB1-2) are able to drive EMT through binding to E-box DNA elements and co-recruitment of C-terminal binding protein (CTBP) co-repressor or p300/CBP-binding protein (PCAF) and p300 co-activators and demethylase LSD1 (32). Other transcription factors involved in EMT regulation include fox family (FOXC2, FOXF1, FOXQ1, FOXA1 among others), HMGA2, SOX9 and KLF8 (32). Together those “master-switch” transcription factors directly repress epithelial genes including *CDH1* encoding E-Cadherin and induce mesenchymal genes such as *FN1* (Fibronectin), *CDH2* (N-Cadherin), *VIM* (Vimentin), *COL1A1* (Collagen type 1) and several *MMP* encoding matrix metalloproteases, in addition to reciprocally co-regulating their own expression to establish a positive-feedback loop that drives a global epigenetic reprogramming (22, 32).

In addition to high motility and invasiveness cancer cells undergoing EMT were shown to acquire stem-like phenotype with increased self-renewal capabilities and resistance to apoptosis and chemotherapy (33-36). Induction of EMT in cancer cells results in an elevated expression of transcription factors characteristic of human embryonic stem cells (ESC) including octamer-binding transcription factor 3 and 4 (OCT3-4), Nanog, SRY (sex-determining region Y)-box 2 (SOX2), c-Myc, Kruppel-like factor 4 (KLF4) (22). Concomitantly those

cells show self-renewing potential observed as increased capability to form tumorspheres *in vitro* and initiate tumors under limited dilution in xenograft models *in vivo* (20, 33, 37). Conversely, isolation of cancer initiating cells (CIC or cancer stem cells), based on the expression of cell surface markers associated with stem-like phenotypes, yields tumor cells with activated EMT signature (18). Notably majority of pathways involved in induction of EMT are also known to be essential in a regulation of stem cells populations in embryogenesis and in adult organism. Acquisition of stem-like properties by metastatic cells might be of particular importance during metastatic seeding when a few cancer cells can give raise to a sizeable heterogeneous macrometastatic tumor mass. CIC have been implicated in acquired resistance to chemotherapy and tumor relapses, at least partially due to their intrinsic resistance to apoptosis and high expression of ATP-dependent drug efflux pumps; ABC transporters in a number of malignancies (22, 32). EMT, given its ability to generate CIC, has been shown to be involved in chemoresistance in breast and pancreatic cancers (34-35). Additionally, EMT may also be responsible for acquired resistance of NSCLC *EGFR* mutant cells to TKIs inhibitors as TKI resistant cancer cells display EMT activation (38).

EMT can be induced in NSCLC cells *in vitro* resulting in an increased mesenchymal phenotype, metastatic potential and self-renewal capacity (19-20). Consistently, elevated expression of TGFβ, SNAIL, TWIST, HIF-1α, Vimentin, OCT4, Nanog, ABCG2 and CD133 or decreased expression of E-cadherin all correlate with lymph node metastasis and poor prognosis for NSCLC patients (39-46). Observation of EMT in NSCLC *in vivo* has been obscured by its

transient and reversible nature. Recently circulating tumor cells (CTC) of breast cancer present in blood as either single cells or cell clusters, were shown to carry a signature of activated EMT, including up-regulated expression of FOXC1 and components of TGFβ pathway (18). Induction of EMT in breast cancer *in vivo* has been further confirmed using EMT-dependent fluorescent lineage tracing in mouse model (35). Mesenchymal breast cancer cells were shown to govern tumor chemoresistance and drive tumor metastasis predominantly following cyclophosphamide treatment (35). Similarly conditional knockout of either *TWIST1* or *SNAI1* sensitizes pancreatic cancer cells to gemcitabine treatment in a mouse model of pancreatic tumor (34).

Cancer Metabolism

One of the characteristic features of cancer cells is up-regulated glucose uptake and utilization through glycolytic pathway under aerobic conditions, a phenomenon first described by Warburg in 1920s. Elevated glucose uptake in various cancers including NSCLC is commonly utilized for tumor imaging with positron emission tomography and computer tomography (PET-CT) scan using radiolabeled glucose derivative, ^{18}F-fluoro-2-deoxy-glucose (FDG) (47-54). It is now thought that this metabolic switch is an oncogene-driven response to high proliferation rate and it predominantly serves as a source of metabolic intermediates for the synthesis of lipids, proteins and nucleic acids rather than the source of energy. This is supported by the observation that cancer cells

display unaltered mitochondrial oxidative respiration which often occurs in cancer cells irrespective of the Warburg effect (47-54). Similar elevation of glutamine metabolism has been described in some cancer types which can support redox status and replenish intermediates of the tricarboxylic acid (TCA) cycle in a process of anaplerosis to provide metabolic intermediates for biosynthesis (55-57).

Glucose enters the cell through a family of constitutive or inducible facilitated glucose transporters (GLUT) to be directed into glycolysis pathway in the cytoplasm (48). The first out of nine enzymatic reactions in the glycolysis pathway is carried out by the hexokinase (HK) which phosphorylates glucose to yield glucose-6-phosphate (G6P). G6P is an important substrate for both glycolysis and pentose phosphate pathway (PPP) that generates reducing potential of NADPH and ribose for nucleotide synthesis (48). Hydrolyzed glycogen can additionally contribute to the pool of G6P available for these processes (58). In the glycolytic pathway phosphoglucoisomerase/glucose-6-phosphate isomerase (PGI/GPI) converts G6P into fructose-6-phosphate (F6P) which is subsequently phosphorylated by phosphofructokinase (PFK) into fructose-1, 6-biphosphate (FBP). Following enzymatic reaction converts FBP into two molecules of glyceraldehyde-3-phosphate (G3P) by the enzyme fructose-1, 6-biphosphate aldolase A (ALDOA). G3P may be isomerized into dihydroxyacetone by the enzyme triosephosphate isomerase (TPI) or converted into 1, 3-bisphosphoglycerate (1,3BPG) by glyceraldehyde-3-phosphate dehydrogenase (GAPDH). 1, 3-biphosphoglycerate is further converted into 3-

phosphoglycerate (3PG) by phosphoglyderate kinase (PGK) followed by conversion into 2-phosphoglycerate (2PG) by phosphoglycerate mutase (PGM) to phosphoenolpyruvate (PEP) by enolase (Eno) and into pyruvate by pyruvate kinase (PKM) that can either be reduced to lactate by lactate dehydrogenase (LDH) pumped out of the cell by monocarboxylate transporters (MCT), or oxidatively decarboxylated to acetyl-CoA by pyruvate dehydrogenase complex (PDC) to enter TCA cycle (48). A net result of glycolysis is two molecules of ATP and two molecules of NADH from one glucose molecule. Conversion of pyruvate to lactate yields additional two molecules of ATP per one molecule of glucose and may be used as an energy source in the hypoxic conditions contributing to environment acidification and cancer invasion. The TCA cycle takes place in mitochondria and cycles through eight intermediates; oxaloacetate, citrate, isocitrate, α-ketoglutarate, succinyl-CoA, succinate, fumarate and malate, to yield eight molecules of NADH, two molecules of $FADH_2$, 2 molecules of ATP and six molecules of CO_2 from one molecule of glucose. NADH and $FADH_2$ will donate their electrons onto the electron transport chain system to fuel the synthesis of 38 molecules of ATP from one molecule of glucose in a process of oxidative phosphorylation. Additionally TCA cycle generates intermediates α-ketoglutarate, succinyl-CoA, fumarate and oxaloacetate important for numerous biosynthetic processes. Glutamine uptake is facilitated by several membrane transporters belonging to different families encoded by *SLC1*, *SLC6-7* and *SLC38* (55). Glutamine can be either deaminated by glutamine deaminase (GLS) and converted into α-ketoglutarate to enter TCA or directly used for synthesis of

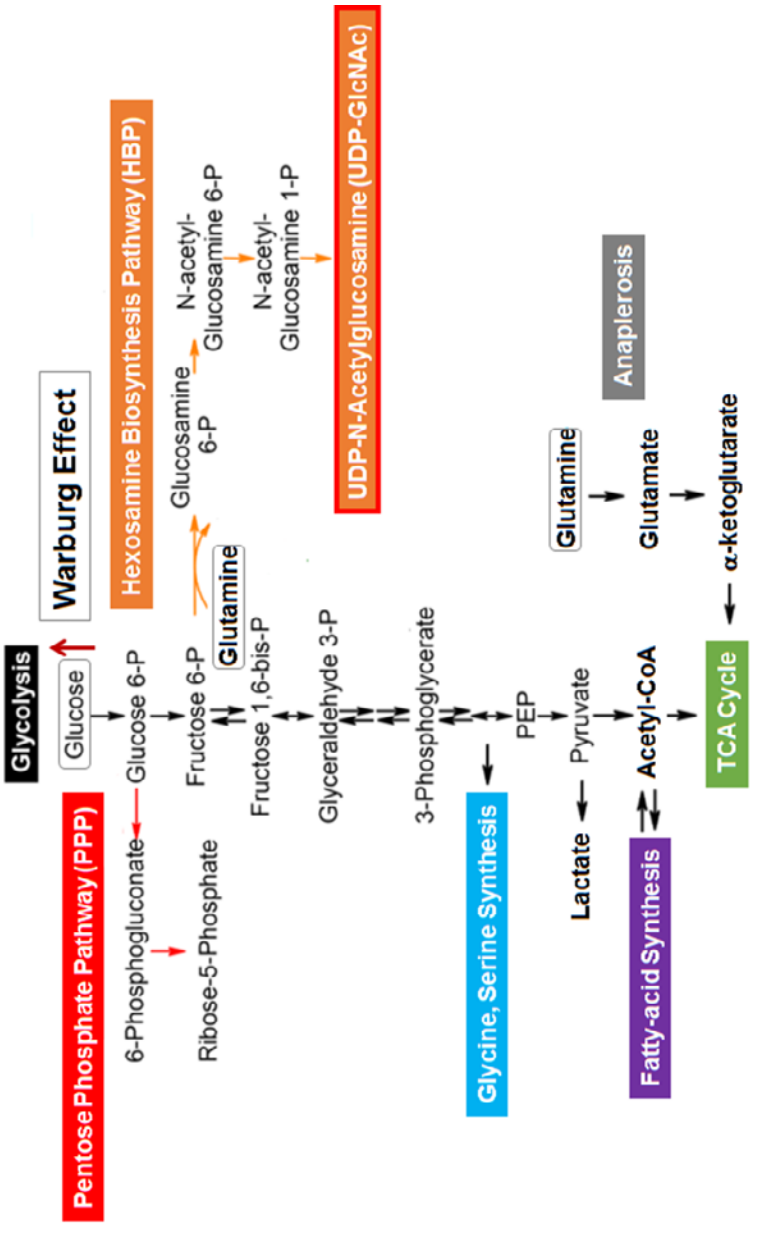
Glycolysis
Glucose
Warburg Effect
Pentose Phosphate Pathway (PPP)
Glucose 6-P
6-Phosphogluconate
Ribose-5-Phosphate
Hexosamine Biosynthesis Pathway (HBP)
Fructose 6-P
Glutamine
Glucosamine 6-P
N-acetyl-Glucosamine 6-P
N-acetyl-Glucosamine 1-P
UDP-N-Acetylglucosamine (UDP-GlcNAc)
Fructose 1,6-bis-P
Glyceraldehyde 3-P
3-Phosphoglycerate
Glycine, Serine Synthesis
PEP
Pyruvate
Lactate
Glutamine
Anaplerosis
Glutamate
Fatty-acid Synthesis
Acetyl-CoA
TCA Cycle
α-ketoglutarate

Introduction Figure 1. Metabolic pathways of glucose and glutamine in a cancer cell. Glucose transported into the cancer cell at elevated rate is directed into the glycolysis pathway and converted primarily into lactate, the phenomenon called “Warburg effect”. Increased flux through glycolysis generates intermediate metabolites for the synthesis of amino acids glycine and serine, fatty acids and ribose sugars in the pentose phosphate pathway (PPP). Glutamine transported into the cancer cell may be converted to glutamate and further into α-ketoglutarate to directly enter TCA cycle for the energy generation. Both glutamine and glucose feed into hexosamine biosynthesis pathway (HBP) in which glutamine and fructose-6-phpsphate are converted into glucosamine-6-phpsphate by the first and rate-limiting enzyme of the pathway, glutamine: fructose-6-phpsphate aminotransferase (GFPT). Glucosamine-6-phpsphate is further converted in four enzymatic steps into UDP-N-acetylglucosamine (UDP-GlcNAc), a key precursor molecule for the synthesis of majority of glycans in the cell.

glutathione (GSH) by glutathione cysteine ligase (GCL) to regulate redox status (55). Fueling TCA promotes biosynthesis whereas GSH is an essential antioxidant scavenging increased levels of reactive oxygen species (ROS) generated as a result of elevated metabolism of highly proliferative cell (55).

Several pathways dysregulated in cancer are known to drive glycolysis. Activated RAS can signal through PI3K/Akt pathway that regulates the expression of GLUT transporters and modifies the activity of glycolytic enzymes including hexokinase 2 (HK2) in addition to activating mammalian target of rapamycin (mTOR) pathway that can directly stimulate protein and lipid biosynthesis and indirectly up-regulate glycolysis through HIF-1α activation (48). HIF-1α is the main regulator of glycolysis in hypoxic conditions and directly induces the expression of GLUT1 and GLUT3, HK1 and HK2, lactate dehydrogenase A (LDHA), monocarboxylate transporter 4 (MCT4) and pyruvate dehydrogenase kinase 1 (PDK1) which phosphorylates and inactivates pyruvate dehydrogenase (PDH) resulting in decreased oxidative phosphorylation and oxygen consumption (48). Liver kinase B1 (LKB1) is an important tumor-suppressor that directly activates AMP-activated protein kinase (AMPK), an important sensor of metabolic state of the cell responsive to the ATP/AMP concentration and negative regulator of mTOR (48). Consequently, loss of LKB1 leads to abnormal mTOR activation (48). Similarly p53 tumor-suppressor induces expression of HK2 and TP-53-induced glycolysis and apoptosis regulator (TIGAR) that decreases levels of fructose-2, 6-biphosphate, together leading to increased flux through PPP (48). Additionally p53 induced expression of PTEN

tumor suppressor and negative regulator of PI3K and expression of SCO2, component of the mitochondrial electron chain transport system and mutation of p53 is sufficient to recapitulate Warburg effect in cancer cells (48). Notably many cancers up-regulate expression of pyruvate kinase M2 (PKM2), an isoenzyme catalyzing last and rate-limiting step of glycolysis of phosphorylation of phosphoenolpyruvate (PEP) to pyruvate (48). Pyruvate kinase M2 has low enzymatic activity and decreases the rate of pyruvate conversion which results in an accumulation of intermediate metabolites of glycolysis (48). Myc proto-oncogene is known to induce PKM2 expression and elevate NADPH pool through PPP, supporting the notion that elevated glycolysis in cancer cells may be primarily utilized for biosynthesis rather than energy generation (48). Myc is also the main regulator of glutamine metabolism in cancer cell, known to directly induce SLC5A1, SLC7A1 and GLS1 to promote both elevated cycling through TCA and generation of intermediates for biosynthetic processes and synthesis of GSH which together with NADPH regulate redox status (55).

Abnormal activation of oncogenic signaling often renders cancer more susceptible to glucose or glutamine withdrawal, phenomena termed glucose- or glutamine-addiction, respectively. Consistently glutamine starvation induces cell death of Myc-dependent but not of Myc-independent cancer cells and targeting GLS enzyme inhibits oncogenic transformation (59, 60). Similarly glucose deprivation induces cell death in Ras and Akt hyperactive cancer cells by triggering ER stress response (61). Recent insights into cancer metabolism sparked a search for potential druggable targets for therapy. Currently under

investigation in preclinical or early clinical phase are inhibitors of GLUT1, GLS1, HK, MCT1, PDK1 and PKM2, amongst others (51, 63). Signaling pathways regulating cancer metabolism including HIF1 and PI3K/Akt are also feasible targets. Inhibitors of mTOR were shown to decrease tumor growth and are available as prescription drugs for graft rejection (51, 63). Similarly metformin, an anti-diabetic drug that inhibits AMPK and mitochondrial complex I, has been reported to improve survival of breast and colorectal cancer patients however further clinical trials are necessary (63-64).

Hexosamine Biosynthesis Pathway

Glutamine and fructose-6-phosphate (F6P) are both substrates of hexosamine biosynthesis pathway (HBP) that generates uridine diphosphate N-acetylglucosamine (UDP-GlcNAc). UDP-GlcNAc is a precursor amino sugar molecule required for protein glycosylation and the synthesis of proteoglycans, glycolipids and glycosylphosphatidylinositol anchors (65). HBP comprises of four enzymatic steps, first of which is a rate-limiting but reversible conversion of glycolysis intermediate fructose-6 phosphate (F6P) and glutamine into glucosamine-6 phosphate (GlcN6P) and glutamate, catalyzed by glutamine: fructose-6P aminotransferases 1 and 2 (GFPT or GFAT) (65). GlcN6P can be converted back to F6P by the action of glucosamine-6 phosphate deaminases 1 and 2. Subsequently GlcN6P is acetylated on a primary amine group by glucosamine-6 phosphate N-acetyltransferase (GNPNAT1/Emeg32/GNA) to form

N-acetylglucosamine-6 phosphate (GlcNAc-6P) using acetyl-CoA as a donor of an acetyl group (65). This process is irreversible in mammals as mammalian cells lack GlcNAc-6P deacetylase activity (65). GlcNAc-6P isomerization to GlcNAc-1P is catalyzed by phosphoacetylglucosamine mutase (PGM3) followed by a transfer of uridine group onto GlcNAc-1P by the enzyme UDP-N-acetylglucosamine pyrophosphorylase (UAP1) to generate the final product of HBP, UDP-GlcNAc (65).

Cellular level of UDP-GlcNAc is tightly linked to global metabolic state of the cell. Notably the rate of glycolysis and glutamine uptake as well as glycogen degradation, acetyl-CoA availability and UTP synthesis can all affect UDP-GlcNAc biosynthesis. Thus UDP-GlcNAc is along with 5' AMP-activated protein kinase (AMPK), mTOR and NAD-dependent deacetylases from sirtuin family, considered an important sensor of the cellular metabolism. In the resting state 3 to 5% of the glucose that enters the cell is directed into HBP but UDP-GlcNAc synthesis can be fueled by additional GlcNAc salvaged through endocytosis and degradation of existing glycans following its phosphorylation to GlcNAc-6P by N-acetylglucosamine kinase (NAGK) (65-67). Similar to other metabolic pathways, flow through HBP is a subject to a complex regulation by its metabolites including GlcNAc-6P and UDP-GlcNAc (68-75). GlcNAc-6P is a potent inhibitor of GFPT1 enzyme and may limit shunting of F6P from glycolysis in an abundance of salvaged GlcNAc. Similarly the end product of HBP, UDP-GlcNAc is an inhibitor of GFPT1 but not GFPT2 (68-76).

First and rate-limiting reaction of HBP, conversion of F6P and glutamine into GlcN6P and glutamate is catalyzed by GFPT enzymes (65-67). Two isoforms are present in humans: GFPT1 and GFPT2 encoded by genes *GFPT1* on chromosome 2 and *GFPT2* on chromosome 5 respectively. GFPTs belong to class II of L-glutamine-dependent amidotransferase (GATs) family of enzymes that utilize their N-terminal cysteine to cleave glutamine amide bond and transfer amide nitrogen onto the substrate (77). Human GFPT1 and GFPT2 proteins comprise of 681aa and 682aa respectively and share about 78% amino acid sequence similarity based on BLAST analysis. They contain two enzymatic domains; N-terminal glutaminase domain that hydrolyzes glutamine to glutamate and ammonia and C-terminal synthase domain composed of two synthase (SIS) domains that transfer ammonia onto F6P and form homotetramers (77). K_D for F6P has been estimated for 2.4 to 5μM and for glutamine 99μM as deduced for *S. typhimurium* enzyme. Binding of F6P GFPT increases its glutaminase enzymatic activity by a fold of 74 to 130 (77). Notably two GFPT isoforms show different tissue expression and opposite regulation by UDP-GlcNAc and cellular signaling pathways (78). GFPT1 is ubiquitously expressed thorough the organism on a basal level whereas GFPT1 isoform (GFPT1-L1) containing an insertion of 54bp within GFPT1 coding sequence is specific to skeletal and heart muscle. GFPT1 is potently feedback-inhibited by HBP metabolites GlcNAc-6P (K_I of 6μM) and UDP-GlcNAc (K_I of 4μM) and by phosphorylation at the serine 205 by cAMP-dependent protein kinase A (PKA), a common effector kinase of G-protein-coupled receptors (GPCRs) that respond to variety of hormones including

glucagon and adrenaline (76, 79). Additionally phosphorylation at serine 261 by AMPK decreases GFPT1 enzymatic activity (80). Under normal physiological conditions expression of GFPT2 is predominantly limited to the central nervous system (CNS) (87). GFPT2 show limited feedback-inhibition by GlcNAc-6P and UDP-GlcNAc and the enzyme activity is increases following PKA phosphorylation at serine 202 (81). Second irreversible reaction of HBP, acetylation of glucosamine-6-phosphate to N-acetylglucosamine-6-phosphate is catalyzed by GNPNAT1 enzyme. Glucosamine-6-phosphate may be generated from F6P or come from salvage pathway and N-acetylglucosamine-6-phosphate is a potent inhibitor of GFPT enzymes. Homozygous deletion of *GNPNAT1* is embryonic lethal whereas isolated mouse embryonic fibroblasts (MEF) show decreased proliferation and adhesiveness (82). Third reaction of HBP, isomerization of GlcNAc-6P to GlcNAc-1P is catalyzed by phosphoacetylglucosamine mutase (PGM3). Homozygous PGM3 deletion is embryonically lethal whereas knockdown of PGM3 in human prostate cancer cell line results in the growth inhibition (83-84). Final reaction of HBP, synthesis of UDP-GlcNAc is catalyzed by UAP1 enzyme. Recently UAP1 expression has been shown to protect cancer cells from endoplasmic reticulum stress induced by inhibitors of N-glycosylation (85).

Little is known about transcriptional regulation of HBP. Proximal promoters of both *GFPT1* and *GFPT2* were partially characterized. They both lack canonical TATA box and contain several Sp-1 sites important for basal transcription (86-87). EGF has been shown to induce expression of *GFPT1* in

breast cancer possibly through Sp1 binding (88). Additionally proximal promoters of *GFPT1* and *GFPT2* contain several AP-1 sites (86-87). Down-regulation of Kras or c-Myc decreases the expression of *GFPT1* in pancreatic cancer (89). Hypoxia has been shown to elevate both *GFPT1* and *GFPT2* transcripts in pancreatic cancer and *GFPT1* proximal promoter contain hypoxia-responsive element (HRE) (90). Recently unfolded protein response (UPR) activated in endoplasmic reticulum (ER) in response to improper protein glycosylation and protein aggregation has been shown to directly regulate *GFPT1* expression through activation of X-box binding protein 1 (Xbp1s) transcription factor binding to X-box motif within a proximal promoter of *GFPT1* (91-92)

GFPT2 expression has been shown to protect hippocampal neuronal cell line from oxidative stress following H_2O_2 treatment and has been shown to be elevated in glioblastoma (93-94). Similarly *GFPT1* homologue (GFA1) protects *Saccharomyces* from methylmercury cytotoxicity (95). Of note, transgenic mice over-expressing *GFPT1* in adipocytes develop insulin resistance and metabolic syndrome and short nucleotide polymorphisms (SNPs) in *GFPT1* and *GFPT2* have been associated with type 2 diabetes (T2D) in several human genetic studies (96-99). Recently *GFPT1* and *GFPT2* expression has been shown to correlate with poor clinical outcome of patients with breast cancer and *GFPT2* expression has been identified as a metabolic signature gene of mesenchymal state (100-101). Additionally ectopic GFPT2 expression in lung adenocarcinoma has been shown to elevate O-linked glycosylation of oncofetal fibronectin, an effect that impacts induction of EMT (198-200).

UDP-GlcNAc can be directly utilized for N- and O-glycosylation including O-GlcNAcylation and the synthesis of proteoglycans and hyaluronan as well as glycolipids and GPI-anchors. UDP-GlcNAc is also an important precursor molecule for the synthesis of other amino sugars in the cell and can be further converted to either uridine diphosphate N-acetylgalactosamine (UDP-GalNAc) or uridine diphosphate N-acetylmannosamine (UDP-ManNAc) by UDP-GlcNAc 4-Epimerase (GALE) and UDP-GlcNAc 2-Epimerase (GNE) respectively (102-103). UDP-GalNAc is used directly for N- and O-glycosylation and the synthesis of glycosaminoglycans and hyaluronan whereas UDP-ManNAc can be further converted into CMP-5-acetylneuraminic acid/sialic acid (CMP-Neu5Ac), an important component of sialylated glycoconjugates (102-103).

Proteoglycans and Hyaluronan in Cancer Biology

Glycosaminoglycans (GAG) are linear polymers of monosaccharides and amino sugars that can either be attached onto a group of extracellular proteins through N- and O- glycosylation to form proteoglycans (PGs) or secreted from the cell on their own in the case of hyaluronan (HA) to form a network of extracellular matrix (ECM) (104). GAGs are polymers of a disaccharide units that can be classified based on their sugar composition into five types; keratan sulfate (KS) composed of 5 – 50 units of galactose and N-acetylglucosamine, dermatan sulfate (DS) containing 50 – 150 of iduronic acid and N-acetylgalactosamine disaccharides, chondroitin sulfate (CS) built 50 – 150 glucuronic acid and N-

acetylgalactosamine disaccharides, heparan sulfate (HS) containing 50 – 150 units of iduronic acid and N-acetylglucosamine and hyaluronan (HA) composed of 2000 – 25000 units of glucuronic acid and N-acetylglucosamine (104). CS, HS, DS and HS are synthesized in a stepwise manner by specific glycosyltransferase enzymes and added sequentially onto their core proteins in the Golgi apparatus from monosaccharides and amino sugars actively transported to Golgi from the cytoplasm (104). These GAGs additionally undergo several modifications including sulfation, epimerization, desulfation and phosphorylation. KS core proteins are predominantly present in the cornea and cartilage and connective tissue (104). CS and DS core proteins belong to a heterogeneous group containing proteins such as aggrecan, versican, neurocan, neuroglycan and tenascin amongst others that play essential role in neuronal biology (104). HS core proteins include syndecans, glypians and secreted molecules including perlecan and collagen XVIII, mutations of which affect cell migration and cause developmental defects or embryonic lethality (104). Fifth and perhaps the best studied class of GAG is hyaluronan. Interestingly this polymer of glucuronic acid and N-acetylglucosamine is synthesized by transmembrane hyaluronan synthases enzymes (HAS1-3) from a cytoplasmic pool of these monosaccharides and translocated outside of the cell during its synthesis (104). Excreted HA can interacts with other proteoglycans, structural proteins and growth factors to build in ECM. It may also remain attached to the cell surface through HAS to form along with several HA binding proteins extensive pericellular coating. Importantly HA may act as a signaling ligand for its receptors CD44 to activate downstream

signaling (105-106). HA matrix is highly dynamic and can be digested by a group of hyaluronidases (HYAL) enzymes and recycled by the cell through the salvage pathway (107). HA chains of varied molecular size from 5 to 10,000 kDa exert different often opposite effect with high molecular weight hyaluronan (HMW) reported to suppress tumor formation and low molecular weight hyaluronan (LMW) fragments promoting cell migration, invasion and metastasis (105-106).

HA synthesis is elevated during injury and inflammation and number of cytokines and growth factors have been shown to stimulate HA secretion including TNF, IL-1β and INFγ amongst others (108). Increased formation of hyaluronan matrix is observed around migrating cells in morphogenesis during mesenchymal cell differentiation and migrating neuronal cells as well as in wound healing (109-111). Of three HAS encoding genes, mutation of HAS2 is embryonically lethal and has been identified as a major HAS during organogenesis and possibly implicated in cancer development (111-112).

Elevated hyaluronan secretion has been associated with cancer development and progression. Increased hyaluronan deposition in the stroma of malignant tumors as compared to benign or normal tissues and elevated serum levels of hyaluronan has been observed in several malignancies including breast, colorectal and NSCLC (112, 116). Similarly overexpression of HAS1 or HAS2 increases tumorigenic and metastatic potential of several cancer types including prostate, colon and breast cancers (117-120). HA is often enriched at the invasive front of tumors and high HAS2 expression has been shown to correlate with mesenchymal phenotypes of cancer cells (101, 112). HA has been shown to

promote migration and invasion, EMT and self-renewal phenotypes in cancer initiating cells (CIC) (121-132). Often characteristics attributed to HA include pro-survival signaling, chemoresistance and immuno-suppression and HAS2 has been identified as a metabolic signature gene on mesenchymal cancer cells (121-132).

Number of studies indicates that HA can promote cancer cell migration and survival through cell-autonomous signaling via CD44 receptor. Importantly expression of a splice variant isoform of CD44 (CD44v) is often observed in variety of cancers and is able to induce metastatic phenotype in carcinoma *in situ* cells (105). Binding of CD44 to its ligands including HA, collagen and fibronectin initiates activation of several downstream effectors. One of them is Rho guanine exchange factor (GEF) which activates small GTP-protein RHOA. Cytoplasmic tail of CD44 is associated with actin cytoskeleton through and adaptor proteins ankyrin and ezrin-radixin-moesin (ERM). Activated RHOA signals to its downstream serine/threonine kinase Rho kinase (ROK) which phosphorylates ankyrin to strengthen its interaction with CD44 (105). ROK also phosphorylates Na^+/H^+ exchanger which creates acidic environment promoting ECM degradation through HYAL2 and cathepsin B (133). Furthermore upon HA binding, CD44 associates with $\alpha 4\beta 1$ integrin receptor and activates focal adhesion kinase (FAK) via SRC which weakens CD44/integrin association with paxillin and allows their translocation to the leading edge of the cell (105). Together those changes promote formation of lamellipodia and cell migration. HA has been shown to be implicated in TNF and TGFβ induced EMT (134). TNF has been shown to induce

CD44 and HAS expression in retinal pigmental epithelial cells which promoted HA/CD44 interaction and moesin phosphorylation and cell migration. HA/CD44/moesin complex was found to be associated with TGFβ receptor II which led the activation of TGFβ downstream cascade of Smad signaling and induction of EMT (134). Several studies have implicated HA/CD44 signaling in the regulation of CIC phenotypes (105). Indeed CD44 is one of the earliest identified cell surface marker used to sort stem cell population from variety of cancers types. HA/CD44 interaction has been suggested to promote Nanog signaling through CD44-dependent activation of protein kinase Cε (PKCε) and expression of stemness transcription factors and chemoresistance and anti-apoptotic genes (122-123, 126-127). Finally HA/CD44 may promote signaling through receptor tyrosine kinases (RTKs) including ERBB2 (105). CD44 has been shown to interact with ERBB2 in colorectal cancer and HA/CD44 initiates ERBB2 phosphorylation and downstream signaling (105, 112). Similarly CD44 may promote signaling from MET receptor by binding to HGF which activates downstream PI3K and Ras signaling (105, 112).

In addition to the cell-autonomous effect of HA/CD44 on cancer cells, HA may also affect tumor progression through shaping of the tumor microenvironment. HA along with other proteoglycans comprises a scaffold for migrating cancer cells. Additionally HA has been shown to induce formation of immunosuppressive tumor infiltrating macrophages that secrete growth factors and MMPs to promote tumor invasion without exerting cytotoxicity (135). HA may also contribute to tumor angiogenesis as oligosaccharide fragments of HA induce

neovascularization and promote endothelial cell proliferation (105). Similarly HAS2 overexpression in breast cancer mouse model elevates tumor vasculature formation (136). Finally ECM binds a variety of growth factors that may be released during ECM remodeling to stimulate cancer cell proliferation and metastasis.

HA is tightly linked to the flux through glycolytic pathway and cellular concentration of UDP-GlcNAc. Elevated glucose promotes HA synthesis and HAS enzymes has been shown to be sensitive to UDP-GlcNAc (137-140). Notably HA synthesis is also regulated by protein O-GlcNAcylation, type of O-linked glycosylation that also utilizes UDP-GlcNAc as a substrate acting as a metabolic sensor of the cell (140). HAS2 has been shown to be modified by O-GlcNAcylation at serine 221 which potentiates its enzymatic activity and HA secretion (140). Interestingly O-GlcNAcylation also negatively affects *HAS2* gene expression through modifying transcription factors YY1 and SP1 which forms a feedback loop of HA synthesis (138). Additionally HA may undergo turnover through receptor-mediated uptake and lysosomal degradation to refuel a pool of cytosolic UDP-GlcNAc (141-142).

N- and O-Glycosylation and Cancer Biology

Glycosylation is a post translational modification that relies on the addition of a single or complex glycan group onto the amide groups of asparagines (N-linked) or hydroxyl groups of serine/threonine or hyrdoxylisines (O-linked).

Complex glycosylation occurs predominantly on transmembrane or secreted proteins and is facilitated in endoplasmic reticulum (ER) and Golgi apparatus. A special type of O-linked glycosylation with a single N-acetylglucosamine is called O-GlcNAcylation and occurs predominantly on the nucleocytoplasmic proteins. A number of simple monosaccharides including glucose, galactose, fucose and xylulose and amino sugars generated in HBP GlcNAc, GalNAc and sialic acid are used in the glycosylation process (143).

The most abundant types of O-liked glycosylation are GAGs, O-GlcNAcylation and O-linked mucin-type glycosylation (143). Additionally domain-specific non-mucin-like O-glycosylation types have been described including O-fucosylation of EGF-repeat domains and O-mannosylation α-dystroglycan (143). O-linked mucin-type glycosylation occur on a number of proteins including mucins (MUC) and oncofetal fibronectin. Mucins are large extracellular or membrane-associated proteins that form a gel-like protective layer on epithelial cells lining internal tracts of respiratory system, stomach, intestines and other organs (145). O-linked glycosylation is initiated in Golgi apparatus where monosaccharides starting with UDP-GalNAc, are added directly onto serine or threonine hydroxyl groups on mucins by a group of N-acetylgalactosaminyltransferases (GalNAcTs). In a subsequent reactions additional oligosaccharide branching, elongation and terminal modifications occur (145).

Aberrant mucins expression and O-glycosylation have long been associated with cancer development, particularly adenocarcinomas and elevated

levels of mucins correlate with tumor progression and poor clinical outcome (145). Some of the early identified tumor associated antigens (TAAs) used for diagnostics are O-glycosylated mucins. In addition to being a component of ECM that provides a substrate for cell attachment and migration and sequesters ECM-binding growth factors, membrane-associated mucins including MUC1 have been shown to facilitate signal transduction via cytoplasmic tail domain associated with β-catenin and MAPK kinase (145). MUC1 overexpression correlates with invasive and metastatic cancers of the colon and pancreas (145). Increased mucin-type O-linked glycosylation of oncofetal fibronectin following TGFβ treatment has been shown to promote EMT in prostate and lung adenocarcinoma cells whereas silencing of GalNAc-T6 and T3 resulted in loss of oncofetal fibronectin expression and inhibition of EMT (198-200).

N-linked glycosylation occurs initially in the ER and later in Golgi apparatus (143). N-glycosylation is initiated by the synthesis of a lipid-linked oligosaccharide (LLO) linker attached to dolichol lipid. Initial steps of linker synthesis occurs on the cytoplasmic site of ER membrane is then flipped onto the luminal site of the ER, converted to LLO and covalently added co-translationally onto polypeptide chain emerging in ER by oligosaccharyltransferase (OST) through GlcNAc residue (143). The linkage occurs at the asparagine residue within a sequence Asn-X-Ser/Thr where X is any amino acid except proline (143). Glycan groups serve as recognition sites for ER-associated chaperones that ensure proper protein folding (143). Improper protein glycosylation due to protein overload or defects in N-glycosylation results in ER stress and activation

unfolded protein response (UPR) (143). Subsequent processing of oligosaccharide chain occurs in Golgi and includes removal of mannose residues by a group of mannosidases and introduction specific types of branching in oligosaccharide backbone facilitated by a group of β-N-acetylglucosaminyltransferase enzymes (GnTs) using UDP-GlcNAc as a substrate (143). Further addition of monosaccharide units occurs across cis-to-trans Golgi trafficking and results in a vast variety of generated structures that differ by the number of branching, saccharide composition and type of glycosidic bonds (143). Majority of transmembrane and secreted proteins undergo glycosylation including growth factors, cytokines, receptors and adhesion molecules. Consequently a number of cellular processes may be affected by changes in glycosylation including inflammation, immune surveillance, cellular signaling and metabolism, cell survival, adhesion and motility.

Aberrant N-linked glycosylation is observed in a number of malignancies and has been associated with increased metastatic potential and poor clinical outcome (144, 146-148). Particularly, elevated amount of tetraantenary N-glycans generated by mannoside acetylglucosaminyltransferase 5 (MGAT5) often overexpressed in cancer cells promotes tumorigenesis (146-149). Overexpression of MGAT5 induces increased cell motility, tumor formation and metastasis in immortalized lung epithelial and mammary carcinoma cells (146-148). Conversely downregulation of MGAT5 reduces tumor growth and metastasis of mammary cancer cells (149). Interestingly MGAT5 expression is regulated by Kras signaling pathway (146-148). The effect of MGAT5 is opposed

by the activity of MGAT3 enzyme that generates simple bisected N-glycans that cannot undergo further branching (146-148). Consequently overexpression of MGAT3 reduces tumor growth and metastasis (146-148). Aberrant N-glycosylation in cancer cells may alter growth factor signaling as majority of growth factors and growth factor receptors are undergo glycosylation. It has been proposed that elevated number of tetraantenary glycans which have high affinity to extracellular lectin proteins called gallectins that can cross-link glycosylated transmembrane proteins and prolong their retention at the cell surface promote sustained signaling from EGFR (146). On the other hand abundance of bisecting N-glycans produced by MGAT3 decreases the affinity to galectins and counteracts receptor activation (146). Similar effect of aberrant N-glycosylation was observed on TGFβ and VEGF pathways which promoted cancer angiogenesis and mediated resistance to anti-VEGF treatment (150). Similarly cell motility and invasion might be affected by altered N-glycosylation. Integrins receptors that mediate cell-ECM interactions and participate in focal adhesion formation and cell movement through signaling via focal adhesion kinase (FAK) are N-glycosylated (146). Overexpression of MGAT5 resulted in elevated migration on fibronectin by elevation of tetraantenary N-glycans on integrin $\alpha 5\beta 1$ that binds fibronectin (146). Aberrant E-cadherin N-glycosylation due to MGAT5 overexpression results in its mislocalization from the plasma membrane contributing to invasiveness and metastasis (146). Conversely elevation of bisecting N-glycans delayed E-cadherin turnover from cell membrane, increasing stability of adherens-junctions and decreasing tumor progression (146).

Interestingly, during TGFβ-induced EMT, expression of MGAT3 is downregulated which leads to a decrease in bisecting N-glycosylation (151-152). Conversely TGFβ withdrawal results in mesenchymal to epithelial transition (MET) which restores MGAT3 expression and E-cadherin bisecting N-glycosylation (151). Overexpression of MGAT3 opposed EMT and inhibited cell migration (146). Notably β-catenin acting downstream of E-cadherin and Wnt pathway which also utilizes β-catenin, both negatively regulate MGAT3 expression to form an auto regulation loop (153).

Protein glycosylation is tightly linked to the flux of HBP and the metabolic state of the cell. Glucose starvation of Kras tumors leads to improper glycosylation in ER and the induction of unfolded protein response (UPR) (61). This effect can be rescued by supplementation with GlcNAc, indicating the importance of HBP (61). Importantly recently *GFPT1* gain of function mutation has been shown to protect *Caenorhabditis elegans* from UPR and proteotoxic stress and resulted in prolonged lifespan as did supplementation with GlcNAc (91). Similarly UAP1 overexpression has been shown to protect prostate cancer cells against inhibitors of N-linked glycosylation and UPR (85). Interestingly UPR has been shown to regulate the flux through HBP via direct binding of spliced X-box binding protein 1 (Xbp1s), a conserved signal transducer of the UPR, to the promoter of GFPT1 which results in protein expression and elevation of protein O-GlcNAcylation (92). The rate of metabolic flux through HBP may also affect N-glycans branching. It has been shown that MGAT5 has much lower Km for the UDP-GlcNAc that other GnTs, and is highly sensitive to UDP-GlcNAc

concentration in the cell (154). Consequently supplementation with GlcNAc has been shown to induce tetraantenary branching of N-glycans in melanoma cells. Additionally N-glycosylation has been shown to regulate cell metabolism. Glucose starvation leads to cell death due to decreased cytokine receptor-mediated uptake of glutamine resulting from improper receptor glycosylation and membrane localization (155). This effect can be reversed with GlcNAc supplementation. Moreover N-glycosylation of glucose transporters increases their membrane localization and elevates glucose uptake and the Warburg effect (156-157). Similarly O-linked glycosylation of oncofetal fibronectin has been shown to be elevated in lung adenocarcinoma cells following overexpression of GFAT2 (200).

O-GlcNAcylation in Cancer Biology

A single UDP-GlcNAc molecule can be directly added onto hydroxyl groups of serines or threonines of target proteins as a post-translational modification (PTM) called O-GlcNAcylation (O-GlcNAc) (158). Similar to other PTMs O-GlcNAcylation is highly dynamic and reversible, catalyzed by O-GlcNAc transferase (OGT) and O-GlcNAcase (OGA) that adds and removes O-GlcNAc modification respectively (159). Unlike N-glycosylation, O-GlcNAcylation occurs predominantly on the nucleocytoplasmic proteins to regulate their stability, localization and activity (159). Close to 4000 proteins modified by O-GlcNAcylation have been identified, including enzymes, transcription factors, chaperones, structural proteins, ribosomes and histones (159, 165). OGT and

OGA are the only two enzymes facilitating deposition and removal of O-GlcNAcylation, respectively. The *OGT* gene resides on the X chromosome whereas *MGEA5* gene is located on the chromosome 10. Importantly, the loss of either gene results in embryonic lethality (160-161). Three OGT splice isoforms are present in humans that share identical C-terminal glycosyltransferase domain but differ in the number of N-terminal tetraticopeptide repeat (TPR) motifs that mediate interactions with substrates and the subcellular localization (162). Nucleocytoplasmic OGT (ncOGT), short OGT (sOGT) and mitochondrial-specific OGT (mOGT) contain 13.5, 2 and 9 TPR motifs and are 116kDa, 78kDa and 103kDa respectively (162, 165). OGT possesses a non-canonical PIP3-binding domain at the C-terminus which facilitates its recruitment to inner cell membrane following PI3K activation (163). Interestingly OGT has been shown to possess a protease activity and is capable of the cleavage of host cell factor-1 (HCF-1), a transcriptional co-regulator of cell-cycle progression (164). Two identified OGA splice isoforms; long (OGA-L) cytoplasmic 130kDa form and short (OGA-S) 75kDa form localized in nucleus and lipid droplets share N-terminal β-N-acetylglucosaminidase enzymatic domain but differ in the presence or absence of putative C-terminal histone acetyltransferase (HAT) domain respectively (165). OGA-S shows lower enzymatic activity *in vitro*. Substrate specificities of OGT and OGA are thought to be regulated by interactions with targeting protein complexes. The level of O-GlcNAcylation is determined primarily by the rate of the flux through HBP and changes rapidly with varied glucose and glutamine concentration. Importantly UDP-GlcNAc is an obligate activator of the OGT

enzyme and cellular concentration of UDP-GlcNAc can modulate both enzymatic activity and the specificity of the OGT towards its substrates. Expression of OGT and OGA appear to be co-regulated in untransformed cells possibly to limit the abnormal changes in protein O-GlcNAcylation. Both OGT and OGA undergo several posttranslational modifications (PTMs) with possible regulatory function. OGT phosphorylation by activated IGF receptor (IGFR) results in the elevation of its enzymatic activity (163). OGT has also been shown to be phosphorylated by AMPK at threonine 444, which affects its enzymatic activity and nuclear localization (166). Additionally OGT can catalyze its auto-O-GlcNAcylation (167).

Protein O-GlcNAcylation appears to act both as a sensor of metabolic state of the cell that fine-tunes activation of signaling pathways to the nutrient availability as well as a pro-survival stress-response modification (165, 169). Several signaling pathways have been shown to be modulated by O-GlcNAc in hyperglycemic conditions. Components of FGF receptor (FGFR) are O-GlcNAcylated in *Drosophila*, which is required for a proper signal transduction to the downstream mitogen-activated protein kinase (MAPK) and cell migration during development (168). Similarly several components of IGF pathway including insulin receptor substrate 1 (IRS1), PIP3-dependent kinase (PDK1) and Akt itself become O-GlcNAcylated by OGT recruited to cell membrane by activated IGF receptor (IGFR) which results in an inhibition of the pathway and is believed to play a causative role in the development of insulin resistance in hyperglycemic conditions in pre-diabetic patients (163). TGF-β-activated kinase 1 binding protein 1 (TAB1) that transduces signaling from multiple pro-inflammatory

cytokines including TNF, TGFβ, interleukin-1 (IL-1) and bacterial lipopolysaccharide (LPS) has been shown to be O-GlcNAcylated on serine 395 which is required for full activation of its partner serine/threonine kinase TGFβ-activated kinase1 (TAK1) and signal transduction to downstream effector nuclear factor kappa B (NF-κB) and MAPK kinases (170). Similarly AMPK has been shown to be O-GlcNAcylated which is required for its full enzymatic activity (166). O-GlcNAcylation may also act as a feedback regulator of glycolysis. A number of glycolytic enzymes have been shown to undergo O-GlcNAcylation including HK, GPI, PFK1, ALDOA, TPI, GAPDH, PGK2, Eno1, PKM2, LDHA which cumulatively results in an accumulation of glycolytic metabolites (171-172). O-GlcNAcylation of Oct4 and Sox2 regulates their stability and transcriptional activity and regulates pluripotency and stem cell reprogramming of embryonic stem cells (ESC) (173). Concomitantly inhibition of O-GlcNAcylation results in a loss of pluripotency and self-renewal in ESC (173). Recently O-GlcNAcylation has been shown to act as an epigenetic modification (174). OGT can be associated with chromatin and directly interacts with ten eleven translocation (TET) 2 and 3 proteins through its TPR domain and mSin3A corepressor (175-178). TET proteins convert 5-methylcytosine (5mC) to 5-hydroxymethylcytosine (5hmC), which promotes loss of DNA methylation and gene regulation with particular implication in embryonic stem cells (179). Additionally OGT can O-GlcNAcylate histone 2B (H2B) at serine 112 in mouse embryonic stem cells which serves as an anchor for ubiquitin ligase and promotes H2B monoubiquitination at lysine 120 (180).

O-GlcNAcylation is induced in response to multiple stress signals including heat shock, heavy metals, DNA damage, endoplasmic reticulum stress, hypoxia, and starvation, to promote cell survival and inhibit apoptosis (169, 181-184). O-GlcNAcylation is tightly linked to heat shock response. Increase O-GlcNAcylation enhances expression of heat shock factor 1 (HSF1) a main transcription factor orchestrating heat shock response as well as its transcriptional targets heat shock proteins (HSP) including HSP70 and HSP90 that act as a chaperone for misfolded proteins (169). HSP70 itself is O-GlcNAcylated and display lectin-like binding activity towards O-GlcNAcylated proteins (169, 185). Indeed O-GlcNAcylation prevents aggregation of several proteins including tau and α-Synuclein with potential implication in neurodegenerative diseases (169, 186). Additionally O-GlcNAcylation of 26S proteasome inhibits its activity and prevents protein degradation (187). Recently O-GlcNAcylation has been shown to be induced during unfolded protein response (UPR) through direct induction of *GFPT1* and HBP flux by a spliced isoform of a transcription factor X-Box Binding Protein 1 (Xbp1s), which promoted cell survival (91-92). Moreover O-GlcNAcylation can prevent apoptosis through direct modification of the components of NF-κB signaling pathway which leads to its full transcriptional activation and induction of expression of several anti-apoptotic genes (188-191).

Elevated O-GlcNAcylation has been associated with cellular transformation and hyper O-GlcNAcylation has been observed in all examined cancer types including breast, prostate, colorectal, liver and pancreatic cancer and chronic lymphocytic leukemia (CLL) due to both changes in the metabolic

flux in cancer cells and de-regulation of OGT and OGA expression (192-196). OGT is over-expressed in multiple cancer types including breast, prostate, colorectal, pancreatic and lung cancers *in vitro* and *in vivo* whereas OGA levels are down-regulated in lymphoma and leukemia, brain and ovarian cancers (171, 192-196). Aberrant O-GlcNAcylation has been shown to promote tumor development by regulating various aspects of cancer cell biology including cell proliferation, resistance to apoptosis, EMT and invasion and metabolic reprogramming (171). O-GlcNAcylation of FoxM1 in breast cancer leads to increased protein stability resulting in elevated cell proliferation and invasion through regulation of FoxM1 targets $p27^{Kip1}$ and MMP2 respectively (196). Snail1 transcription factor has been shown to undergo O-GlcNAcylation which results in its stabilization and increased transcriptional activity, suppression of E-cadherin and induction of EMT in lung and breast cancer cell lines (197). Increased O-GlcNAcylation of actin-binding protein cofilin further promotes cell migration through the regulation of actin cytoskeleton dynamics in breast cancer (231). Notably a proto-oncogene c-Myc has been shown to be O-GlcNAcylated at threonine 58. This modification of c-Myc results in protein stabilization and elevated HBP. Indeed protein O-GlcNAcylation has been shown to drive pancreatic cancer cell proliferation through regulation of c-Myc whereas reducing O-GlcNAcylation causes degradation of c-Myc in prostate cancer cells (201-202). Similarly tumor suppressor p53 has been shown to be O-GlcNAcylated at serine 149, leading to protein stabilization by blocking its ubiquitin-dependent degradation (203). Hyper-O-GlcNAcylation can affect cancer cell metabolism. O-

GlcNAcylation of HK in cancer cells elevates its enzymatic activity and promotes the Warburg effect, whereas O-GlcNAcylation of PFK1 and PKM2 decreases their activities which results in the accumulation of glycolytic intermediates for utilization in PPP and HBP (172). Moreover hyper-O-GlcNAcylation of NF-κB prevents apoptosis in cancer cells. Consequently blocking O-GlcNAcylation by silencing of OGT has been shown to reduce cancer cell proliferation and invasion and tumor formation *in vivo* in a number of malignancies including breast prostate and colorectal cancers (192-196).

NF-κB Pathway and Cancer

NF-κB is a family of pleiotropic transcription factors that regulate a broad range of biological processes including lymphocyte activation, pro-inflammatory signaling, cell proliferation, differentiation and apoptosis (204-207). Dysregulation of NF-κB pathway is implicated in the development of a number of pathological conditions including autoimmune diseases, diabetes and cancer (204-207).

Multitude of extra- and intracellular stimuli can induce canonical NF-κB pathway, including T- and B-cell receptors (TCR and BCR), pro-inflammatory cytokines, Toll-like receptors, growth factors, DNA damage and UPR (204). All stimuli converge on the activation of IκB kinase (IKK) complex, a critical component of NF-κB signaling pathway (204). TNF is a key pro-inflammatory cytokine that signals through NF-κB. Following TNF binding to TNF receptor 1 (TNFR1) adaptor proteins TNF receptor associated factor 2/5 (TRAF2/5) and

receptor interacting protein (RIP) as well as TAK1 kinase are recruited to TNFR1 along with IKK complex which leads to IKK activation (204). Similarly, signaling from Toll-like receptors (TLRs) and interleukin 1 receptor (IL-1R) proceeds through adaptor proteins MyD88, TRAF6 and kinase TAK1 to activate IKK (204). TGFβ may induce NF-κB through TAK1 kinase and TAB1 adaptor protein whereas stimulation of T- and B-cell receptors results in IKK activation through CARD-containing proteins BCL10 and CARD11 (208). Intracellular signals such as DNA damage and UPR can also activate NF-κB. DNA damage appears to induce IKK through RIP1/NEMO/PIDD complex formed in the nucleus and the ATM-mediated phosphorylation of NEMO whereas UPR can activates IKK through endoplasmic reticulum (ER) membrane receptor inositol-requiring protein 1α (IRE1α) and TRAF2 adaptor (209-210). IKK complex is composed of two catalytic subunits IKKα/IKK1 (*CHUK*), IKKβ/IKK2 (*IKBKB*) and a regulatory NF-κB essential modulator (NEMO)/IKKγ (*IKBKG*) (204). Activated IKK phosphorylates IκB complex composed of IκBα (*NFKBIA*), IκBβ (*NFKBIB*) and IκBε (*NFKBIE*) that binds NF-κB transcription factors and sequesters NF-κB in the cytoplasm by masking its nuclear localization signal (NLS) (204). In the canonical pathway, IKK-dependent phosphorylation of IκB leads to IκB poly-ubiquitination by SCF-type E3 ligase $E3RS^{IκB/β\text{-}TrCP}$ and its 26S proteasomal degradation which allows NF-κB translocation into the nucleus to activate transcription (204). NF-κB family consists of five proteins; p65/RelA (*RELA*), c-Rel (*REL*), RelB (*RELB*), p105/p50 (*NFKB1*) and p100/p52 (*NFKB2*) that act as

homo- and heterodimers. They all share N-terminal Rel homology domain (RHD) that mediates dimer formation and DNA binding to kappa B (κB) motifs within gene promoters and enhancers (204). Three NF-κB proteins p65/RelA, c-Rel or RelB contain an additional C-terminal transcription activation domain (TAD) responsible for the recruitment of coactivators including CREB-binding protein (CBP)/p300 and activation of transcription (204). Consequently, NF-κB dimers containing p65/RelA, c-Rel or RelB, predominantly p65:p50 heterodimer, are able to drive transcription activation (204). Conversely homodimers of p105/p50 and p100/p52 that lack TAD repress transcription in the absence of stimuli by binding to κB sites and tethering core repression complexes comprised of HDAC3 and one of two homologous corepressors, SMRT or nuclear receptor corepressor (N-CoR), until displaced by transcriptionally competent NF-κB dimers (204). Notably activated NF-κB undergoes several posttranslational modifications that regulate its transcriptional potential (211). PKA phosphorylation of p65 at serine 276 is necessary for its full activity and promotes p65 interaction with coactivators CBP/p300 (211). Serine 276 may be also phosphorylated by mitogen- and stress-activated protein kinase 1 and 2 (MSK1 and MSK2), a nuclear effector kinases of ERK and p38/MAPK pathways (211). Similarly serine 536 of p65 may be phosphorylated by IKKα and IKKβ (211). CBP/p300 facilitate p65 acetylation at lysine 310 which is further required for its full activation in response to cellular cues (211). Phosphorylation of serine 276 is necessary for the subsequent p65 acetylation at lysine 310, whereas phosphorylation at serine 536 can further

increase acetylation of lysine 310 possibly by altering p65 interaction with co-repressor and histone deacetylase SMRT/HDAC3 complex (211).

NF-κB activation has been implicated in cancer development and progression in both cell autonomous and non-autonomous fashion. As a key regulator of innate and adaptive immune system NF-κB can contribute to cancer development by affecting inflammation and immunosurveillance (212). Inflammation is a known tumor promoter and low doses of non-steroidal anti-inflammatory drugs (NSAID) decreases a risk of development of a number of malignancies. NF-κB is also activated in cancer cells and regulates variety of biological processes by upregulating a multitude of target genes that encode for anti-apoptotic proteins (Mcl-1, Bcl-xl, Bcl-2, , XIAP, cIAPs), cyclins (Cyclin D1, D2 and D3), proto-oncogenes (c-Myc, c-Fos, c-Rel, JunD), growth factors (Activin A, BMP2, BMP4, PDGF, WNT10B), inflammatory cytokines (IL-1, IL-2, IL-6, IL-8, TNF) and their receptors (EGFR, Erbb2), cell adhesion molecules (CD44, Fibronectin), heat shock proteins (HSP90), reactive oxygen scavengers (SOD1 and 2), transcription factors (Elf3, HIF1α, p53, Snail, Sox9), histone modifiers (JMJD3) and metabolic enzymes (Eno, HAS, MMP3, MMP9, SCO2, GLUT3) amongst others (213). Cellular transformation by proto-oncogenes and viral oncogenes often activates NF-κB pathway and exploits its anti-apoptotic activity (205). Aberrant activation of NF-κB has been observed in multiple cancer types, including lung and promotes tumor development (207, 214-218). Conversely silencing of NF-κB in the airway epithelial cells decreases lung inflammation and tumor formation and elevates apoptosis in lung epithelial cells due to reduced

expression of anti-apoptotic Bcl-2 in mouse model of urethane-induced lung cancer (216). NF-κB is activated in Kras mutant and p53 null lung cancer cells and inhibition of NF-κB decreased lung adenocarcinoma formation in a mouse model of lung cancer driven by these mutations (214). In a different study silencing of NF-κB decreased lung cancer formation in mouse model of Kras-driven lung tumor regardless of p53 status (217). Similarly depletion of IKK2 reduces cancer cell proliferation and prolongs survival in Kras-driven mouse model of lung adenocarcinoma (215). Consistently, increased NF-κB expression in NSCLC patients correlates with higher tumor grade and poor clinical outcome (219).

NF-κB activation is also implicated in an induction of EMT and stem-like phenotype in cancer cells in several malignancies including lung tumors (223-229). TNF has been shown to synergize with TGFβ by inducing EMT in NSCLC and other cancers (220-222). Importantly NF-κB is required for the EMT induction in NSCLC and inhibition of NF-κB is sufficient to block TGFβ-driven EMT *in vitro* and cancer metastasis *in vivo* (19). NF-κB has been shown to directly regulate the expression of several “master-switch” EMT transcription factors including Snail, Twist and SIP1 as well as other mesenchymal genes including Vimentin, Fibronectin and MMPs (224-225). Additionally NF-κB may also indirectly promote EMT through stabilization of Snail protein and preventing its ubiquitin-dependent degradation (229). Recently our laboratory showed that NF-κB-dependent up-regulation of Activin A sets up an auto-activation loop of growth factor signaling and is required for the maintenance of mesenchymal

phenotype following EMT in NSCLC (20). Notably NF-κB activation has recently been associated with self-renewal and regulation cancer-initiating cells (CIC) in prostate cancer (230)

NF-κB pathway is an important regulator of cellular metabolism and is itself responsive to metabolic state of the cell. NF-κB has been shown to promote oxidative mitochondrial oxidative phosphorylation through upregulation of mitochondrial synthesis of cytochrome c oxidase 2 (SCO2), one of the enzymes of electron transfer chain (231). Concomitantly, silencing of RelA elevates aerobic glycolysis, promotes glucose addiction and renders cells susceptible to mitochondrial stress and necrosis under glucose starvation (231). This effect of NF-κB on metabolism appears to require p53 as a downstream effector and NF-κB can directly upregulate p53 (231). Loss of p53 elevates IKK1 and IKK2 activity and NF-κB signaling. This activation of IKK was linked to elevated rate of aerobic glycolysis following p53 loss, and required upregulation of GLUT3 which may be directly regulated by p65. The same group identified that IKK2 is modified by O-GlcNAcylation at serine 733 which potentiates IKK2 activity. O-GlcNAcylation of IKK was elevated in p53 deficient cells or by high glucose concentration. Similarly several O-GlcNAcylation sites on p65 were identified. O-GlcNAcylation of p65 at threonine 352 has been shown to decrease p65 binding to IκB and resulted in increased NF-κB activity. Additionally the Mayo laboratory has shown that O-GlcNAcylation of p65 on threonine 305 is required for its subsequent acetylation on lysine 310 and full transcriptional activation. Subsequently hyper O-GlcNAcylation has been implicated in sustained NF-κB

signaling in pancreatic cancer and was required for anchorage-independent growth. Similarly O-GlcNAcylation of c-Rel on serine 350 has been shown to promote its transcriptional activity downstream of TCR. Thus, NF-κB and critical components within the NF-κB signaling pathway are post-transcriptionally regulated by the O-GlcNAc moiety. Despite this understanding, NF-κB has not been shown to regulate enzymes in the HBP or enzymes critical for O-GlcNAc deposition.

Here we hypothesize that mesenchymal NSCLC cells undergo metabolic reprogramming to upregulate the flux through the HBP, the synthesis of UDP-GlcNAc and the content of cellular glycans. Furthermore we aim at determining the role of elevated glycans during EMT and in mesenchymal cells and their effect on progression and metastasis of lung cancer.

REFERENCES

1. www.cancer.org

2. Bender E. Epidemiology: The dominant malignancy. *Nature.* 2014 Sep 11; 513(7517): S2-3.

3. www.who.int

4. Devita Clinical Oncology

5. Herbst RS, Heymach JV, Lippman SM. Lung cancer. *N Engl J Med.* 2008 Sep 25; 359(13): 1367-1380.

6. Aisner DL, Marshall CB. Molecular pathology of non-small cell lung cancer: A practical guide. *Am J Clin Pathol.* 2012 Sep; 138(3): 332-346.

7. Gaikwad A, Gupta A, Hare S, Gomes M, Sekhon H, Souza C, Inacio J, Lad S, Seely J. Primary adenocarcinoma of lung: A pictorial review of recent updates. *Eur J Radiol.* 2012 Dec; 81(12): 4146-4155.

8. Cancer Genome Atlas Research Network. Comprehensive molecular profiling of lung adenocarcinoma. *Nature.* 2014 Jul 31; 511(7511): 543-550. PMCID: PMC4231481.

9. Cancer Genome Atlas Research Network. Comprehensive genomic characterization of squamous cell lung cancers. *Nature.* 2012 Sep 27; 489(7417): 519-525. PMCID: PMC3466113.

10. Chen Z, Fillmore CM, Hammerman PS, Kim CF, Wong KK. Non-small-cell lung cancers: A heterogeneous set of diseases. *Nat Rev Cancer.* 2014 Aug; 14(8): 535-546.

11. Petersen I. The morphological and molecular diagnosis of lung cancer. *Dtsch Arztebl Int.* 2011 Aug; 108(31-32): 525-531. PMCID: PMC3163783.

12. Zhou C, Wu YL, Chen G, Feng J, Liu XQ, Wang C, Zhang S, Wang J, Zhou S, Ren S, Lu S, Zhang L, Hu C, Hu C, Luo Y, Chen L, Ye M, Huang J, Zhi X, Zhang Y, Xiu Q, Ma J, Zhang L, You C. Erlotinib versus chemotherapy as first-line treatment for patients with advanced EGFR mutation-positive non-small-cell lung cancer (OPTIMAL, CTONG-0802): A multicentre, open-label, randomised, phase 3 study.*Lancet Oncol.* 2011 Aug; 12(8): 735-742.

13. Rosell R, Carcereny E, Gervais R, Vergnenegre A, Massuti B, Felip E, Palmero R, Garcia-Gomez R, Pallares C, Sanchez JM, Porta R, Cobo M, Garrido P, Longo F, Moran T, Insa A, De Marinis F, Corre R, Bover I, Illiano A, Dansin E, de Castro J, Milella M, Reguart N, Altavilla G, Jimenez U, Provencio M, Moreno MA, Terrasa J, Munoz-Langa J, Valdivia J, Isla D, Domine M, Molinier O, Mazieres J, Baize N, Garcia-Campelo R, Robinet G, Rodriguez-Abreu D, Lopez-Vivanco G, Gebbia V, Ferrera-Delgado L, Bombaron P, Bernabe R, Bearz A, Artal A, Cortesi E, Rolfo C, Sanchez-Ronco M, Drozdowskyj A, Queralt C, de Aguirre I, Ramirez JL, Sanchez JJ, Molina MA, Taron M, Paz-Ares L, Spanish Lung Cancer Group in collaboration with Groupe Francais de Pneumo-Cancerologie and Associazione Italiana Oncologia Toracica. Erlotinib versus standard chemotherapy as first-line treatment for european patients with advanced EGFR mutation-positive non-small-cell lung cancer (EURTAC): A multicentre, open-label, randomised phase 3 trial. *Lancet Oncol.* 2012 Mar; 13(3): 239-246.

14. Solomon BJ, Mok T, Kim DW, Wu YL, Nakagawa K, Mekhail T, Felip E, Cappuzzo F, Paolini J, Usari T, Iyer S, Reisman A, Wilner KD, Tursi J, Blackhall F, PROFILE 1014 Investigators. First-line crizotinib versus chemotherapy in ALK-positive lung cancer. *N Engl J Med.* 2014 Dec 4; 371(23): 2167-2177.

15. Thomas A, Liu SV, Subramaniam DS, Giaccone G. Refining the treatment of NSCLC according to histological and molecular subtypes. *Nat Rev Clin Oncol.* 2015 Sep; 12(9): 511-526.

16. Janku F, Stewart DJ, Kurzrock R. Targeted therapy in non-small-cell lung cancer--is it becoming a reality? *Nat Rev Clin Oncol.* 2010 Jul; 7(7): 401-414.

17. Nguyen DX, Bos PD, Massague J. Metastasis: From dissemination to organ-specific colonization. *Nat Rev Cancer.* 2009 Apr; 9(4): 274-284.

18. Aceto N, Bardia A, Miyamoto DT, Donaldson MC, Wittner BS, Spencer JA, Yu M, Pely A, Engstrom A, Zhu H, Brannigan BW, Kapur R, Stott SL, Shioda T, Ramaswamy S, Ting DT, Lin CP, Toner M, Haber DA, Maheswaran S. Circulating tumor cell clusters are oligoclonal precursors of breast cancer metastasis. *Cell.* 2014 Aug 28; 158(5): 1110-1122. PMCID: PMC4149753.

19. Kumar M, Allison DF, Baranova NN, Wamsley JJ, Katz AJ, Bekiranov S, Jones DR, Mayo MW. NF-kappaB regulates mesenchymal transition for the

induction of non-small cell lung cancer initiating cells.*PLoS One.* 2013 Jul 30; 8(7): e68597. PMCID: PMC3728367.

20. Wamsley JJ, Kumar M, Allison DF, Clift SH, Holzknecht CM, Szymura SJ, Hoang SA, Xu X, Moskaluk CA, Jones DR, Bekiranov S, Mayo MW. Activin upregulation by NF-kappaB is required to maintain mesenchymal features of cancer stem-like cells in non-small cell lung cancer. *Cancer Res.* 2015 Jan 15; 75(2): 426-435. PMCID: PMC4297542.

21. Thiery JP. Epithelial-mesenchymal transitions in tumour progression. *Nat Rev Cancer.* 2002 Jun; 2(6): 442-454.

22. De Craene B, Berx G. Regulatory networks defining EMT during cancer initiation and progression. *Nat Rev Cancer.* 2013 Feb; 13(2): 97-110.

23. Cirri P, Chiarugi P. Cancer-associated-fibroblasts and tumour cells: A diabolic liaison driving cancer progression. *Cancer Metastasis Rev.* 2012 Jun; 31(1-2): 195-208.

24. Fuxe J, Karlsson MC. TGF-beta-induced epithelial-mesenchymal transition: A link between cancer and inflammation. *Semin Cancer Biol.* 2012 Oct; 22(5-6): 455-461.

25. Gao D, Vahdat LT, Wong S, Chang JC, Mittal V. Microenvironmental regulation of epithelial-mesenchymal transitions in cancer. *Cancer Res.* 2012 Oct 1; 72(19): 4883-4889. PMCID: PMC3649848.

26. Floor S, van Staveren WC, Larsimont D, Dumont JE, Maenhaut C. Cancer cells in epithelial-to-mesenchymal transition and tumor-propagating-cancer stem cells: Distinct, overlapping or same populations. *Oncogene.* 2011 Nov 17; 30(46): 4609-4621.

27. Heldin CH, Vanlandewijck M, Moustakas A. Regulation of EMT by TGFbeta in cancer. *FEBS Lett.* 2012 Jul 4; 586(14): 1959-1970.

28. Xu J, Lamouille S, Derynck R. TGF-beta-induced epithelial to mesenchymal transition. *Cell Res.* 2009 Feb; 19(2): 156-172. PMCID: PMC4720263.

29. Wakefield LM, Hill CS. Beyond TGFbeta: Roles of other TGFbeta superfamily members in cancer. *Nat Rev Cancer.* 2013 May; 13(5): 328-341.

30. Oshimori N, Fuchs E. The harmonies played by TGF-beta in stem cell biology. *Cell Stem Cell.* 2012 Dec 7; 11(6): 751-764. PMCID: PMC3612991.

31. Loomans HA, Andl CD. Intertwining of activin A and TGFbeta signaling: Dual roles in cancer progression and cancer cell invasion. *Cancers (Basel).* 2014 Dec 30; 7(1): 70-91. PMCID: PMC4381251.

32. Lamouille S, Xu J, Derynck R. Molecular mechanisms of epithelial-mesenchymal transition. *Nat Rev Mol Cell Biol.* 2014 Mar; 15(3): 178-196. PMCID: PMC4240281.

33. Scheel C, Weinberg RA. Cancer stem cells and epithelial-mesenchymal transition: Concepts and molecular links. *Semin Cancer Biol.* 2012 Oct; 22(5-6): 396-403.

34. Zheng X, Carstens JL, Kim J, Scheible M, Kaye J, Sugimoto H, Wu CC, LeBleu VS, Kalluri R. Epithelial-to-mesenchymal transition is dispensable for metastasis but induces chemoresistance in pancreatic cancer. *Nature.* 2015 Nov 26; 527(7579): 525-530.

35. Fischer KR, Durrans A, Lee S, Sheng J, Li F, Wong ST, Choi H, El Rayes T, Ryu S, Troeger J, Schwabe RF, Vahdat LT, Altorki NK, Mittal V, Gao D. Epithelial-to-mesenchymal transition is not required for lung metastasis but contributes to chemoresistance. *Nature.* 2015 Nov 26; 527(7579): 472-476. PMCID: PMC4662610.

36. Ye X, Tam WL, Shibue T, Kaygusuz Y, Reinhardt F, Ng Eaton E, Weinberg RA. Distinct EMT programs control normal mammary stem cells and tumour-initiating cells. *Nature.* 2015 Sep 10; 525(7568): 256-260. PMCID: PMC4764075.

37. Labelle M, Begum S, Hynes RO. Direct signaling between platelets and cancer cells induces an epithelial-mesenchymal-like transition and promotes metastasis. *Cancer Cell.* 2011 Nov 15; 20(5): 576-590. PMCID: PMC3487108.

38. Yauch RL, Januario T, Eberhard DA, Cavet G, Zhu W, Fu L, Pham TQ, Soriano R, Stinson J, Seshagiri S, Modrusan Z, Lin CY, O'Neill V, Amler LC. Epithelial versus mesenchymal phenotype determines in vitro sensitivity and predicts clinical activity of erlotinib in lung cancer patients. *Clin Cancer Res.* 2005 Dec 15; 11(24 Pt 1): 8686-8698.

39. Hasegawa Y, Takanashi S, Kanehira Y, Tsushima T, Imai T, Okumura K. Transforming growth factor-beta1 level correlates with angiogenesis, tumor progression, and prognosis in patients with nonsmall cell lung carcinoma. *Cancer.* 2001 Mar 1; 91(5): 964-971.

40. Yanagawa J, Walser TC, Zhu LX, Hong L, Fishbein MC, Mah V, Chia D, Goodglick L, Elashoff DA, Luo J, Magyar CE, Dohadwala M, Lee JM, St John MA, Strieter RM, Sharma S, Dubinett SM. Snail promotes CXCR2

ligand-dependent tumor progression in non-small cell lung carcinoma. *Clin Cancer Res.* 2009 Nov 15; 15(22): 6820-6829. PMCID: PMC2783274.

41. Ho MM, Ng AV, Lam S, Hung JY. Side population in human lung cancer cell lines and tumors is enriched with stem-like cancer cells. *Cancer Res.* 2007 May 15; 67(10): 4827-4833.

42. Shih JY, Tsai MF, Chang TH, Chang YL, Yuan A, Yu CJ, Lin SB, Liou GY, Lee ML, Chen JJ, Hong TM, Yang SC, Su JL, Lee YC, Yang PC. Transcription repressor slug promotes carcinoma invasion and predicts outcome of patients with lung adenocarcinoma. *Clin Cancer Res.* 2005 Nov 15; 11(22): 8070-8078.

43. Al-Saad S, Al-Shibli K, Donnem T, Persson M, Bremnes RM, Busund LT. The prognostic impact of NF-kappaB p105, vimentin, E-cadherin and Par6 expression in epithelial and stromal compartment in non-small-cell lung cancer. *Br J Cancer.* 2008 Nov 4; 99(9): 1476-1483. PMCID: PMC2579693.

44. Kase S, Sugio K, Yamazaki K, Okamoto T, Yano T, Sugimachi K. Expression of E-cadherin and beta-catenin in human non-small cell lung cancer and the clinical significance. *Clin Cancer Res.* 2000 Dec; 6(12): 4789-4796.

45. Li F, Zeng H, Ying K. The combination of stem cell markers CD133 and ABCG2 predicts relapse in stage I non-small cell lung carcinomas. *Med Oncol.* 2011 Dec; 28(4): 1458-1462.

46. Chiou SH, Wang ML, Chou YT, Chen CJ, Hong CF, Hsieh WJ, Chang HT, Chen YS, Lin TW, Hsu HS, Wu CW. Coexpression of Oct4 and nanog enhances malignancy in lung adenocarcinoma by inducing cancer stem cell-like properties and epithelial-mesenchymal transdifferentiation. *Cancer Res.* 2010 Dec 15; 70(24): 10433-10444.

47. Kroemer G, Pouyssegur J. Tumor cell metabolism: Cancer's achilles' heel. *Cancer Cell.* 2008 Jun; 13(6): 472-482.

48. Cairns RA, Harris IS, Mak TW. Regulation of cancer cell metabolism. *Nat Rev Cancer.* 2011 Feb; 11(2): 85-95.

49. Vander Heiden MG, Cantley LC, Thompson CB. Understanding the warburg effect: The metabolic requirements of cell proliferation. *Science.* 2009 May 22; 324(5930): 1029-1033. PMCID: PMC2849637.

50. DeBerardinis RJ, Lum JJ, Hatzivassiliou G, Thompson CB. The biology of cancer: Metabolic reprogramming fuels cell growth and proliferation. *Cell Metab.* 2008 Jan; 7(1): 11-20.

51. Tennant DA, Duran RV, Gottlieb E. Targeting metabolic transformation for cancer therapy. *Nat Rev Cancer.* 2010 Apr; 10(4): 267-277.

52. Mikawa T, LLeonart ME, Takaori-Kondo A, Inagaki N, Yokode M, Kondoh H. Dysregulated glycolysis as an oncogenic event. *Cell Mol Life Sci.* 2015 May; 72(10): 1881-1892.

53. Koppenol WH, Bounds PL, Dang CV. Otto warburg's contributions to current concepts of cancer metabolism. *Nat Rev Cancer.* 2011 May; 11(5): 325-337.

54. Gatenby RA, Gillies RJ. Why do cancers have high aerobic glycolysis? *Nat Rev Cancer.* 2004 Nov; 4(11): 891-899.

55. Hensley CT, Wasti AT, DeBerardinis RJ. Glutamine and cancer: Cell biology, physiology, and clinical opportunities. *J Clin Invest.* 2013 Sep; 123(9): 3678-3684. PMCID: PMC3754270.

56. Lukey MJ, Wilson KF, Cerione RA. Therapeutic strategies impacting cancer cell glutamine metabolism. *Future Med Chem.* 2013 Sep; 5(14): 1685-1700. PMCID: PMC4154374.

57. Blum R, Kloog Y. Metabolism addiction in pancreatic cancer. *Cell Death Dis.* 2014 Feb 20; 5: e1065. PMCID: PMC3944253.

58. Kang JG, Park SY, Ji S, Jang I, Park S, Kim HS, Kim SM, Yook JI, Park YI, Roth J, Cho JW. O-GlcNAc protein modification in cancer cells increases in response to glucose deprivation through glycogen degradation. *J Biol Chem.* 2009 Dec 11; 284(50): 34777-34784. PMCID: PMC2787340.

59. Wang JB, Erickson JW, Fuji R, Ramachandran S, Gao P, Dinavahi R, Wilson KF, Ambrosio AL, Dias SM, Dang CV, Cerione RA. Targeting mitochondrial glutaminase activity inhibits oncogenic transformation. *Cancer Cell.* 2010 Sep 14; 18(3): 207-219. PMCID: PMC3078749.

60. Yuneva M, Zamboni N, Oefner P, Sachidanandam R, Lazebnik Y. Deficiency in glutamine but not glucose induces MYC-dependent apoptosis in human cells. *J Cell Biol.* 2007 Jul 2; 178(1): 93-105. PMCID: PMC2064426.

61. Palorini R, Cammarata FP, Balestrieri C, Monestiroli A, Vasso M, Gelfi C, Alberghina L, Chiaradonna F. Glucose starvation induces cell death in K-ras-transformed cells by interfering with the hexosamine biosynthesis pathway and activating the unfolded protein response. *Cell Death Dis.* 2013 Jul 18; 4: e732. PMCID: PMC3730427.

62. El Mjiyad N, Caro-Maldonado A, Ramirez-Peinado S, Munoz-Pinedo C. Sugar-free approaches to cancer cell killing. *Oncogene.* 2011 Jan 20; 30(3): 253-264.

63. Vander Heiden MG. Targeting cancer metabolism: A therapeutic window opens. *Nat Rev Drug Discov.* 2011 Aug 31; 10(9): 671-684.

64. Pernicova I, Korbonits M. Metformin--mode of action and clinical implications for diabetes and cancer. *Nat Rev Endocrinol.* 2014 Mar; 10(3): 143-156.

65. Abdel Rahman AM, Ryczko M, Pawling J, Dennis JW. Probing the hexosamine biosynthetic pathway in human tumor cells by multitargeted tandem mass spectrometry. *ACS Chem Biol.* 2013 Sep 20; 8(9): 2053-2062.

66. Hanover JA, Krause MW, Love DC. The hexosamine signaling pathway: O-GlcNAc cycling in feast or famine. *Biochim Biophys Acta.* 2010 Feb; 1800(2): 80-95. PMCID: PMC2815088.

67. Metallo CM, Vander Heiden MG. Metabolism strikes back: Metabolic flux regulates cell signaling. *Genes Dev.* 2010 Dec 15; 24(24): 2717-2722. PMCID: PMC3003187.

68. KORNFELD S, KORNFELD R, NEUFELD EF, O'BRIEN PJ. The feedback control of sugar nucleotide biosynthesis in liver. *Proc Natl Acad Sci U S A.* 1964 Aug; 52: 371-379. PMCID: PMC300286.

69. Marshall S, Nadeau O, Yamasaki K. Dynamic actions of glucose and glucosamine on hexosamine biosynthesis in isolated adipocytes: Differential effects on glucosamine 6-phosphate, UDP-N-acetylglucosamine, and ATP levels. *J Biol Chem.* 2004 Aug 20; 279(34): 35313-35319.

70. Miyagi T, Tsuiki S. Effect of phosphoglucose isomerase and glucose 6-phosphate on UDP-N-acetylglucosamine inhibition of L-glutamine-D-fructose 6-phosphate aminotransferase. *Biochim Biophys Acta.*1971 Oct; 250(1): 51-62.

71. Benson RL, Friedman S. Allosteric control of glucosamine phosphate isomerase from the adult housefly and its role in the synthesis of glucosamine 6-phosphate. *J Biol Chem.* 1970 May 10; 245(9): 2219-2228.

72. Kornfeld R. Studies on L-glutamine D-fructose 6-phosphate amidotransferase. I. feedback inhibition by uridine diphosphate-N-acetylglucosamine. *J Biol Chem.* 1967 Jul 10; 242(13): 3135-3141.

73. Endo A, Kakiki K, Misato T. Feedback inhibition of L-glutamine D-fructose 6-phosphate amidotransferase by uridine diphosphate N-acetylglucosamine

in neurospora crassa. *J Bacteriol.* 1970 Sep; 103(3): 588-594. PMCID: PMC248130.

74. Ellis DB, Sommar KM. Regulation of L-glutamine:D-fructose-6-phosphate aminotransferase activity in bovine trachea. *Biochim Biophys Acta.* 1971; 230(3): 531-534

75. Broschat KO, Gorka C, Page JD, Martin-Berger CL, Davies MS, Huang Hc HC, Gulve EA, Salsgiver WJ, Kasten TP. Kinetic characterization of human glutamine-fructose-6-phosphate amidotransferase I: Potent feedback inhibition by glucosamine 6-phosphate. *J Biol Chem.* 2002 Apr 26; 277(17): 14764-14770.

76. Graack HR, Cinque U, Kress H. Functional regulation of glutamine:Fructose-6-phosphate aminotransferase 1 (GFAT1) of drosophila melanogaster in a UDP-N-acetylglucosamine and cAMP-dependent manner. *Biochem J.* 2001 Dec 1; 360(Pt 2): 401-412. PMCID: PMC1222241.

77. Durand P, Golinelli-Pimpaneau B, Mouilleron S, Badet B, Badet-Denisot MA. Highlights of glucosamine-6P synthase catalysis. *Arch Biochem Biophys.* 2008 Jun 15; 474(2): 302-317.

78. Schleicher ED, Weigert C. Role of the hexosamine biosynthetic pathway in diabetic nephropathy. *Kidney Int Suppl.* 2000 Sep; 77: S13-8.

79. Chang Q, Su K, Baker JR, Yang X, Paterson AJ, Kudlow JE. Phosphorylation of human glutamine:Fructose-6-phosphate amidotransferase by cAMP-dependent protein kinase at serine 205 blocks the enzyme activity. *J Biol Chem.* 2000 Jul 21; 275(29): 21981-21987.

80. Eguchi S, Oshiro N, Miyamoto T, Yoshino K, Okamoto S, Ono T, Kikkawa U, Yonezawa K. AMP-activated protein kinase phosphorylates glutamine : Fructose-6-phosphate amidotransferase 1 at Ser243 to modulate its enzymatic activity. *Genes Cells.* 2009 Feb; 14(2): 179-189

81. Hu Y, Riesland L, Paterson AJ, Kudlow JE. Phosphorylation of mouse glutamine-fructose-6-phosphate amidotransferase 2 (GFAT2) by cAMP-dependent protein kinase increases the enzyme activity. *J Biol Chem.* 2004 Jul 16; 279(29): 29988-29993.

82. Boehmelt G, Wakeham A, Elia A, Sasaki T, Plyte S, Potter J, Yang Y, Tsang E, Ruland J, Iscove NN, Dennis JW, Mak TW. Decreased UDP-GlcNAc levels abrogate proliferation control in EMeg32-deficient cells. *EMBO J.* 2000 Oct 2; 19(19): 5092-5104. PMCID: PMC302091.

83. Russell PJ, Srb AM. A study of L-glutamine: D-fructose 6-phosphate amidotransferase in certain developmental mutants of neurospora crassa. *Mol Gen Genet.* 1974 Mar 6; 129(1): 77-86.

84. Greig KT, Antonchuk J, Metcalf D, Morgan PO, Krebs DL, Zhang JG, Hacking DF, Bode L, Robb L, Kranz C, de Graaf C, Bahlo M, Nicola NA, Nutt SL, Freeze HH, Alexander WS, Hilton DJ, Kile BT. Agm1/Pgm3-mediated sugar nucleotide synthesis is essential for hematopoiesis and development. *Mol Cell Biol.* 2007 Aug; 27(16): 5849-5859. PMCID: PMC1952135.

85. Itkonen HM, Engedal N, Babaie E, Luhr M, Guldvik IJ, Minner S, Hohloch J, Tsourlakis MC, Schlomm T, Mills IG. UAP1 is overexpressed in prostate cancer and is protective against inhibitors of N-linked glycosylation. *Oncogene.* 2015 Jul; 34(28): 3744-3750.

86. Sayeski PP, Wang D, Su K, Han IO, Kudlow JE. Cloning and partial characterization of the mouse glutamine:Fructose-6-phosphate amidotransferase (GFAT) gene promoter. *Nucleic Acids Res.* 1997 Apr 1; 25(7): 1458-1466. PMCID: PMC146605

87. Yamazaki K, Mizui Y, Oki T, Okada M, Tanaka I. Cloning and characterization of mouse glutamine:Fructose-6-phosphate amidotransferase 2 gene promoter. *Gene.* 2000 Dec 31; 261(2): 329-336.

88. Paterson AJ, Kudlow JE. Regulation of glutamine:Fructose-6-phosphate amidotransferase gene transcription by epidermal growth factor and glucose. *Endocrinology.* 1995 Jul; 136(7): 2809-2816.

89. Ying H, Kimmelman AC, Lyssiotis CA, Hua S, Chu GC, Fletcher-Sananikone E, Locasale JW, Son J, Zhang H, Coloff JL, Yan H, Wang W, Chen S, Viale A, Zheng H, Paik JH, Lim C, Guimaraes AR, Martin ES, Chang J, Hezel AF, Perry SR, Hu J, Gan B, Xiao Y, Asara JM, Weissleder R, Wang YA, Chin L, Cantley LC, DePinho RA. Oncogenic kras maintains pancreatic tumors through regulation of anabolic glucose metabolism. *Cell.* 2012 Apr 27; 149(3): 656-670. PMCID: PMC3472002.

90. Guillaumond F, Leca J, Olivares O, Lavaut MN, Vidal N, Berthezene P, Dusetti NJ, Loncle C, Calvo E, Turrini O, Iovanna JL, Tomasini R, Vasseur S. Strengthened glycolysis under hypoxia supports tumor symbiosis and hexosamine biosynthesis in pancreatic adenocarcinoma. *Proc Natl Acad Sci U S A.* 2013 Mar 5; 110(10): 3919-3924. PMCID: PMC3593894

91. Denzel MS, Storm NJ, Gutschmidt A, Baddi R, Hinze Y, Jarosch E, Sommer T, Hoppe T, Antebi A. Hexosamine pathway metabolites enhance protein quality control and prolong life. *Cell.* 2014 Mar 13; 156(6): 1167-1178.

92. Wang ZV, Deng Y, Gao N, Pedrozo Z, Li DL, Morales CR, Criollo A, Luo X, Tan W, Jiang N, Lehrman MA, Rothermel BA, Lee AH, Lavandero S, Mammen PP, Ferdous A, Gillette TG, Scherer PE, Hill JA. Spliced X-box binding protein 1 couples the unfolded protein response to hexosamine biosynthetic pathway. *Cell.* 2014 Mar 13; 156(6): 1179-1192. PMCID: PMC3959665.

93. Zitzler J, Link D, Schafer R, Liebetrau W, Kazinski M, Bonin-Debs A, Behl C, Buckel P, Brinkmann U. High-throughput functional genomics identifies genes that ameliorate toxicity due to oxidative stress in neuronal HT-22 cells: GFPT2 protects cells against peroxide. *Mol Cell Proteomics.* 2004 Aug; 3(8): 834-840.

94. Verbovsek U, Motaln H, Rotter A, Atai NA, Gruden K, Van Noorden CJ, Lah TT. Expression analysis of all protease genes reveals cathepsin K to be overexpressed in glioblastoma. *PLoS One.* 2014 Oct 30; 9(10): e111819. PMCID: PMC4214761.

95. Miura N, Kaneko S, Hosoya S, Furuchi T, Miura K, Kuge S, Naganuma A. Overexpression of L-glutamine:D-fructose-6-phosphate amidotransferase provides resistance to methylmercury in saccharomyces cerevisiae. *FEBS Lett.* 1999 Sep 17; 458(2): 215-218.

96. Hebert LF,Jr, Daniels MC, Zhou J, Crook ED, Turner RL, Simmons ST, Neidigh JL, Zhu JS, Baron AD, McClain DA. Overexpression of glutamine:Fructose-6-phosphate amidotransferase in transgenic mice leads to insulin resistance. *J Clin Invest.* 1996 Aug 15; 98(4): 930-936. PMCID: PMC507507.

97. Zhang H, Jia Y, Cooper JJ, Hale T, Zhang Z, Elbein SC. Common variants in glutamine:Fructose-6-phosphate amidotransferase 2 (GFPT2) gene are associated with type 2 diabetes, diabetic nephropathy, and increased GFPT2 mRNA levels. *J Clin Endocrinol Metab.* 2004 Feb; 89(2): 748-755.

98. Elbein SC, Zheng H, Jia Y, Chu W, Cooper JJ, Hale T, Zhang Z. Molecular screening of the human glutamine-fructose-6-phosphate amidotransferase 1 (GFPT1) gene and association studies with diabetes and diabetic nephropathy. *Mol Genet Metab.* 2004 Aug; 82(4): 321-328.

99. Srinivasan V, Sandhya N, Sampathkumar R, Farooq S, Mohan V, Balasubramanyam M. Glutamine fructose-6-phosphate amidotransferase (GFAT) gene expression and activity in patients with type 2 diabetes: Inter-relationships with hyperglycaemia and oxidative stress. *Clin Biochem.* 2007 Sep; 40(13-14): 952-957.

100. Simpson NE, Tryndyak VP, Beland FA, Pogribny IP. An in vitro investigation of metabolically sensitive biomarkers in breast cancer progression. *Breast Cancer Res Treat.* 2012 Jun; 133(3): 959-968.

101. Shaul YD, Freinkman E, Comb WC, Cantor JR, Tam WL, Thiru P, Kim D, Kanarek N, Pacold ME, Chen WW, Bierie B, Possemato R, Reinhardt F, Weinberg RA, Yaffe MB, Sabatini DM. Dihydropyrimidine accumulation is required for the epithelial-mesenchymal transition. *Cell.* 2014 Aug 28; 158(5): 1094-1109. PMCID: PMC4250222.

102. Chen SC, Huang CH, Lai SJ, Yang CS, Hsiao TH, Lin CH, Fu PK, Ko TP, Chen Y. Mechanism and inhibition of human UDP-GlcNAc 2-epimerase, the key enzyme in sialic acid biosynthesis. *Sci Rep.* 2016 Mar 16; 6: 23274. PMCID: PMC4793188.

103. Schulz JM, Watson AL, Sanders R, Ross KL, Thoden JB, Holden HM, Fridovich-Keil JL. Determinants of function and substrate specificity in human UDP-galactose 4'-epimerase. *J Biol Chem.* 2004 Jul 30; 279(31): 32796-32803.

104. Bulow HE, Hobert O. The molecular diversity of glycosaminoglycans shapes animal development. *Annu Rev Cell Dev Biol.* 2006; 22: 375-407.

105. Zoller M. CD44: Can a cancer-initiating cell profit from an abundantly expressed molecule? *Nat Rev Cancer.* 2011 Apr; 11(4): 254-267.

106. Ponta H, Sherman L, Herrlich PA. CD44: From adhesion molecules to signalling regulators. *Nat Rev Mol Cell Biol.* 2003 Jan; 4(1): 33-45.

107. Stern R. Hyaluronidases in cancer biology. *Semin Cancer Biol.* 2008 Aug; 18(4): 275-280.

108. Ijuin C, Ohno S, Tanimoto K, Honda K, Tanne K. Regulation of hyaluronan synthase gene expression in human periodontal ligament cells by tumour necrosis factor-alpha, interleukin-1beta and interferon-gamma. *Arch Oral Biol.* 2001 Aug; 46(8): 767-772.

109. Kosher RA, Savage MP. Glycosaminoglycan synthesis by the apical ectodermal ridge of chick limb bud. *Nature.* 1981 May 21; 291(5812): 231-232.

110. Verna JM, Fichard A, Saxod R. Influence of glycosaminoglycans on neurite morphology and outgrowth patterns in vitro. *Int J Dev Neurosci.* 1989; 7(4): 389-399.

111. Adamia S, Maxwell CA, Pilarski LM. Hyaluronan and hyaluronan synthases: Potential therapeutic targets in cancer. *Curr Drug Targets Cardiovasc Haematol Disord.* 2005 Feb; 5(1): 3-14.

112. Toole BP. Hyaluronan: From extracellular glue to pericellular cue. *Nat Rev Cancer.* 2004 Jul; 4(7): 528-539.

113. Itano N, Kimata K. Altered hyaluronan biosynthesis in cancer progression. *Semin Cancer Biol.* 2008 Aug; 18(4): 268-274.

114. Ponting J, Howell A, Pye D, Kumar S. Prognostic relevance of serum hyaluronan levels in patients with breast cancer. *Int J Cancer.* 1992 Dec 2; 52(6): 873-876.

115. Ropponen K, Tammi M, Parkkinen J, Eskelinen M, Tammi R, Lipponen P, Agren U, Alhava E, Kosma VM. Tumor cell-associated hyaluronan as an unfavorable prognostic factor in colorectal cancer. *Cancer Res.* 1998 Jan 15; 58(2): 342-347.

116. Tammi RH, Kultti A, Kosma VM, Pirinen R, Auvinen P, Tammi MI. Hyaluronan in human tumors: Pathobiological and prognostic messages from cell-associated and stromal hyaluronan. *Semin Cancer Biol.* 2008 Aug; 18(4): 288-295.

117. Kosaki R, Watanabe K, Yamaguchi Y. Overproduction of hyaluronan by expression of the hyaluronan synthase Has2 enhances anchorage-independent growth and tumorigenicity. *Cancer Res.* 1999 Mar 1; 59(5): 1141-1145.

118. Itano N, Sawai T, Miyaishi O, Kimata K. Relationship between hyaluronan production and metastatic potential of mouse mammary carcinoma cells. *Cancer Res.* 1999 May 15; 59(10): 2499-2504.

119. Liu N, Gao F, Han Z, Xu X, Underhill CB, Zhang L. Hyaluronan synthase 3 overexpression promotes the growth of TSU prostate cancer cells. *Cancer Res.* 2001 Jul 1; 61(13): 5207-5214.

120. Jacobson A, Rahmanian M, Rubin K, Heldin P. Expression of hyaluronan synthase 2 or hyaluronidase 1 differentially affect the growth rate of transplantable colon carcinoma cell tumors. *Int J Cancer.*2002 Nov 20; 102(3): 212-219.

121. Bourguignon LY, Peyrollier K, Gilad E, Brightman A. Hyaluronan-CD44 interaction with neural wiskott-aldrich syndrome protein (N-WASP) promotes actin polymerization and ErbB2 activation leading to beta-catenin nuclear translocation, transcriptional up-regulation, and cell migration in ovarian tumor cells. *J Biol Chem.* 2007 Jan 12; 282(2): 1265-1280.

122. Bourguignon LY, Spevak CC, Wong G, Xia W, Gilad E. Hyaluronan-CD44 interaction with protein kinase C(epsilon) promotes oncogenic signaling by the stem cell marker nanog and the production of microRNA-21, leading to down-regulation of the tumor suppressor protein PDCD4, anti-apoptosis, and chemotherapy resistance in breast tumor cells. *J Biol Chem.* 2009 Sep 25; 284(39): 26533-26546. PMCID: PMC2785342.

123. Bourguignon LY, Peyrollier K, Xia W, Gilad E. Hyaluronan-CD44 interaction activates stem cell marker nanog, stat-3-mediated MDR1 gene expression, and ankyrin-regulated multidrug efflux in breast and ovarian tumor cells. *J Biol Chem.* 2008 Jun 20; 283(25): 17635-17651. PMCID: PMC2427357.

124. Bourguignon LY, Gilad E, Brightman A, Diedrich F, Singleton P. Hyaluronan-CD44 interaction with leukemia-associated RhoGEF and epidermal growth factor receptor promotes Rho/Ras co-activation, phospholipase C epsilon-Ca2+ signaling, and cytoskeleton modification in head and neck squamous cell carcinoma cells. *J Biol Chem.* 2006 May 19; 281(20): 14026-14040.

125. Bourguignon LY, Wong G, Earle C, Krueger K, Spevak CC. Hyaluronan-CD44 interaction promotes c-src-mediated twist signaling, microRNA-10b expression, and RhoA/RhoC up-regulation, leading to rho-kinase-associated cytoskeleton activation and breast tumor cell invasion. *J Biol Chem.* 2010 Nov 19; 285(47): 36721-36735. PMCID: PMC2978601.

126. Bourguignon LY, Wong G, Earle C, Chen L. Hyaluronan-CD44v3 interaction with Oct4-Sox2-nanog promotes miR-302 expression leading to self-renewal, clonal formation, and cisplatin resistance in cancer stem cells from head and neck squamous cell carcinoma. *J Biol Chem.* 2012 Sep 21; 287(39): 32800-32824. PMCID: PMC3463333.

127. Bourguignon LY, Earle C, Wong G, Spevak CC, Krueger K. Stem cell marker (nanog) and stat-3 signaling promote MicroRNA-21 expression and chemoresistance in hyaluronan/CD44-activated head and neck squamous cell carcinoma cells. *Oncogene.* 2012 Jan 12; 31(2): 149-160. PMCID: PMC3179812.

128. Bourguignon LY, Singleton PA, Zhu H, Diedrich F. Hyaluronan-mediated CD44 interaction with RhoGEF and rho kinase promotes Grb2-associated binder-1 phosphorylation and phosphatidylinositol 3-kinase signaling leading to cytokine (macrophage-colony stimulating factor) production and breast tumor progression. *J Biol Chem.* 2003 Aug 8; 278(32): 29420-29434.

129. Bourguignon LY, Zhu H, Shao L, Chen YW. CD44 interaction with c-src kinase promotes cortactin-mediated cytoskeleton function and hyaluronic acid-dependent ovarian tumor cell migration. *J Biol Chem.* 2001 Mar 9; 276(10): 7327-7336.

130. Bourguignon LY, Zhu H, Shao L, Chen YW. CD44 interaction with tiam1 promotes Rac1 signaling and hyaluronic acid-mediated breast tumor cell migration. *J Biol Chem.* 2000 Jan 21; 275(3): 1829-1838.

131. Bourguignon LY, Zhu H, Zhou B, Diedrich F, Singleton PA, Hung MC. Hyaluronan promotes CD44v3-Vav2 interaction with Grb2-p185(HER2) and

induces Rac1 and ras signaling during ovarian tumor cell migration and growth. *J Biol Chem.* 2001 Dec 28; 276(52): 48679-48692.

132. Bernert B, Porsch H, Heldin P. Hyaluronan synthase 2 (HAS2) promotes breast cancer cell invasion by suppression of tissue metalloproteinase inhibitor 1 (TIMP-1). *J Biol Chem.* 2011 Dec 9; 286(49): 42349-42359. PMCID: PMC3234988.

133. Bourguignon LY, Singleton PA, Diedrich F, Stern R, Gilad E. CD44 interaction with Na+-H+ exchanger (NHE1) creates acidic microenvironments leading to hyaluronidase-2 and cathepsin B activation and breast tumor cell invasion. *J Biol Chem.* 2004 Jun 25; 279(26): 26991-27007.

134. Takahashi E, Nagano O, Ishimoto T, Yae T, Suzuki Y, Shinoda T, Nakamura S, Niwa S, Ikeda S, Koga H, Tanihara H, Saya H. Tumor necrosis factor-alpha regulates transforming growth factor-beta-dependent epithelial-mesenchymal transition by promoting hyaluronan-CD44-moesin interaction. *J Biol Chem.* 2010 Feb 5; 285(6): 4060-4073. PMCID: PMC2823547.

135. Kuang DM, Wu Y, Chen N, Cheng J, Zhuang SM, Zheng L. Tumor-derived hyaluronan induces formation of immunosuppressive macrophages through transient early activation of monocytes. *Blood.*2007 Jul 15; 110(2): 587-595.

136. Koyama H, Hibi T, Isogai Z, Yoneda M, Fujimori M, Amano J, Kawakubo M, Kannagi R, Kimata K, Taniguchi S, Itano N. Hyperproduction of hyaluronan in neu-induced mammary tumor accelerates angiogenesis through stromal cell recruitment: Possible involvement of versican/PG-M. *Am J Pathol.* 2007 Mar; 170(3): 1086-1099. PMCID: PMC1864876.

137. Siiskonen H, Karna R, Hyttinen JM, Tammi RH, Tammi MI, Rilla K. Hyaluronan synthase 1 (HAS1) produces a cytokine-and glucose-inducible, CD44-dependent cell surface coat. *Exp Cell Res.* 2014 Jan 1; 320(1): 153-163.

138. 99. Jokela TA, Makkonen KM, Oikari S, Karna R, Koli E, Hart GW, Tammi RH, Carlberg C, Tammi MI. Cellular content of UDP-N-acetylhexosamines controls hyaluronan synthase 2 expression and correlates with O-linked N-acetylglucosamine modification of transcription factors YY1 and SP1. *J Biol Chem.* 2011 Sep 23; 286(38): 33632-33640. PMCID: PMC3190925.

139. Rilla K, Oikari S, Jokela TA, Hyttinen JM, Karna R, Tammi RH, Tammi MI. Hyaluronan synthase 1 (HAS1) requires higher cellular UDP-GlcNAc concentration than HAS2 and HAS3. *J Biol Chem.* 2013 Feb 22; 288(8): 5973-5983. PMCID: PMC3581382.

140. Vigetti D, Deleonibus S, Moretto P, Karousou E, Viola M, Bartolini B, Hascall VC, Tammi M, De Luca G, Passi A. Role of UDP-N-acetylglucosamine (GlcNAc) and O-GlcNAcylation of hyaluronan synthase 2 in the control of chondroitin sulfate and hyaluronan synthesis. *J Biol Chem.* 2012 Oct 12; 287(42): 35544-35555. PMCID: PMC3471761.

141. Knudson W, Chow G, Knudson CB. CD44-mediated uptake and degradation of hyaluronan. *Matrix Biol.* 2002 Jan; 21(1): 15-23.

142. Hascall VC, Wang A, Tammi M, Oikari S, Tammi R, Passi A, Vigetti D, Hanson RW, Hart GW. The dynamic metabolism of hyaluronan regulates the cytosolic concentration of UDP-GlcNAc. *Matrix Biol.* 2014 Apr; 35: 14-17. PMCID: PMC4039572.

143. Moremen KW, Tiemeyer M, Nairn AV. Vertebrate protein glycosylation: Diversity, synthesis and function. *Nat Rev Mol Cell Biol.* 2012 Jun 22; 13(7): 448-462. PMCID: PMC3934011.

144. Stowell SR, Ju T, Cummings RD. Protein glycosylation in cancer. *Annu Rev Pathol.* 2015; 10: 473-510. PMCID: PMC4396820.

145. Hollingsworth MA, Swanson BJ. Mucins in cancer: Protection and control of the cell surface. *Nat Rev Cancer.* 2004 Jan; 4(1): 45-60.

146. Pinho SS, Reis CA. Glycosylation in cancer: Mechanisms and clinical implications. *Nat Rev Cancer.* 2015 Sep; 15(9): 540-555.

147. Mendelsohn R, Cheung P, Berger L, Partridge E, Lau K, Datti A, Pawling J, Dennis JW. Complex N-glycan and metabolic control in tumor cells. *Cancer Res.* 2007 Oct 15; 67(20): 9771-9780.

148. Lau KS, Dennis JW. N-glycans in cancer progression. *Glycobiology.* 2008 Oct; 18(10): 750-760.

149. Granovsky M, Fata J, Pawling J, Muller WJ, Khokha R, Dennis JW. Suppression of tumor growth and metastasis in Mgat5-deficient mice. *Nat Med.* 2000 Mar; 6(3): 306-312.

150. Croci DO, Cerliani JP, Dalotto-Moreno T, Mendez-Huergo SP, Mascanfroni ID, Dergan-Dylon S, Toscano MA, Caramelo JJ, Garcia-Vallejo JJ, Ouyang J, Mesri EA, Junttila MR, Bais C, Shipp MA, Salatino M, Rabinovich GA. Glycosylation-dependent lectin-receptor interactions preserve angiogenesis in anti-VEGF refractory tumors. *Cell.* 2014 Feb 13; 156(4): 744-758.

151. Pinho SS, Oliveira P, Cabral J, Carvalho S, Huntsman D, Gartner F, Seruca R, Reis CA, Oliveira C. Loss and recovery of Mgat3 and GnT-III mediated E-cadherin N-glycosylation is a mechanism involved in epithelial-

mesenchymal-epithelial transitions. *PLoS One.* 2012; 7(3): e33191. PMCID: PMC3302839.

152. Xu Q, Isaji T, Lu Y, Gu W, Kondo M, Fukuda T, Du Y, Gu J. Roles of N-acetylglucosaminyltransferase III in epithelial-to-mesenchymal transition induced by transforming growth factor beta1 (TGF-beta1) in epithelial cell lines. *J Biol Chem.* 2012 May 11; 287(20): 16563-16574. PMCID: PMC3351319.

153. Xu Q, Akama R, Isaji T, Lu Y, Hashimoto H, Kariya Y, Fukuda T, Du Y, Gu J. Wnt/beta-catenin signaling down-regulates N-acetylglucosaminyltransferase III expression: The implications of two mutually exclusive pathways for regulation. *J Biol Chem.* 2011 Feb 11; 286(6): 4310-4318. PMCID: PMC3039325.

154. Sasai K, Ikeda Y, Fujii T, Tsuda T, Taniguchi N. UDP-GlcNAc concentration is an important factor in the biosynthesis of beta1,6-branched oligosaccharides: Regulation based on the kinetic properties of N-acetylglucosaminyltransferase V. *Glycobiology.* 2002 Feb; 12(2): 119-127.

155. Wellen KE, Lu C, Mancuso A, Lemons JM, Ryczko M, Dennis JW, Rabinowitz JD, Coller HA, Thompson CB. The hexosamine biosynthetic pathway couples growth factor-induced glutamine uptake to glucose metabolism. *Genes Dev.* 2010 Dec 15; 24(24): 2784-2799. PMCID: PMC3003197.

156. Fang M, Shen Z, Huang S, Zhao L, Chen S, Mak TW, Wang X. The ER UDPase ENTPD5 promotes protein N-glycosylation, the warburg effect, and proliferation in the PTEN pathway. *Cell.* 2010 Nov 24; 143(5): 711-724.

157. Ohtsubo K, Takamatsu S, Minowa MT, Yoshida A, Takeuchi M, Marth JD. Dietary and genetic control of glucose transporter 2 glycosylation promotes insulin secretion in suppressing diabetes. *Cell.* 2005 Dec 29; 123(7): 1307-1321.

158. Wells L, Vosseller K, Hart GW. Glycosylation of nucleocytoplasmic proteins: Signal transduction and O-GlcNAc. *Science.* 2001 Mar 23; 291(5512): 2376-2378.

159. Bond MR, Hanover JA. O-GlcNAc cycling: A link between metabolism and chronic disease. *Annu Rev Nutr.* 2013; 33: 205-229.

160. Shafi R, Iyer SP, Ellies LG, O'Donnell N, Marek KW, Chui D, Hart GW, Marth JD. The O-GlcNAc transferase gene resides on the X chromosome and is essential for embryonic stem cell viability and mouse ontogeny. *Proc Natl Acad Sci U S A.* 2000 May 23; 97(11): 5735-5739. PMCID: PMC18502.

161. Keembiyehetty C, Love DC, Harwood KR, Gavrilova O, Comly ME, Hanover JA. Conditional knock-out reveals a requirement for O-linked N-acetylglucosaminase (O-GlcNAcase) in metabolic homeostasis. *J Biol Chem.* 2015 Mar 13; 290(11): 7097-7113. PMCID: PMC4358131.

162. Janetzko J, Walker S. The making of a sweet modification: Structure and function of O-GlcNAc transferase. *J Biol Chem.* 2014 Dec 12; 289(50): 34424-34432. PMCID: PMC4263849.

163. Yang X, Ongusaha PP, Miles PD, Havstad JC, Zhang F, So WV, Kudlow JE, Michell RH, Olefsky JM, Field SJ, Evans RM. Phosphoinositide signalling links O-GlcNAc transferase to insulin resistance. *Nature.*2008 Feb 21; 451(7181): 964-969.

164. Lazarus MB, Jiang J, Kapuria V, Bhuiyan T, Janetzko J, Zandberg WF, Vocadlo DJ, Herr W, Walker S. HCF-1 is cleaved in the active site of O-GlcNAc transferase. *Science.* 2013 Dec 6; 342(6163): 1235-1239. PMCID: PMC3930058.

165. Bond MR, Hanover JA. A little sugar goes a long way: The cell biology of O-GlcNAc. *J Cell Biol.* 2015 Mar 30; 208(7): 869-880. PMCID: PMC4384737.

166. Bullen JW, Balsbaugh JL, Chanda D, Shabanowitz J, Hunt DF, Neumann D, Hart GW. Cross-talk between two essential nutrient-sensitive enzymes: O-GlcNAc transferase (OGT) and AMP-activated protein kinase (AMPK). *J Biol Chem.* 2014 Apr 11; 289(15): 10592-10606. PMCID: PMC4036179.

167. Butkinaree C, Park K, Hart GW. O-linked beta-N-acetylglucosamine (O-GlcNAc): Extensive crosstalk with phosphorylation to regulate signaling and transcription in response to nutrients and stress.*Biochim Biophys Acta.* 2010 Feb; 1800(2): 96-106. PMCID: PMC2815129.

168. Ghabrial AS. A sweet spot in the FGFR signal transduction pathway. *Sci Signal.* 2012 Jan 17; 5(207): pe1. PMCID: PMC3362922.

169. Zachara NE, O'Donnell N, Cheung WD, Mercer JJ, Marth JD, Hart GW. Dynamic O-GlcNAc modification of nucleocytoplasmic proteins in response to stress. A survival response of mammalian cells. *J Biol Chem.* 2004 Jul 16; 279(29): 30133-30142.

170. Pathak S, Borodkin VS, Albarbarawi O, Campbell DG, Ibrahim A, van Aalten DM. O-GlcNAcylation of TAB1 modulates TAK1-mediated cytokine release. *EMBO J.* 2012 Mar 21; 31(6): 1394-1404. PMCID: PMC3321193.

171. Ma Z, Vosseller K. O-GlcNAc in cancer biology. *Amino Acids.* 2013 Oct; 45(4): 719-733.

172. Li Z, Yi W. Regulation of cancer metabolism by O-GlcNAcylation. *Glycoconj J.* 2014 Apr; 31(3): 185-191.

173. Jang H, Kim TW, Yoon S, Choi SY, Kang TW, Kim SY, Kwon YW, Cho EJ, Youn HD. O-GlcNAc regulates pluripotency and reprogramming by directly acting on core components of the pluripotency network.*Cell Stem Cell.* 2012 Jul 6; 11(1): 62-74.

174. Sakabe K, Wang Z, Hart GW. Beta-N-acetylglucosamine (O-GlcNAc) is part of the histone code. *Proc Natl Acad Sci U S A.* 2010 Nov 16; 107(46): 19915-19920. PMCID: PMC2993388.

175. Chen Q, Chen Y, Bian C, Fujiki R, Yu X. TET2 promotes histone O-GlcNAcylation during gene transcription. *Nature.* 2013 Jan 24; 493(7433): 561-564. PMCID: PMC3684361.

176. Vella P, Scelfo A, Jammula S, Chiacchiera F, Williams K, Cuomo A, Roberto A, Christensen J, Bonaldi T, Helin K, Pasini D. Tet proteins connect the O-linked N-acetylglucosamine transferase ogt to chromatin in embryonic stem cells. *Mol Cell.* 2013 Feb 21; 49(4): 645-656.

177. Deplus R, Delatte B, Schwinn MK, Defrance M, Mendez J, Murphy N, Dawson MA, Volkmar M, Putmans P, Calonne E, Shih AH, Levine RL, Bernard O, Mercher T, Solary E, Urh M, Daniels DL, Fuks F. TET2 and TET3 regulate GlcNAcylation and H3K4 methylation through OGT and SET1/COMPASS. *EMBO J.* 2013 Mar 6; 32(5): 645-655. PMCID: PMC3590984.

178. Yang X, Zhang F, Kudlow JE. Recruitment of O-GlcNAc transferase to promoters by corepressor mSin3A: Coupling protein O-GlcNAcylation to transcriptional repression. *Cell.* 2002 Jul 12; 110(1): 69-80.

179. Cimmino L, Abdel-Wahab O, Levine RL, Aifantis I. TET family proteins and their role in stem cell differentiation and transformation. *Cell Stem Cell.* 2011 Sep 2; 9(3): 193-204. PMCID: PMC3244690.

180. Fujiki R, Hashiba W, Sekine H, Yokoyama A, Chikanishi T, Ito S, Imai Y, Kim J, He HH, Igarashi K, Kanno J, Ohtake F, Kitagawa H, Roeder RG, Brown M, Kato S. GlcNAcylation of histone H2B facilitates its monoubiquitination. *Nature.* 2011 Nov 27; 480(7378): 557-560.

181. Chatham JC, Not LG, Fulop N, Marchase RB. Hexosamine biosynthesis and protein O-glycosylation: The first line of defense against stress, ischemia, and trauma. *Shock.* 2008 Apr; 29(4): 431-440.

182. Zachara NE, Molina H, Wong KY, Pandey A, Hart GW. The dynamic stress-induced "O-GlcNAc-ome" highlights functions for O-GlcNAc in regulating

DNA damage/repair and other cellular pathways.*Amino Acids.* 2011 Mar; 40(3): 793-808. PMCID: PMC3329784.

183. Groves JA, Lee A, Yildirir G, Zachara NE. Dynamic O-GlcNAcylation and its roles in the cellular stress response and homeostasis. *Cell Stress Chaperones.* 2013 Sep; 18(5): 535-558. PMCID: PMC3745259.

184. Taylor RP, Parker GJ, Hazel MW, Soesanto Y, Fuller W, Yazzie MJ, McClain DA. Glucose deprivation stimulates O-GlcNAc modification of proteins through up-regulation of O-linked N-acetylglucosaminyltransferase. *J Biol Chem.* 2008 Mar 7; 283(10): 6050-6057.

185. Lefebvre T, Cieniewski C, Lemoine J, Guerardel Y, Leroy Y, Zanetta JP, Michalski JC. Identification of N-acetyl-d-glucosamine-specific lectins from rat liver cytosolic and nuclear compartments as heat-shock proteins. *Biochem J.* 2001 Nov 15; 360(Pt 1): 179-188. PMCID: PMC1222216.

186. Marotta NP, Lin YH, Lewis YE, Ambroso MR, Zaro BW, Roth MT, Arnold DB, Langen R, Pratt MR. O-GlcNAc modification blocks the aggregation and toxicity of the protein alpha-synuclein associated with parkinson's disease. *Nat Chem.* 2015 Nov; 7(11): 913-920. PMCID: PMC4618406.

187. Zhang F, Su K, Yang X, Bowe DB, Paterson AJ, Kudlow JE. O-GlcNAc modification is an endogenous inhibitor of the proteasome. *Cell.* 2003 Dec 12; 115(6): 715-725.

188. Allison DF, Wamsley JJ, Kumar M, Li D, Gray LG, Hart GW, Jones DR, Mayo MW. Modification of RelA by O-linked N-acetylglucosamine links glucose metabolism to NF-kappaB acetylation and transcription.*Proc Natl Acad Sci U S A.* 2012 Oct 16; 109(42): 16888-16893. PMCID: PMC3479489.

189. Ma Z, Vocadlo DJ, Vosseller K. Hyper-O-GlcNAcylation is anti-apoptotic and maintains constitutive NF-kappaB activity in pancreatic cancer cells. *J Biol Chem.* 2013 May 24; 288(21): 15121-15130. PMCID: PMC3663532.

190. Kawauchi K, Araki K, Tobiume K, Tanaka N. Loss of p53 enhances catalytic activity of IKKbeta through O-linked beta-N-acetyl glucosamine modification. *Proc Natl Acad Sci U S A.* 2009 Mar 3; 106(9): 3431-3436. PMCID: PMC2651314.

191. Yang WH, Park SY, Nam HW, Kim do H, Kang JG, Kang ES, Kim YS, Lee HC, Kim KS, Cho JW. NFkappaB activation is associated with its O-GlcNAcylation state under hyperglycemic conditions. *Proc Natl Acad Sci U S A.* 2008 Nov 11; 105(45): 17345-17350. PMCID: PMC2582288.

192. Chaiyawat P, Netsirisawan P, Svasti J, Champattanachai V. Aberrant O-GlcNAcylated proteins: New perspectives in breast and colorectal cancer. *Front Endocrinol (Lausanne).* 2014 Nov 11; 5: 193. PMCID: PMC4227529.

193. Yehezkel G, Cohen L, Kliger A, Manor E, Khalaila I. O-linked beta-N-acetylglucosaminylation (O-GlcNAcylation) in primary and metastatic colorectal cancer clones and effect of N-acetyl-beta-D-glucosaminidase silencing on cell phenotype and transcriptome. *J Biol Chem.* 2012 Aug 17; 287(34): 28755-28769. PMCID: PMC3436545.

194. Onodera Y, Nam JM, Bissell MJ. Increased sugar uptake promotes oncogenesis via EPAC/RAP1 and O-GlcNAc pathways. *J Clin Invest.* 2014 Jan; 124(1): 367-384. PMCID: PMC3871217.

195. Lynch TP, Ferrer CM, Jackson SR, Shahriari KS, Vosseller K, Reginato MJ. Critical role of O-linked beta-N-acetylglucosamine transferase in prostate cancer invasion, angiogenesis, and metastasis. *J Biol Chem.* 2012 Mar 30; 287(14): 11070-11081. PMCID: PMC3322861.

196. Caldwell SA, Jackson SR, Shahriari KS, Lynch TP, Sethi G, Walker S, Vosseller K, Reginato MJ. Nutrient sensor O-GlcNAc transferase regulates breast cancer tumorigenesis through targeting of the oncogenic transcription factor FoxM1. *Oncogene.* 2010 May 13; 29(19): 2831-2842.

197. Park SY, Kim HS, Kim NH, Ji S, Cha SY, Kang JG, Ota I, Shimada K, Konishi N, Nam HW, Hong SW, Yang WH, Roth J, Yook JI, Cho JW. Snail1 is stabilized by O-GlcNAc modification in hyperglycaemic condition. *EMBO J.* 2010 Nov 17; 29(22): 3787-3796. PMCID: PMC2989108.

198. Freire-de-Lima L, Gelfenbeyn K, Ding Y, Mandel U, Clausen H, Handa K, Hakomori SI. Involvement of O-glycosylation defining oncofetal fibronectin in epithelial-mesenchymal transition process. *Proc Natl Acad Sci U S A.* 2011 Oct 25; 108(43): 17690-17695. PMCID: PMC3203762.

199. Ding Y, Gelfenbeyn K, Freire-de-Lima L, Handa K, Hakomori SI. Induction of epithelial-mesenchymal transition with O-glycosylated oncofetal fibronectin. *FEBS Lett.* 2012 Jun 21; 586(13): 1813-1820. PMCID: PMC3377767.

200. Alisson-Silva F, Freire-de-Lima L, Donadio JL, Lucena MC, Penha L, Sa-Diniz JN, Dias WB, Todeschini AR. Increase of O-glycosylated oncofetal fibronectin in high glucose-induced epithelial-mesenchymal transition of cultured human epithelial cells. *PLoS One.* 2013 Apr 12; 8(4): e60471. PMCID: PMC3625189.

201. Chou TY, Dang CV, Hart GW. Glycosylation of the c-myc transactivation domain. *Proc Natl Acad Sci U S A.* 1995 May 9; 92(10): 4417-4421. PMCID: PMC41955.

202. Itkonen HM, Minner S, Guldvik IJ, Sandmann MJ, Tsourlakis MC, Berge V, Svindland A, Schlomm T, Mills IG. O-GlcNAc transferase integrates metabolic pathways to regulate the stability of c-MYC in human prostate cancer cells. *Cancer Res.* 2013 Aug 15; 73(16): 5277-5287.

203. Yang WH, Kim JE, Nam HW, Ju JW, Kim HS, Kim YS, Cho JW. Modification of p53 with O-linked N-acetylglucosamine regulates p53 activity and stability. *Nat Cell Biol.* 2006 Oct; 8(10): 1074-1083.

204. Napetschnig J, Wu H. Molecular basis of NF-kappaB signaling. *Annu Rev Biophys.* 2013; 42: 443-468. PMCID: PMC3678348.

205. Perkins ND. The diverse and complex roles of NF-kappaB subunits in cancer. *Nat Rev Cancer.* 2012 Jan 19; 12(2): 121-132.

206. Karin M, Cao Y, Greten FR, Li ZW. NF-kappaB in cancer: From innocent bystander to major culprit. *Nat Rev Cancer.* 2002 Apr; 2(4): 301-310.

207. Karin M. Nuclear factor-kappaB in cancer development and progression. *Nature.* 2006 May 25; 441(7092): 431-436.

208. Perkins ND. Integrating cell-signalling pathways with NF-kappaB and IKK function. *Nat Rev Mol Cell Biol.* 2007 Jan; 8(1): 49-62.

209. Janssens S, Tschopp J. Signals from within: The DNA-damage-induced NF-kappaB response. *Cell Death Differ.* 2006 May; 13(5): 773-784.

210. Tam AB, Mercado EL, Hoffmann A, Niwa M. ER stress activates NF-kappaB by integrating functions of basal IKK activity, IRE1 and PERK. *PLoS One.* 2012; 7(10): e45078. PMCID: PMC3482226.

211. Huang B, Yang XD, Lamb A, Chen LF. Posttranslational modifications of NF-kappaB: Another layer of regulation for NF-kappaB signaling pathway. *Cell Signal.* 2010 Sep; 22(9): 1282-1290. PMCID: PMC2893268.

212. Ben-Neriah Y, Karin M. Inflammation meets cancer, with NF-kappaB as the matchmaker. *Nat Immunol.* 2011 Jul 19; 12(8): 715-723.

213. http://www.bu.edu/nf-kb/gene-resources/target-genes/

214. Meylan E, Dooley AL, Feldser DM, Shen L, Turk E, Ouyang C, Jacks T. Requirement for NF-kappaB signalling in a mouse model of lung adenocarcinoma. *Nature.* 2009 Nov 5; 462(7269): 104-107. PMCID: PMC2780341.

215. Xia Y, Yeddula N, Leblanc M, Ke E, Zhang Y, Oldfield E, Shaw RJ, Verma IM. Reduced cell proliferation by IKK2 depletion in a mouse lung-cancer model. *Nat Cell Biol.* 2012 Feb 12; 14(3): 257-265. PMCID: PMC3290728.

216. Stathopoulos GT, Sherrill TP, Cheng DS, Scoggins RM, Han W, Polosukhin VV, Connelly L, Yull FE, Fingleton B, Blackwell TS. Epithelial NF-kappaB activation promotes urethane-induced lung carcinogenesis. *Proc Natl Acad Sci U S A.* 2007 Nov 20; 104(47): 18514-18519. PMCID: PMC2141808.

217. Basseres DS, Ebbs A, Levantini E, Baldwin AS. Requirement of the NF-kappaB subunit p65/RelA for K-ras-induced lung tumorigenesis. *Cancer Res.* 2010 May 1; 70(9): 3537-3546. PMCID: PMC2862109.

218. Finco TS, Westwick JK, Norris JL, Beg AA, Der CJ, Baldwin AS,Jr. Oncogenic ha-ras-induced signaling activates NF-kappaB transcriptional activity, which is required for cellular transformation. *J Biol Chem.* 1997 Sep 26; 272(39): 24113-24116.

219. Chen W, Li Z, Bai L, and Lin Y. NF-kappaB in lung cancer, a carcinogenesis mediator and a prevention and therapy target. Frontiers in Bioscience. 2011;16:1172–85.

220. Kawata M, Koinuma D, Ogami T, Umezawa K, Iwata C, Watabe T, Miyazono K. TGF-beta-induced epithelial-mesenchymal transition of A549 lung adenocarcinoma cells is enhanced by pro-inflammatory cytokines derived from RAW 264.7 macrophage cells. *J Biochem.* 2012 Feb; 151(2): 205-216.

221. Asiedu MK, Ingle JN, Behrens MD, Radisky DC, Knutson KL. TGFbeta/TNF(alpha)-mediated epithelial-mesenchymal transition generates breast cancer stem cells with a claudin-low phenotype. *Cancer Res.* 2011 Jul 1; 71(13): 4707-4719. PMCID: PMC3129359.

222. Bates RC, Mercurio AM. Tumor necrosis factor-alpha stimulates the epithelial-to-mesenchymal transition of human colonic organoids. *Mol Biol Cell.* 2003 May; 14(5): 1790-1800. PMCID: PMC165077.

223. Maier HJ, Schmidt-Strassburger U, Huber MA, Wiedemann EM, Beug H, Wirth T. NF-kappaB promotes epithelial-mesenchymal transition, migration and invasion of pancreatic carcinoma cells. *Cancer Lett.* 2010 Sep 28; 295(2): 214-228.

224. Huber MA, Azoitei N, Baumann B, Grunert S, Sommer A, Pehamberger H, Kraut N, Beug H, Wirth T. NF-kappaB is essential for epithelial-mesenchymal transition and metastasis in a model of breast cancer progression. *J Clin Invest.* 2004 Aug; 114(4): 569-581. PMCID: PMC503772.

225. Stanisavljevic J, Porta-de-la-Riva M, Batlle R, de Herreros AG, Baulida J. The p65 subunit of NF-kappaB and PARP1 assist Snail1 in activating fibronectin transcription. *J Cell Sci.* 2011 Dec 15; 124(Pt 24): 4161-4171

226. De Craene B, Berx G. Regulatory networks defining EMT during cancer initiation and progression. *Nat Rev Cancer.* 2013 Feb; 13(2): 97-110.

227. Chua HL, Bhat-Nakshatri P, Clare SE, Morimiya A, Badve S, Nakshatri H. NF-kappaB represses E-cadherin expression and enhances epithelial to mesenchymal transition of mammary epithelial cells: Potential involvement of ZEB-1 and ZEB-2. *Oncogene.* 2007 Feb 1; 26(5): 711-724.

228. Julien S, Puig I, Caretti E, Bonaventure J, Nelles L, van Roy F, Dargemont C, de Herreros AG, Bellacosa A, Larue L. Activation of NF-kappaB by akt upregulates snail expression and induces epithelium mesenchyme transition. *Oncogene.* 2007 Nov 22; 26(53): 7445-7456.

229. Stabilization of snail by NF-kappaB is required for inflammation-induced cell migration and invasion. *Cancer Cell.* 2009 May 5; 15(5): 416-428. PMCID: PMC2881229.

230. Rajasekhar VK, Studer L, Gerald W, Socci ND, Scher HI. Tumour-initiating stem-like cells in human prostate cancer exhibit increased NF-kappaB signalling. *Nat Commun.* 2011 Jan 18; 2: 162. PMCID: PMC3105310.

231. Huang X, Pan Q, Sun D, Chen W, Shen A, Huang M, Ding J, Geng M. O-GlcNAcylation of cofilin promotes breast cancer cell invasion. *J Biol Chem.* 2013 Dec 20; 288(51): 36418-36425. PMCID: PMC3868755.

CHAPTER II

Materials and Methods

Cell Culture and Reagents

A549, H358, H1299 NSCLC and HEK293T cell lines were obtained from ATCC. A549 and HEK293T cells were grown in DMEM (Corning 10-017) with 10% fetal bovine serum (FBS, Invitrogen 16000044) and 5% Penicillin/Streptomycin (Pen/Strep, Invitrogen 15070-063). H358 and H1299 cells were grown in RPMI 1640 (Corning 10-040) with 10% FBS and 5% Pen/Strep at 37°C and 5% CO_2. EMT was induced in 3D spheroid cultures by treatment with TNF (Invitrogen PHC3016, 10ng/mL) and TGFb1 (Invitrogen PHG9024, 2ng/mL). PD0329 MEK inhibitor was purchased from Cayman.

Plasmids and Cell Transfection

Untagged GFPT2 was purchased from DNASu repository. Untagged GFPT1 was purchased from Origene. V5-His pcDNA3.1 was obtained from Invitrogen. PIC113 GFP was kindly provided by Dr. Foltz DR. 3xκB Luciferase reporter and β-galactosidase were described previously (1). Rheb, clathrin, Rab1A, Rab39B, RhoG, Rab7A, RRAS2, Rab11A, KIF5A, DYNC1LI1, Rab6C, Rab2A were obtained from Orfeome cDNA library and subcloned into PIC113 using Gateway cloning system (ThermoFisher). Rab5C was kindly provided by Dr. Bloom and Dr. Casanova. Cdc42 and Paxilin were kindly provided by Dr. Horwitz AF. HEK293T cells were seeded onto tissue culture plates and transfected the next day at the confluency of 60-70% using Polyfect reagent (Qiagen) according to

manufacturer protocol with adequate amount of DNA depending on the size of tissue culture plate. Cells were incubated for 24h, washed in PBS, collected and frozen in liquid nitrogen.

Viral Particle Production

For pRetro system HEK293T cells were seeded onto 10-cm tissue culture plates and transfected the next day at the confluency of 50% with total of 8μg of plasmid DNA including GAG-POL, VSV-G and either V5-GFPT2 pRetro-Tight-Pur, pRetro Luciferase or pRetro rTetR using Polyfect reagent (Qiagen). Cells were incubated overnights and the media was changed for a fresh DMEM 10% FBS. Viral supernatants were collected 48h, 72h and 96h following transfection with fresh DMEM 10% FBS added to the cells each time. Supernatants were filtered through 45μM polysulfonic syringe filters, aliquoted and frozen at -80^{o}C. For pTripZ virus production HEK293T cells were transfected with $CaCl_2$ according to manufacturer's protocol using provided trans-lentiviral packaging mix and either GFPT2-shRNA pTripZ of Scrambled pTripZ plasmids and incubated for 16 hours. Media was replaced for 5% FBS DMEM and cells were incubated for additional 48 hours followed by viral supernatant collection. Supernatants were filtered through 45μM PVDF filter. Viral infections of A549 and H1299 cells were performed similarly to pRetro without centrifugation step.

Generation of Stable Cell Lines

Stable knockdown A549 and H1299 cell lines were generated using doxycycline-inducible shRNA targeting 3' UTR region of *GFPT2* mRNA and scrambled control shRNA pTripZ vectors (Dharmacon). Lentiviral particles were produced in HEK293T and used for transduction of target cells according to manufacturer recommendations. Infected cells were selected with puromycin at 1.0 mg/mL for two weeks. Cells were subcloned in 96-well plate and clonal cell lines were tested for the knockdown efficiency in 3D spheroid cultures treated with TNF and TGFβ. Doxycycline at concentration 1.0mg/mL for A549 and 0.5mg/mL for H1299 was administered during 3D spheroid formation and along with cytokine treatments. Stable A549 and H1299 doxycycline-inducible tagged GFPT2 and Luciferase overexpressing cell lines were generated using pRetro Tet-On system (Clontech). Untagged GFPT2 cDNA was obtained from DNASU, and subcloned into pcDNA3.1 vector (Invitrogen) following by cloning of the entire ORF including V5 tag into pRetroX-Tight-Pur vector. HEK293T cells used to produce viral particles containing tetracycline-controlled mutant transactivator rtTA-Advanced (rTetR), V5-GFPT2 pRetro-Tight-Pur and Luciferase pRetro-Tight-Pur. A549 and H1299 cells were infected with combinations of either V5-GFPT2 pRetro-Tight-Pur together with rTetR or Luciferase control together with rTetR pRetro using 10μg/mL of polybrene and centrifugation at 1200g for 90 minutes at RT. Cells were then incubated overnights and he procedure was repeated the next day. Following two rounds of infection cells were selected with puromycin at 1.0

mg/mL and G418 at 1.0 mg/mL for two weeks. 3D spheroid cultures were tested for the efficiency of ectopic GFAT2 expression. Similarly doxycycline at concentration 1.0mg/mL for A549 and 0.5mg/mL for H1299 was administered during 3D spheroid formation and along with cytokine treatments.

Tumorsphere Cultures

Multicellular spheroid cultures were created using a modified hanging droplet method (2). Cells were grown to approximately 80% confluence on the standard tissue culture plates, trypsinized and resuspended in DMEM or RPMI containing 10% FBS and PenStrep. Cell suspension was diluted to 1 x 10^6 cells/mL and 54 of 25μl droplets were pipetted onto the underside of a sterile 10 cm Petri dish to create spheroids of 25,000 cells. The lid was then flipped and placed onto the bottom of Petri plate containing 13mL of PBS. Spheroids were incubated for 48 hours to facilitate cellular aggregation and then transferred onto a polyHEMA-covered 10 cm Petri plates in reduced serum 2% FBS media DMEM or RPMI containing PenStrep. Petri plates were prepared using 8mL per plate of 10mg/mL polyHEMA (Sigma-Aldrich P3932) working solution in 95% ethanol. Plates were allowed to air dry overnight and were washed in PBS before use. Spheroids from two hanging droplet lids were transferred onto one polyHEMA plate (total of 108 spheroids). Spheroids were incubated for additional 96h either without or with two treatments with TNF at 10ng/mL (Invitrogen PHC3016) and TGFb1 at

2ng/mL (Invitrogen PHG9024) at the time of transfer and at 48h time point, to induce EMT.

ChIP-Seq Data Analysis

ChIP-Seq assay for histone modifications in 3D spheroids was described previously. ChIP-Seq data for p65 in TNF stimulated A549 was retrieved from Raskatov et. al. (3) Data was overlaid onto human genome (hg19) and visualized using Integrative Genome Viewer (Broad Institute).

Quantitative Real-Time Polymerase Chain Reaction (QRT-PCR) and PCR

For gene expression analysis total RNA was isolated using RNAesy kit (Zymo Research) and reverse transcribed using iscript reverse polymerase kit (Biorad). QRT-PCR analysis was described previously (4). Primers used are listed (Table 1) or were previously described.

Chromatin Immunoprecipitation (ChIP)

ChIP assay was performed using modified Farnham protocol (5). A549 monolayers cultured on 15-cm tissue culture plates were serum starved for 2 hours before TNF treatments for 45 minutes and 2 hours. Cells were cross-linked with 1% formaldehyde and quenched with 125mM Glycine, washed in PBS,

scraped, spun down and frozen in liquid nitrogen. Cells pellets were thawed on ice and lysed in 300μl cell lysis buffer by passing through 20xG needle 5 times followed by sonication with probeless Bioruptor (Diagenode) to achieve 500bp fragments. Following sonication cell lysates of the same conditions were pooled together and protein concentration was determined using BCA (Pierce). Equal amounts of protein lysates (1.0 – 1.5mg) in adjusted volumes were prepared for immunoprecipitation. Additionally 5% volume of lysate was taken as an input. ChIP-grade p65 antibody (C-20, Santa Cruz) and normal rabbit IgG (Santa Cruz) were used for the immunoprecipitation overnight at 4^{o}C. Protein A/G beads were added the next day for and incubated for an additional 1 hour at 4^{o}C followed by several washes with varied salt concentrations and eluted off the beads. Eluates along with inputs were reversed cross-linked at 65^{o}C overnight and purified the next day using PCR purification columns (Qiagen). Purified DNA samples were used for quantitative PCR (qPCR) using primers listed (Table 1). DNA enrichment was expressed as a percent input.

Adenoviral infections

A549 cells were infected in 2D monolayers with adenovirus particles encoding non-degradable form if IκBα called Super-Repressor (SR-IκBα) and GFP control (6) for 4 hours in low volume of media followed by addition of fresh media and overnight incubation. Next day cells were washed in PBS and serum-free DMEM

was added. Cells were serum starved for 2h following by the treatment with TNF and TGFb1 alone or in a combination. Cells were washed in PBS and harvested.

Transwell migration and invasion assays and wound healing assays

3D spheroid cultures following 96h incubation with or without treatments with TNF and TGFb1 in reduced serum were collected, washed in PBS and trypsinized. Cells were re-suspended in serum free media followed and counted. $1x10^4$ cells for migration assay and $1x10^5$ cells for invasion assays were plated at the top of the Boyden Transwell (BD Biosciences) chamber. Media containing 10% FBS was added at the bottom of the well as a chemoattractant. Cells were incubated for 14 hours for migration assay and 22 hours for invasion assay according to manufacturer protocol. Chambers were washed in PBS and the upper membrane was wiped with cotton swab to remove cells that did not migrated through the membrane. Membranes were fixed in methanol at -20^oC, stained with 0.1% Trypan Blue for 1 hour at RT and photographed. For wound healing assays spheroids were trypsinized and cells were plated in 24-well plates at the near confluency concentration and allowed to attach. A scratch was done with p200 pipette tip the next day followed by a one wash with PBS and fresh media with 2% FBS was added to wells. Gap closure was monitored thorough 72h hour time frame using microscope. Gap surface measurements were done with TScratch software (7).

Immunoprecipitation, succinylated Wheat Germ Agglutinin (sWGA) pull-down and Immunoblotting

Immunoprecipitations were performed as described previously using anti GFP antibody (kindly provided by Dr. Foltz DR) or sWGA agarose beads (B&Y Laboratories) Immunoblotting was performed as described previously (4). Antibodies used are E-cadherin (Santa Cruz), N-cadherin (BD), Vimentin (Sigma), α-tubulin (Sigma), and GAPDH (GeneTex), V5 (Invitrogen), OGT (Sigma), OGA (Sigma), GFAT1 (Cell Signaling), GFAT2 (Cell Signaling), O-GlcNAc RL-2 (Sigma), O-GlcNAc CTD110.1 (Covance), Flag M2 (Sigma), MMP9 (R&D Systems), GFP (Dr. Foltz DR), ERK (Cell Signaling), phospho-ERK (Cell Signaling), MEK (Cell Signaling), phospho-MEK (Cell Signaling), Elk (Cell Signaling), phosphor-Elk (Cell Signaling), IKK (Cell Signaling), phospho-IKK (Cell Signaling), IκB (Santa Cruz), phospho-IκB (Cell Signaling).

Luciferase reporter assay

HEK293T were transfected with 3xκB or pcDNA3.1 along with β-galactosidase plasmid using polyFect according to manufacturer protocol and incubated for 24h. Media was changed for fresh DMEM 10% FBS and cell were incubated additional 24h followed by serum starvation for 4h and TNF treatment for 2h. Cells were washed with PBS, scraped, harvested and frozen in liquid nitrogen. Cells were thawed on ice and lysed in Reporter Lysis Buffer (Promega). Lysates

were used to determine luciferase activity using luciferin substrate (Sigma) using 96-well plate reader. β-galactosidase activity was determined using β-gal (Sigma) as a substrate and protein concentrations were measured using BCA (Promega). Both were used to normalize luciferase activity readouts.

REFERENCES

1. Yeung F, Hoberg JE, Ramsey CS, Keller MD, Jones DR, Frye RA, Mayo MW. Modulation of NF-kappaB-dependent transcription and cell survival by the SIRT1 deacetylase. *EMBO J.* 2004 Jun 16; 23(12): 2369-2380. PMCID: PMC423286.

2. Kelm JM, Timmins NE, Brown CJ, Fussenegger M, Nielsen LK. Method for generation of homogeneous multicellular tumor spheroids applicable to a wide variety of cell types. *Biotechnol Bioeng.* 2003 Jul 20; 83(2): 173-180.

3. Raskatov JA, Meier JL, Puckett JW, Yang F, Ramakrishnan P, Dervan PB. Modulation of NF-kappaB-dependent gene transcription using programmable DNA minor groove binders. *Proc Natl Acad Sci U S A.* 2012 Jan 24; 109(4): 1023-1028. PMCID: PMC3268328.

4. Wamsley JJ, Kumar M, Allison DF, Clift SH, Holzknecht CM, Szymura SJ, Hoang SA, Xu X, Moskaluk CA, Jones DR, Bekiranov S, Mayo MW. Activin upregulation by NF-kappaB is required to maintain mesenchymal features of cancer stem-like cells in non-small cell lung cancer. *Cancer Res.* 2015 Jan 15; 75(2): 426-435. PMCID: PMC4297542.

5. http://farnham.genomecenter.ucdavis.edu/

6. Jobin C, Panja A, Hellerbrand C, Iimuro Y, Didonato J, Brenner DA, Sartor RB. Inhibition of proinflammatory molecule production by adenovirus-mediated expression of a nuclear factor kappaB super-repressor in human intestinal epithelial cells. *J Immunol.* 1998 Jan 1; 160(1): 410-418.

7. Geback T, Schulz MM, Koumoutsakos P, Detmar M. TScratch: A novel and simple software tool for automated analysis of monolayer wound healing assays. *BioTechniques.* 2009 Apr; 46(4): 265-274.

Table 1: Primer Sequences

Gene	Sequence
H. sapiens GAPDH F	GAAGGTGAAGGTCGGAGTC
H. sapiens GAPDH R	GAAGATGGTGATGGGATTTC
H. sapiens SNAI1 F	CACTATGCCGCGCTCTTTC
H. sapiens SNAI1 R	GGTCGTAGGGCTGCTGGAA
H. sapiens SNAI2 F	ATGAGGAATCTGGCTGCTGT
H. sapiens SNAI2 R	CAGGAGAAAATGCCTTTGGA
H. sapiens ZEB2 F	CAATACCGTCATCCTCAGCA
H. sapiens ZEB2 F	CCAATCCCAGGAGGAAAAAC
H. sapiens TWIST1 F	CGGGAGTCCGCAGTCTTA
H. sapiens TWIST1 R	CTTGAGGGTCTGAATCTTGCT
H. sapiens OGT F	AGGAAATGTCTTGAAAGAGGCAC
H. sapiens OGT R	TCGTAGTACACACAAGCCCAGG
H. sapiens SLC2A1 F	CATCAACGCTGTCTTCTATTACTC
H. sapiens SLC2A1 R	ATGCTCAGATAGGACATCCA
H. sapiens SLC1A4 F	CTGTGGACTGGATTGTGGAC
H. sapiens SLC1A4 R	TCCACTTTCACCTCAGCAAG
H. sapiens NT5E F	TGGAGATGGGTTCCAGATGATAA
H. sapiens NT5E R	GGATAAATTACTTTCATTTTGGAGATAT
H. sapiens UUP1 F	ACTGCCCAGGTAGAGACTATC
H. sapiens UUP1 R	CTGCACCAGCTTCTTGTTAAG
H. sapiens GFPT1 F	CCAGCCAGTTTGTATCCCTT
H. sapiens GFPT1 R	CAAGCATGATCTCTTTGCGT
H. sapiens GFPT2 F	AGGTGCATTCGCGCTGGTT
H. sapiens GFPT2 R	TGTGGAGAGCTTGTATTTGCTCCCGGG
H. sapiens UAP1 F	AATGACCTCAAACTCACGTTGT
H. sapiens UAP1 R	GCTCTGCATAAAGTTCTACCTGT
H. sapiens MGEA5 F	TCCATAACCCAAGGTCTTCCA
H. sapiens MGEA5 R	TTGGAGGAGCGGGAGAGCGA
H. sapiens TNFAIP3 F	TTGACCAGGACTTGGGACTT
H. sapiens TNFAIP3 R	ACAGCTTTCCGCATATTGCT
H. sapiens BIRC3 F	GCTGTGATGGTGGACTCAGG
H. sapiens BIRC3 R	TGGCTTGAACTTGACGGATG
H. sapiens CXCL8 F	CTCTTGGCAGCCTTCCTG
H. sapiens CXCL8 R	CTGTGTTGGCGCAGTGTG
H. sapiens HPRT F	TTGGAAAGGGTTATTCCTCA
H. sapiens HPRT R	TCCAGCAGCTCAGCAAAGAA
H. sapiens ChIP site A F	TCCTGCCCTTCCCAGTGATAAA
H. sapiens ChIP site A R	CTTTGCTTATTGTCCTGTTG
H. sapiens ChIP site B F	AGTGGCAAGGGTGAGCTTCT
H. sapiens ChIP site B R	TTGCACAATGCCTGCCTG

CHAPTER III

NF-κB Upregulates Glutamine-Fructose-6-Phosphate Transaminase 2 (GFPT2) to Promote Migration in Non-Small Cell Lung Cancer

This chapter is based on the following manuscript under review for publication.

NF-κB Upregulates Glutamine-Fructose-6-Phosphate Transaminase 2 (GFPT2) to Promote Migration in Non-Small Cell Lung Cancer

Szymon J. Szymura, Jacob P. Zaemes, Sheena H. Clift, David F. Allison, Lisa G. Gray, Xiaojiang Xu, Stefan Bekiranov, David R. Jones and Marty W. Mayo

(Manuscript in preparation)

ABSTRACT

Induction of epithelial-to-mesenchymal transition (EMT) in cancer cells results in changes that promote de-differentiation, migration, and metastasis. While recognized that EMT promotes altered energy utilization, identification of metabolic pathways that directly link EMT with cancer procession is poorly understood. Work presented here indicates that mesenchymal non-small cell lung cancer (NSCLC) cells display altered metabolic gene expression profiles. Among the products upregulated in mesenchymal NSCLC, include glutamine-fructose-6-phosphate transaminase 2 (*GFPT2*) the rate-limiting enzyme in the synthesis of uridine diphosphate *N*-acetylglucosamine (UDP-GlcNAc). UDP-GlcNAc is an obligate activator of O-linked N-acetylglucosamine transferase (OGT), an enzyme intimately linked to EMT and cancer metastasis. Mesenchymal NSCLC cells require NF-κB to transcriptionally upregulate *GFPT2,* which follow similar kinetics as other well established EMT-regulated gene targets. Inducible knockdown of *GFPT2* expression in NSCLC highlight its importance in regulating migration and invasion in response to EMT. Our body of work demonstrates that *GFPT2* is essential for the migratory properties of mesenchymal NSCLC, directly linking its transcriptional upregulation with metastasis.

INTRODUCTION

Lung cancer is the leading cause of cancer-related mortality in the world (1). Non-small cell lung cancer (NSCLC) is the main type of lung cancer and comprises adenocarcinomas (ADC), squamous cell carcinomas (SCC) and large cell carcinomas (LCC) (2). The five-year survival rate for NSCLC is below 17% predominantly due to late-stage diagnosis and metastatic dissemination (2). Epithelial to mesenchymal transition (EMT) triggers the acquisition of the metastatic properties by carcinoma *in situ* (3). This process can be initiated by cytokines and growth factors present in tumor microenvironment and leads to increased migration and invasion, resistance to apoptosis and elevated self-renewal capacity and stem-like properties (3).

Our laboratory showed that tumor necrosis factor (TNF) synergizes with transforming growth factor beta (TGFβ) to induce EMT in NSCLC cells and generate cells with increases migratory and cancer-initiating (CIC) phenotypes (4). Binding of the TNF to its receptor (TNFR), leads to the activation of canonical NF-κB pathway and nuclear translocation of p50/RelA NF-κB heterodimers (5). Upon p50/RelA binding to its cognate κB sites on DNA, RelA is acetylated at Lys310 by p300, for its full transcriptional activation (6). Recently our laboratory showed that constitutive NF-κB activity is required for the induction and maintenance of EMT and CIC phenotypes in NSCLC through the transcriptional regulation of a positive feedback-loop of Activin A signaling (4, 7).

Alteration in energy metabolism has been identified as a hallmark of cancer and increased glucose and glutamine uptake and utilization correlates with the disease progression (8-10). Glucose and glutamine are substrates in the hexosamine biosynthesis pathway (HBP), which generates uridine diphosphate *N*-acetylglucosamine (UDP-GlcNAc) a precursor moiety for the synthesis of glycans and protein glycosylation (11). Glutamine fructose-6-phosphate aminotransferase (GFPT) is the first and rate-limiting enzyme in HBP and two isoforms are present in humans that differ in their tissue expression pattern and the mode of regulation (11). GFPT1 is ubiquitously expressed in majority of tissues whereas GFPT2 is limited primarily to the central nervous system and embryonic stem cells (11).

UDP-GlcNAc is used for the synthesis of hyaluronan, N- and O-glycosylation and protein O-GlcNAcylation, elevation of all of which has been associated with cancer progression and EMT (12-16). O-GlcNAcylation is a post-translational modification that relies on the addition and removal of a single UDP-GlcNAc moiety onto and from the hydroxyl groups of serine and threonine on target proteins by the enzymes O-GlcNAc transferase (OGT) and O-GlcNAcase (OGA), respectively (17). Recently our laboratory has shown that RelA subunit of NF-κB is O-GlcNAcylated at Thr305 which is required for its subsequent acetylation by p300 and full transcriptional activation and anti-apoptotic effect (18). Although the gradual accumulation of O-GlcNAc modification is observed during cancer progression and O-GlcNAcylation and OGT are required for

metastatic phenotype and EMT, regulation of the flux through HBP during EMT is vastly unknown (14-16).

Here we show that global O-GlcNAcylation is elevated in mesenchymal cells and confirm that OGT is necessary for the efficient induction of EMT in NSCLC. We show that the expression *GFPT2* is upregulated in mesenchymal NSCLC. *GFPT2* is a novel NF-κB target gene and an important marker of mesenchymal state that co-relates with poor clinical outcome. Finally, our work implicates GFPT2 as a critical enzyme in the regulation of migratory properties of mesenchymal NSCLC cells.

RESULTS

OGT is required for EMT in A549 cells

Several groups have reported the requirement of O-GlcNAc moiety deposition for metastasis (12-14). To verify these reports and to examine whether OGT is required for induction and maintenance of EMT in the lung adenocarcinoma (LUAD) cell line, A549, we used siRNAs targeting the OGT enzyme. A549 cells transfected with either control (-) or OGT (+) siRNAs were cultured as three dimensional (3D) tumorspheres either left untreated (-) or stimulated with TNF and TGFβ, as previously described (4, Material & Methods). As shown in Figure 1A, TNF/TGFβ-stimulated A549 multicellular tumorspheres showed global increases in O-GlcNAcylated proteins, indicating increased post-translational addition and maintenance of the O-GlcNAc moiety in total protein lysates. Transient knockdown of OGT efficiently silenced OGT expression at both the message and protein level, which was maintained over the six-day time course of EMT induction (Figure 1A and 1B). As predicted, knockdown of OGT effectively abolished the addition of the O-GlcNAc moiety on proteins at a global level. The knockdown of OGT significantly inhibited the gene expression of the EMT mater-switch transcription factors (*SNAI2*, *TWIST1*, and *ZEB2*) without altering *SNAL1* expression (Figure 1B). Moreover, the loss *SNAI2*, *TWIST1* and *ZEB2* gene expression in response to OGT knockdown correlated with the inability of A549 cells to upregulate EMT markers (N-cadherin, fibronectin, and

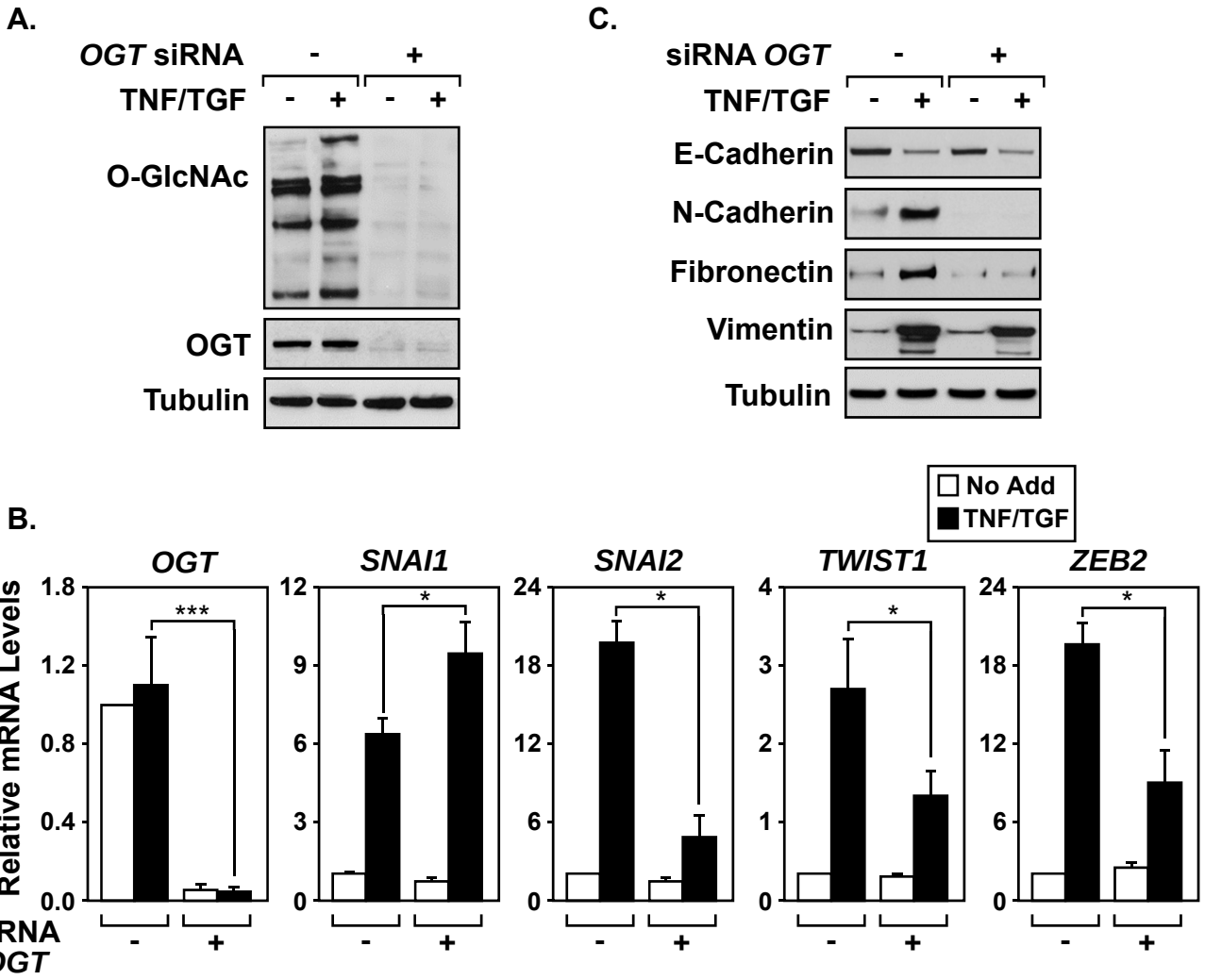
A.
OGT siRNA - +
TNF/TGF - + - +
O-GlcNAc
OGT
Tubulin
C.
siRNA OGT - +
TNF/TGF - + - +
E-Cadherin
N-Cadherin
Fibronectin
Vimentin
Tubulin
B.
No Add
TNF/TGF
OGT
SNAI1
SNAI2
TWIST1
ZEB2
Relative mRNA Levels
1.8
1.2
0.8
0.4
0.0
12
9
6
3
0
24
18
12
6
0
4
3
2
1
0
***
*
siRNA OGT
- +

Figure 1. OGT is required for epithelial to mesenchymal transition in NSCLC. A549 cells were transfected with OGT siRNA (+) or scrambled siRNA (-) followed by culturing in tumorspheres without (-) or with the addition of TNF and TGFβ (+). (A) Total levels of O-GlcNAcylation modification and OGT protein were assessed by immunoblotting. Tubulin probing was used as loading control. (B) Levels of mRNA of *OGT* and master-switch transcription factors *SNAI2*, *SNAI2*, *TWIST1* and *ZEB2* were measured by QRT-PCR and normalized to transcription levels of *GAPDH*. (C) Protein levels of epithelial (E-cadherin) and mesenchymal (N-cadherin, Fibronectin, Vimentin) markers were assessed by immunoblotting. Tubulin expression confirms equal protein loading.

vimentin). The knockdown of OGT was unable to rescue E-Cadherin protein expression following induction of EMT. Collectively, these results extend previous findings that OGT and O-GlcNAcylation are required for the induction of mesenchymal phenotypes in carcinomas and warrants further investigation into the mechanisms governing flux through the HBP (12-14).

Mesenchymal NSCLC cells upregulate genes involved in UDP-GlcNAc synthesis

To examine whether increased O-GlcNAcylation is a commonly observed phenomenon in mesenchymal NSCLC cells, A549 (adenocarcinomas), H358 (mix-cell carcinomas), and H1299 (large cell carcinomas), were cultured as tumorspheres and stimulated with TNF/TGFβ. Cytokine treatment of 3D A549, H358, and H1299 cultures resulted in a modest, but reproducible, increase in O-GlcNAc modified proteins in total cell extracts (Figure 2A, left and right panels). Wheat germ agglutinin pull-down assays confirmed increased detection of O-GlcNAcylated RelA in A549, H358 and H1299 tumorspheres following TNF/TGFβ stimulation (Supplementary S5). The increase in O-GlcNAcylation was not associated with an up-regulation of OGT protein expression or due to a loss of total OGA protein levels in any of the cells analyzed (Figure 2A).

Based on results obtained in Figure 2A, gene expression data was analyzed to determine whether TNF/TGFβ-stimulated A549 tumorspheres

A.

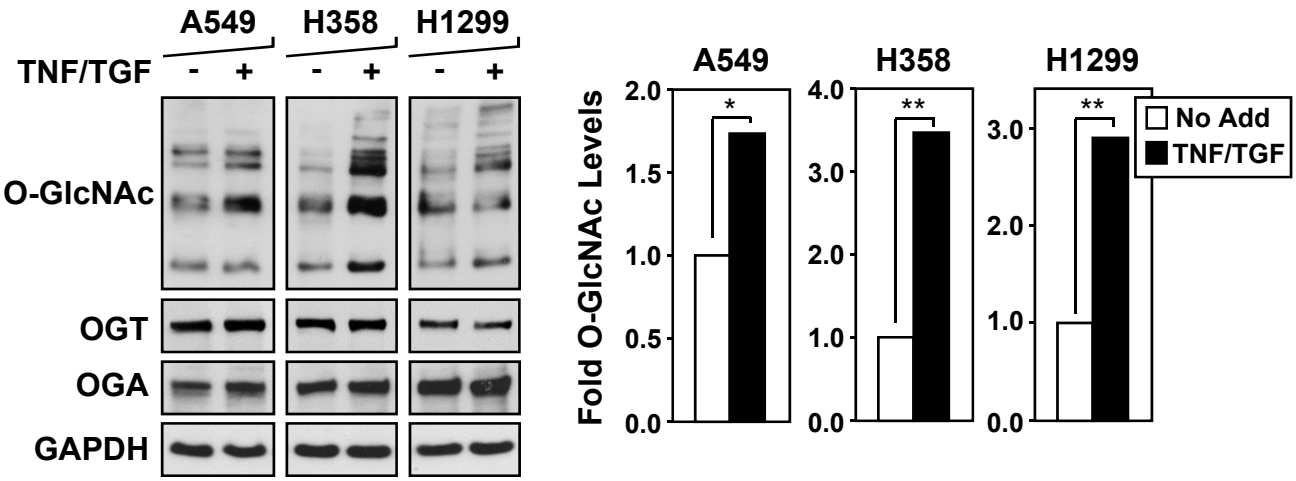

B.

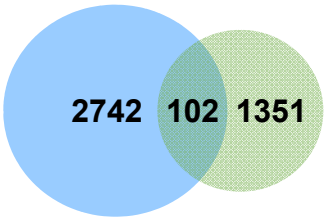

TABLE 1: Upregulated Genes that Contribute to UDP-GlcNAc Synthesis

Symbol	Description	GenBank	Fold Change
GFPT2	glutamine-fructose-6-phosphate transaminase 2	NM_005110	6.567
NT5E	5'-nucleotidase, ecto	NM_002526	3.528
HKDC1	hexokinase domain containing 1	NM_025130	3.414
UPP1	uridine phosphorylase 1	NM_003364	3.209
SLC2A1	solute carrier family 2 (facilitated glucose transporter), member 1	NM_006516	3.003
SLC2A3	solute carrier family 2 (facilitated glucose transporter), member 3	NM_006931	2.700
SLC1A4	solute carrier family 1 (glutamate/ neutral amino acid transporter), member 4	NM_003038	2.695
SLC2A6	solute carrier family 2 (facilitated glucose transporter), member 6	NM_017585	2.672
HK2	hexokinase 2	NM_000189	2.555
PGM2	phosphoglucomutase 2	NM_018290	1.537
CDA	cytidine deaminase	NM_001785	1.515
UAP1	UDP-N-acetylglucosamine pyrophosphorylase 1	NM_003115	1.500

p=<0.05

Figure 2. O-GlcNAcylation and enzymes involved in the synthesis of UDP-GlcNAc are elevated in mesenchymal NSCLC cells. (A) A panel of NSCLC cell lines (A549, H358, H1299) was used for tumorsphere cultures without (-) or with the addition of TNF and TGFβ (+). Total levels of O-GlcNAcylation modification, OGT and OGA proteins were assessed by immunoblotting. GAPDH probing was used as a protein loading control. Levels of O-GlcNAcylation were measured by densitometry. (B) Venn diagram illustrating an overlap between the list of genes upregulated in mesenchymal cells by more than 1.5-fold identified by gene expression microarray (green) and a total number of metabolic genes in human genome (blue). Analysis yielded a list of 102 metabolic genes specifically upregulated in mesenchymal NSCLC cells. (C) A table of mesenchymal metabolic genes identified in (B) involved in the synthesis of a UDP-GlcNAc biomass.

displayed expression changes in metabolic genes that could potentially explain the elevated O-GlcNAcylation observed in whole cell extracts. To identify potential metabolic genes differentially regulated following EMT, we used our previously published microarray (19). Microarray analysis performed on 3D A549 cultures, unstimulated or treated with TNF and TGFβ identified 1351 genes that were transcriptionally upregulated upon stimulation. Next, we used this 1351 upregulated gene list and analyzed for overlap with a library of 2742 metabolic genes (20). As illustrated in the Venn diagram in Figure 2B, a 102 gene overlap was identified between differentially upregulated genes in cytokine-treated 3D cultures and the metabolic gene list. Further analysis of the 102 gene overlap, identified 12 genes that were upregulated (≥1.5-fold) and either generate or transport metabolic precursors required for the synthesis of UDP-GlcNAc (Table 1A). Genes that encode for glucose and glutamate transporters (*SLC2A1*, *SLC2A3*, *SLC1A4*, and *SLC2A6*) and genes that encode for enzymes responsible for phosphorylating and retaining intracellular glucose (*HKDC1*, *HK2* and *PGM2*). Additional metabolic genes include those that alter nucleotide and uridine salvage (*NT5E*, *UPP1*, and *CDA*). Surprisingly, two of the genes in this list are enzymes required for the synthesis of UDP-GlcNAc (*GFPT2*, and *UAP1*). The highest fold upregulated metabolic gene on the list is *glutamine-fructorse-6-phosphate transferase 2* (*GFPT2*), which is the rate-limiting enzyme in the synthesis of the nucleotide-sugar UDP-GlcNAc (21).

Elevated *GFPT2* expression correlates with poor clinical outcomes in NSCLC

To validate results from the microarray analysis, RNA was isolated from A549 tumorspheres either left untreated or stimulated with TNF and TGFβ and QRT-PCR was performed. As shown in Figure 3A, mesenchymal A549 cells displayed elevated expression of *SLC2A1*/*GLUT1*, *SLC1A4*, *NT5E*, and *UPP1*, confirming the upregulation of these metabolic targets following EMT. Transcripts encoding enzymes in the hexosamine biosynthesis pathway, GFPT2 and UAP1 were also elevated following TNF/TGFβ stimulation (Figure 3B). However, transcript for *OGT*, the enzyme required for the deposition of UDP-GlcNAc moiety onto target proteins was not upregulated following EMT. Moreover, MGEA5/OGA, the enzyme required to remove the O-GlcNAc posttranslational modification, was not downregulated but rather was elevated in mesenchymal cells. Collectively, these results suggest that the increase in O-GlcNAcylation observed in mesenchymal A549 cells in Figure 2 was associated with increases in *de novo* synthesis of UDP-GlcNAc via GFPT2 and UAP1 and not through transcriptional modulation of OGT or OGA levels.

Given that GFPT2 is the rate-limiting enzyme in the UDP-GlcNAc synthesis pathway, and because our analysis identified it as one of the highest expressed metabolic genes upregulated following EMT, we asked whether elevated *GFPT2* mRNAs correlated with clinical outcome for NSCLC. To address this we examined the association of *GFPT2* expression in LUAD (n=740)

A.

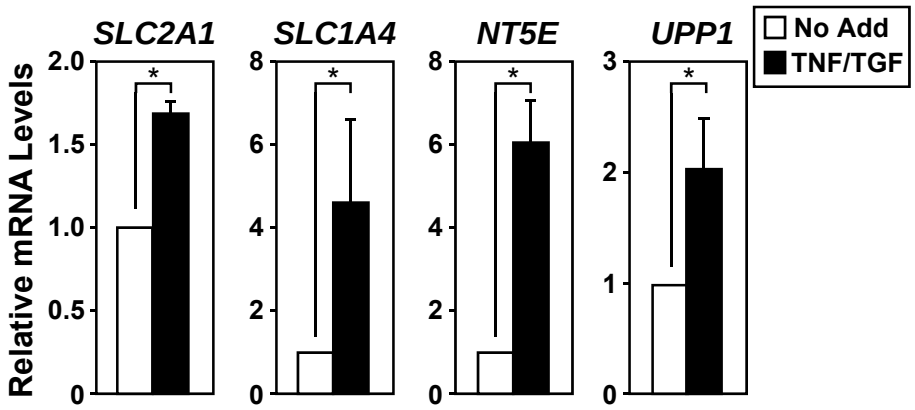
SLC2A1
SLC1A4
NT5E
UPP1
No Add
TNF/TGF
Relative mRNA Levels
2.0
1.5
1.0
0.5
0
8
6
4
2
0
8
6
4
2
0
3
2
1
0
*
*
*
*

B.

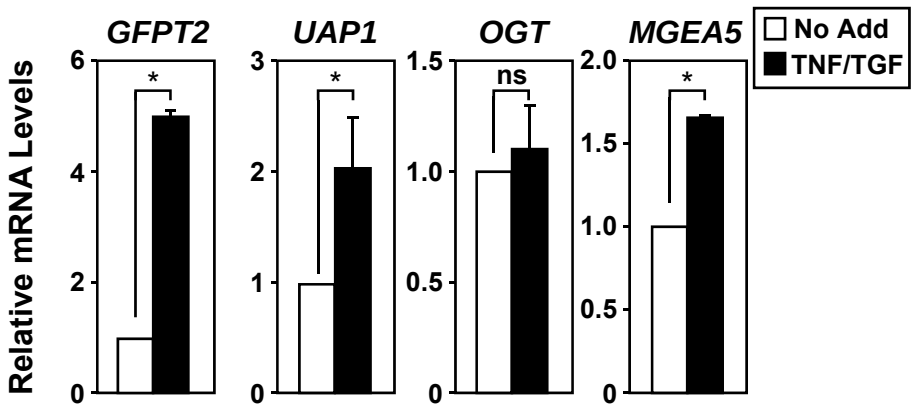
GFPT2
UAP1
OGT
MGEA5
No Add
TNF/TGF
Relative mRNA Levels
6
4
2
0
3
2
1
0
1.5
1.0
0.5
0
2.0
1.5
1.0
0.5
0
*
*
ns
*

C.

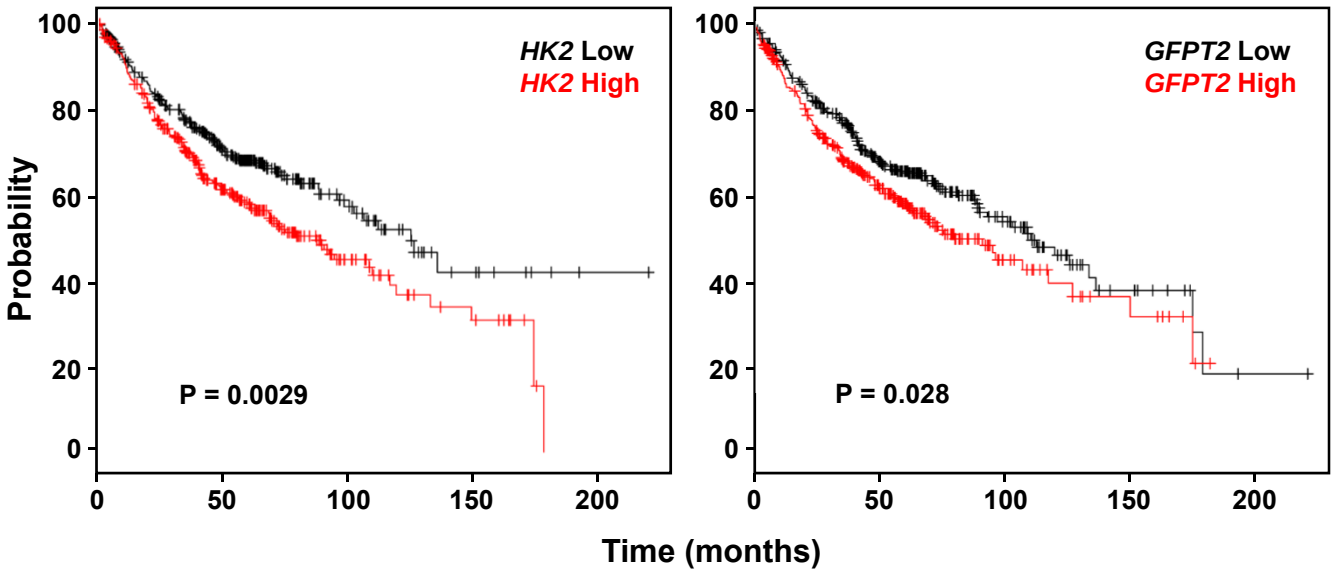
HK2 Low
HK2 High
GFPT2 Low
GFPT2 High
Probability
100
80
60
40
20
0
P = 0.0029
P = 0.028
0
50
100
150
200
Time (months)

D.

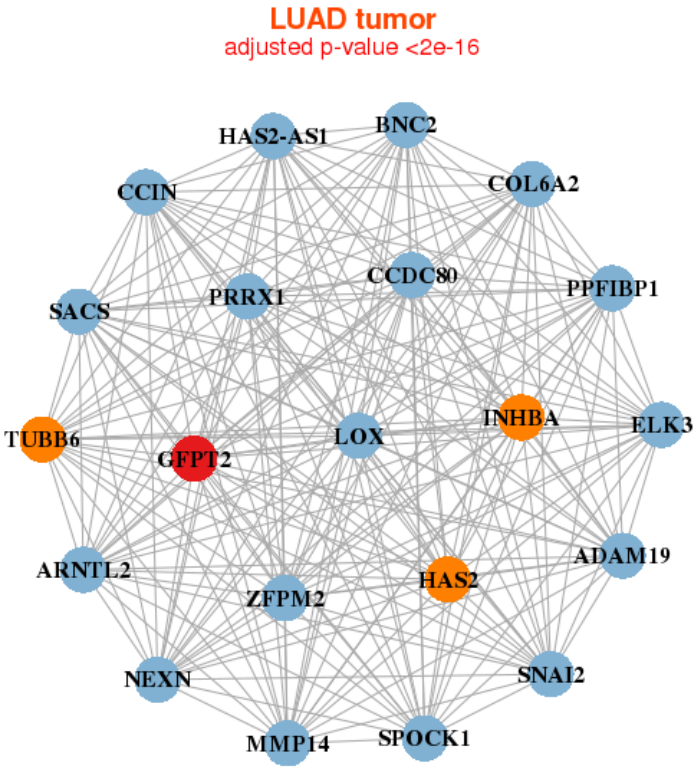
LUAD tumor
adjusted p-value <2e-16
HAS2-AS1
BNC2
CCIN
COL6A2
CCDC80
PPFIBP1
SACS
PRRX1
INHBA
ELK3
TUBB6
LOX
GFPT2
ADAM19
ARNTL2
HAS2
ZFPM2
NEXN
SNAI2
MMP14
SPOCK1

Figure 3. *GFPT2* is induced in mesenchymal NSCLC cells and is co-expressed with mesenchymal markers in LUAD patients. A549 cells were cultured in tumorspheres without or with the addition of TNF and TGFβ (TNF/TGF) (A and B). Transcript levels of proteins that impact UDP-GlcNAc synthesis, deposition and maintenance were measured by QRT-PCR and normalized to mRNA levels of HPRT. (C) Kaplan-Meier survival analysis on the left demonstrates that patients with elevated hexokinase 2 (HK2) (red) have significantly lower probability of survival compared to patients with low HK2 expression (black). Kaplan-Meier survival analysis on the right demonstrates that patients with elevated GFPT2 (red) have a significantly lower probability of survival compared to patients with low GFPT2 expression (black) (n = 720, p = 0.028). Calculations were carried out using www.kmplot.com. D. Network map identifies the top genes co-expressed with GFPT2 (red) in LUAD. Orange color indicates genes known to be associated with mesenchymal phenotypes. Analysis was performed using bioinfo.mc.vanderbilt.edu.

with clinical outcomes using Kaplan-Meier Plot (22). High expression of *GFPT2* mRNAs correlated with poor clinical outcome for patients with LUAD, compared to low *GFPT2* expression (*p = 0.028*, Figure 3C). As expected, patients with elevated *hexokinase 2* (*HK2*), a well-known metabolic gene associated with aggressive PET-positive LUAD, showed significantly reduced survival rates compared to low *HK2* expressing tumors. Thus, similar to *HK2*, elevated *GFPT2* expression in LUAD correlated with poor clinical outcomes, underscoring the importance of this rate-limiting enzyme in the progression of lung cancer. To further investigate the relevance of GFPT2 expression in the progression of lung cancer we examined whether *GFPT2* was co-expressed with other metabolic genes associated with metastatic processes using the Cancer Cell Metabolism Gene DataBase (23). As shown in the network map (Figure 3D), *GFPT2* was significantly co-expressed with several other metabolic genes known for their involvement in the progression of cancer (26-28). To our surprise the top gene co-expressed with *GFPT2* was *INHBA*, which encodes for the TGFβ family member Activin A (7). Our group has recently shown that Activin A acts as a secreted ligand to maintain mesenchymal properties of lung cancer initiating cells (7). Importantly nine out of the twenty genes identified by Cancer Cell Metabolism Gene database as co-expressed with *GFPT2* were also significantly elevated in our EMT gene expression microarray. Interestingly, many of the genes co-expressed with *GFPT2* are known mesenchymal markers associated with invasion and metastasis, namely *SNAI2*, *INHBA*, *SPOCK1*, *LOX*, *HAS2*, *COL6A2*, and *ADAM19* (26-28). Collectively, data provided in Figure 3 indicates

that *GFPT2* is a novel mesenchymal marker significantly elevated in LUAD and its expression correlates with poor clinical outcomes.

GFPT2 is an immediate-early gene product maintained in mesenchymal LUAD cells

HBP flux and protein O-GlcNAcylation has been shown to be elevated in several cancers however the transcriptional regulation of HBP is vastly unknown (12-14). Our data indicates that *GFPT2* is an inducible gene, expressed outside CNS. To further characterize the expression profile of *GFPT2*, a ninety-six hour time course was performed in A549 cells to measure transcript and protein levels. Expression of *GFPT2* mRNA is induces as early as 2h following the addition of TNF/TGFβ and its levels gradually increase in the first twelve hours post TNF/TGF stimulation, to reach plateau and remain steadily expressed through forty-eight and ninety-six hour time points (Figure 4A). This is in stark contrast to *GFPT1* mRNA expression, which shows a modest decrease in gene expression within twenty-four hours, and is then maintained throughout the ninety-six hour time frame. Importantly, consistent with the observed elevation of *GFPT2* mRNA expression, mesenchymal A549 cells display elevated GFPT2 protein expression over the ninety-six hour time course (Figure 4B). In contrast, A594 cells display a modest decrease in GFPT1 protein expression in response to TNF and TGFβ stimulation. Importantly, GFPT2 protein expression increase with similar kinetics to other established protein markers of mesenchymal

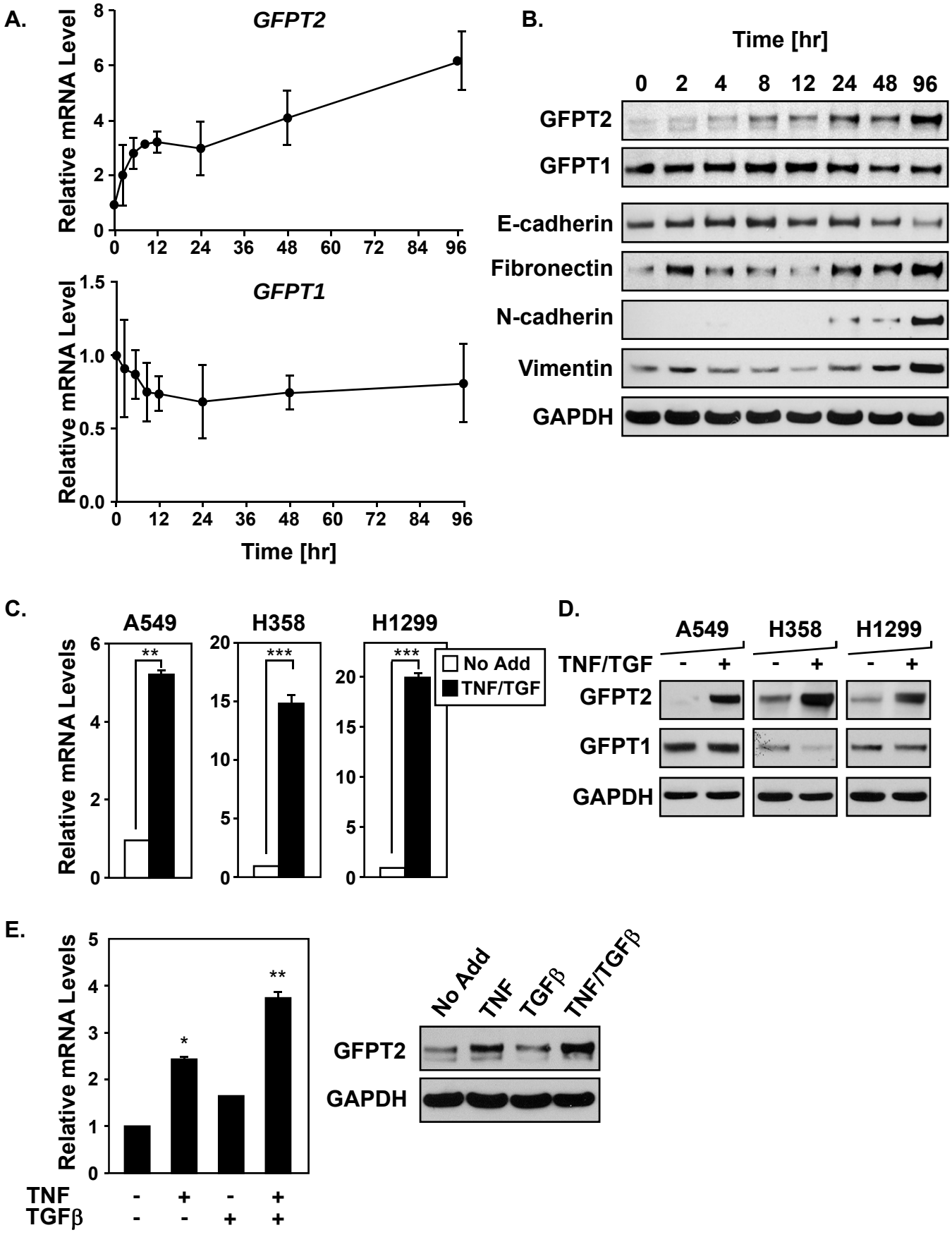
A.
GFPT2
Relative mRNA Level
GFPT1
Time [hr]
B.
Time [hr]
0 2 4 8 12 24 48 96
GFPT2
GFPT1
E-cadherin
Fibronectin
N-cadherin
Vimentin
GAPDH
C.
A549
H358
H1299
No Add
TNF/TGF
Relative mRNA Levels
D.
A549
H358
H1299
TNF/TGF
GFPT2
GFPT1
GAPDH
E.
Relative mRNA Levels
TNF
TGFβ
No Add
TNF
TGFβ
TNF/TGFβ
GFPT2
GAPDH

Figure 4. *GFPT2* is an immediate-early gene induced by TNF and maintained in mesenchymal NSCLC. A549 cells were cultured in tumorspheres without or with the addition of TNF and TGFβ for indicated times before collection. (A) mRNA levels of *GFPT2* and *GFPT1* isoforms were measured with qRT-PCR and normalized to HPRT. (B) Protein levels of GFAT2 and GFAT1 along with epithelial marker E-cadherin and mesenchymal markers N-cadherin, Fibronectin, N-cadherin and Vimentin were assessed by immunoblotting. GAPDH probing was used as a loading control. (C, D) A panel of NSCLC cell lines A549, H358 and H1299 were cultured in 3D spheroids without (-) or with the addition of TNF and TGFβ (+). (C) mRNA levels of *GFPT2* were measured by QRT-PCR. (D) Protein levels of GFAT2 and GFAT1 were assessed by immunoblotting. GAPDH probing was used as a loading control. (E) A549 cells were grown in tumorspheres without or with the addition of TNF, TGFβ of a combination of cytokines as indicated. mRNA levels of *GFPT2* were measured by QRT-PCR and normalized to HPRT (left). Protein levels of GFAT2 were assessed by immunoblotting. GAPDH probing was used as a loading control.

transition, including elevated Fibronectin, N-cadherin and Vimentin and decreased E-Cadherin expression. Similar increase in the transcript and protein expression for *GFPT2* was observed in two other NSCLC cell lines representing mixed-squamous cell (H358) and large cell (H1299) carcinoma. Importantly the increase in mRNA and protein expression was specific for *GFPT2*, not *GFPT1* (Figure 4C, 4D and Supplementary S1).

Since LUAD tumorspheres are stimulated to undergo EMT by a combination of TNF/TGFβ, we were interested in determining whether *GFPT2* expression was regulated by TNF, TGFβ or by the additive action of both cytokines. To test that A549 tumorspheres were treated with each of the cytokines alone or in a combination for the time of 96h. As shown in Figure 4E, A549 cells upregulated *GFPT2* transcripts and protein in response to TNF but not TGFβ. Additionally, the most robust upregulation of *GFPT2* expression is observed when both cytokines are used to stimulate tumorspheres. Collectively results shown in Figure 4 indicate that *GFPT2* is an immediate early gene target upregulated in response to TNF alone and in combination with TGFβ and that elevated protein expression of this rate-limiting enzyme in UDP-GlcNAc synthesis occurs with similar kinetics as other markers of mesenchymal transition in LUAD. This is the first report indicating that *GFPT2* is an inducible gene expressed in NSCLC.

The *GFPT2* gene is transcriptionally regulated by NF-κB

Data shown in Figure 4E indicate that *GFPT2* is an immediate-early transcriptional target upregulated in response to TNF alone. Thus decided to examine whether *GFPT2* is a target of NF-κB, a canonical pathway activated downstream of the TNF receptor (5). To address this we analyzed the chromatin occupancy of the *GFPT2* promoter for RelA/p65 subunit of NF-κB in TNF stimulated A549 cells using publically available ChIP-Seq dataset (24). Interestingly ChIP-Seq reads for RelA/p65 show a significant enrichment within two peaks (sites A and B) located between intron four and six of the *GFPT2* gene, relative to unstimulated A549 control cells (Figure 5A). Our inability to detect binding of p65 to the proximal promoter of the gene is consistent with previous reports (46). Importantly the RelA/p65 enrichment sites A and B correlated with histone modifications associated with active enhancers, namely histone H3K4me1 and H3K4me2, and with marks known to correlate with active promoters, H3K4me3, H3K9Ac and H3K27Ac (19). Both RelA/p65 enrichments and histone H3 modifications overlapped specifically at sites A and B and were not observed at distal sites surrounding the *GFPT2* proximal promoter (Supplementary S2). This unique pattern of chromatin occupancy for RelA/p65 suggests that NF-κB was regulating *GFPT2* gene expression through the distal enhancer sites A and B located deep within the body of the gene. To confirm that NF-κB is directly regulating *GFPT2* expression, we utilized a super-repressor IκBα construct (SR-IκBα) encoding for the IκB protein mutated at residues 32

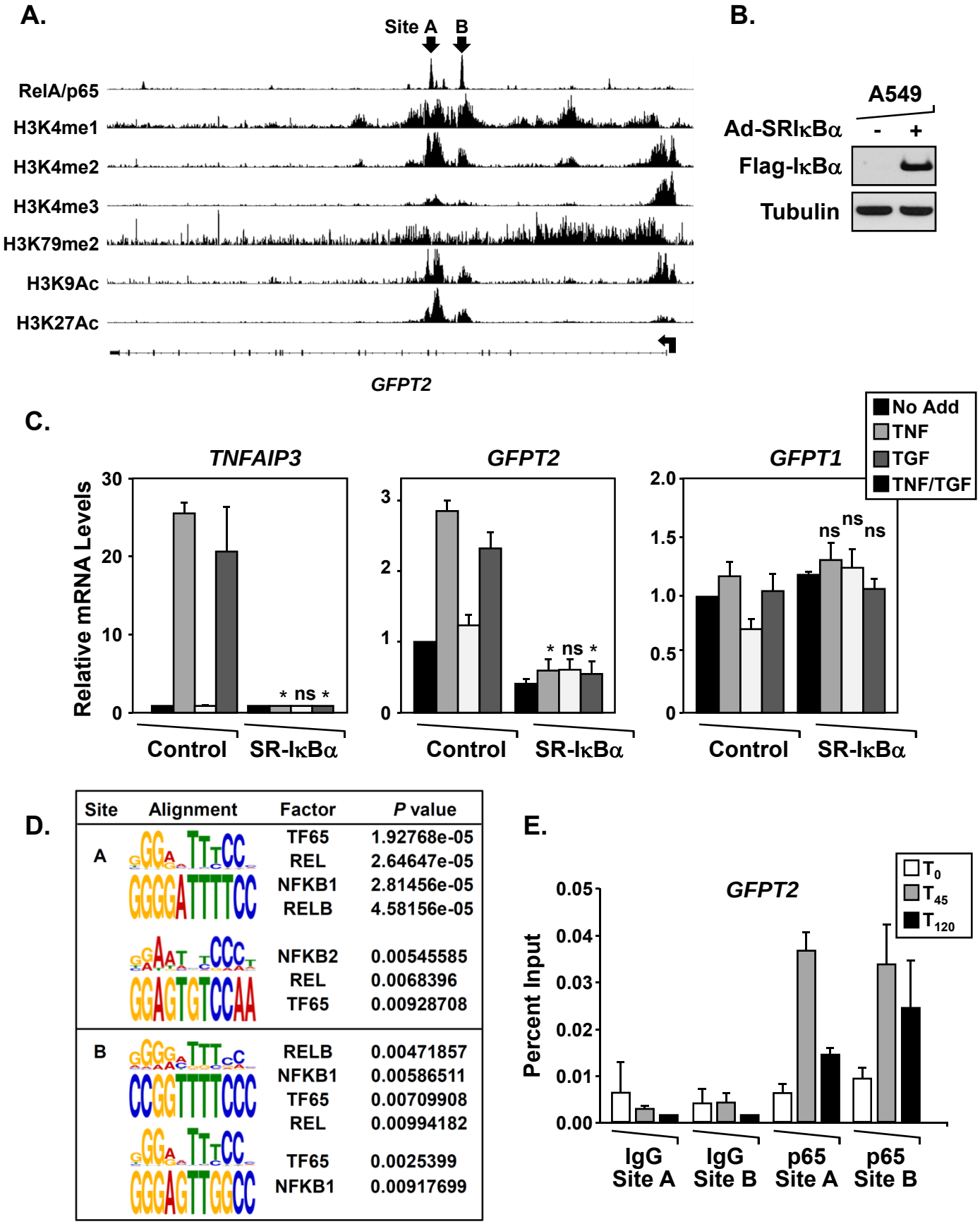
A.
Site A
B
RelA/p65
H3K4me1
H3K4me2
H3K4me3
H3K79me2
H3K9Ac
H3K27Ac
GFPT2
B.
A549
Ad-SRIκBα
-
+
Flag-IκBα
Tubulin
C.
No Add
TNF
TGF
TNF/TGF
TNFAIP3
GFPT2
GFPT1
Relative mRNA Levels
30
20
10
0
3
2
1
2.0
1.5
1.0
0.5
* ns *
* ns *
ns ns ns
Control
SR-IκBα
Control
SR-IκBα
Control
SR-IκBα
D.
Site
Alignment
Factor
P value
A
TF65
1.92768e-05
REL
2.64647e-05
NFKB1
2.81456e-05
RELB
4.58156e-05
NFKB2
0.00545585
REL
0.0068396
TF65
0.00928708
B
RELB
0.00471857
NFKB1
0.00586511
TF65
0.00709908
REL
0.00994182
TF65
0.0025399
NFKB1
0.00917699
E.
GFPT2
T0
T45
T120
Percent Input
0.05
0.04
0.03
0.02
0.01
0.00
IgG Site A
IgG Site B
p65 Site A
p65 Site B

Figure 5. *GFPT2* is a direct target of NF-κB. (A) A caption of ChIP-Seq data for H3K4me1, H3K4me2, H3K4me3, H3K79me2, H3K9Ac and H3K27Ac from mesenchymal A549 cells and p65 ChIP-seq across *GFPT2* gene as visualized by Integrated Genome Viewer. Site A and B indicate two RelA/p65 binding peaks within the body of *GFPT2*. An arrow indicates transcription start of *GFPT2* from right to left. (B) A549 cells were infected with adenovirus encoding GFP control (-) or Flag-tagged non-degradable form of IκBα, called super-repressor (SR-IκBα)**.** Expression of the construct was confirmed by immunoblotting. Tubulin probing was used as a loading control. (C) A549 cells infected with adenovirus encoding GFP (Control) or super-repressor (SR-IκBα) were treated with TNF (TNF), TGFβ (TGF), or TNF and TGFβ (TNF/TGF). Levels of mRNA of *GFPT2*, *GFPT1* and TNFAIP3 were measured by QRT-PCR and normalized to mRNA levels of HPRT. (D) DNA sequences corresponding to site A and B were analyzed using Jaspar (jaspar.genereg.net). Weighted alignments for NF-κB cis-elements are shown along with p values and bases depicted with different colors (E) A549 cells were treated with TNF for indicated times followed by ChIP-PCR for p65 and IgG control. Two primer sets that bind to Site A and Site B within *GFPT2* gene were used for qPCR to quantify the amount of immunoprecipitated DNA that is represented as percent input.

and 36, rendering it resistant to ubiquitin-mediated proteasomal degradation, to specifically block NF-κB pathway (25). A549 cell line was infected with adenovirus encoding for Flag-tagged SR-IκBα or GFP control and treated with TNF or TGFβ for 2hrs. The expression of epitope-tagged SR- IκBα was confirmed by immunoblotting with Flag antibody (Figure 5B). Consistent with our previous observations TNF and combination of TNF/TGFβ but not TGFβ alone was able to up-regulate *GFPT2* levels in GFP-expressing control cells (Figure 5C). Remarkably inhibition of NF-κB pathway by SR-IκBα expression completely abolished TNF-dependent induction of *GFPT2* and decreased basal *GFPT2* mRNA levels (Figure 5C). Similar effect of SR-IκBα expression was observed for TNFAIP3 gene, a known NF-κB regulated target but not *GFPT1* isoform (Figure 5C). These observations indicate that NF-κB pathway is required for *GFPT2* expression on the basal level and following TNF/TGFβ treatment in A549 adenocarcinoma cells. To further confirm direct binding of p65 to the distal enhancer sited of *GFPT2* we performed ChIP-PCR for p65 on A549 cell line treated with TNF for 0, 45 and 120 min. Two sets of primers were used that amplify 200bp region around the center of the peaks A and B. Consistent with ChIP-seq data we observe a time-dependent increase in p65 binding to both site A and site B within body of *GFPT2* in response to TNF treatment as compared to control IgG (Figure 5D). For the first time, our results identify *GFPT2* as a novel NF-κB-regulated gene in NSCLC.

GFPT2 regulates protein O-GlcNAcylation and migration of mesenchymal NSCLC cells

Next we sought to determine the biological function of *GFPT2* in mesenchymal NSCLC cells. To address this we first generated a stable A549 cell line with doxycycline-inducible shRNA-mediated silencing of *GFPT2* and control cell line expressing scrambled shRNAs (Materials & Methods). Generated cell lines were either pre-treated with doxycycline for 2 days or left untreated followed by the induction of EMT in tumorspheres with a combination of TNF/TGFβ. The analysis of *GFPT2* mRNA levels shows the knock-down efficiency of 60-70% which correlates with a decrease in GFPT2 protein level in doxycycline pre-treated cells (Figure 6A and 6B). Importantly *GFPT2* knock-down results in a decrease in a global protein O-GlcNAcylation levels detected by immunoblotting in both epithelial and mesenchymal cells, consistent with its role as the rate-limiting enzyme in UDP-GlcNAc synthesis (Figure 6B). Remarkably, we observed a decrease in migration and invasion of mesenchymal A549 cells as measured by Boyden Chamber assay following *GFPT2* silencing (Figure 6C). The effect of doxycycline on cell migration was ruled out using scrambled RNA-expressing cell line in which the effect on migration and invasion was not observed. Similar results were observed after siRNA-mediated silencing of *GFPT2* in H1299 cell line, compared to control siRNA cells (Supplemental S4). Notably *GFPT2* knockdown did not visibly affect the efficacy of EMT since changes of epithelial and mesenchymal markers were still observed following induction of

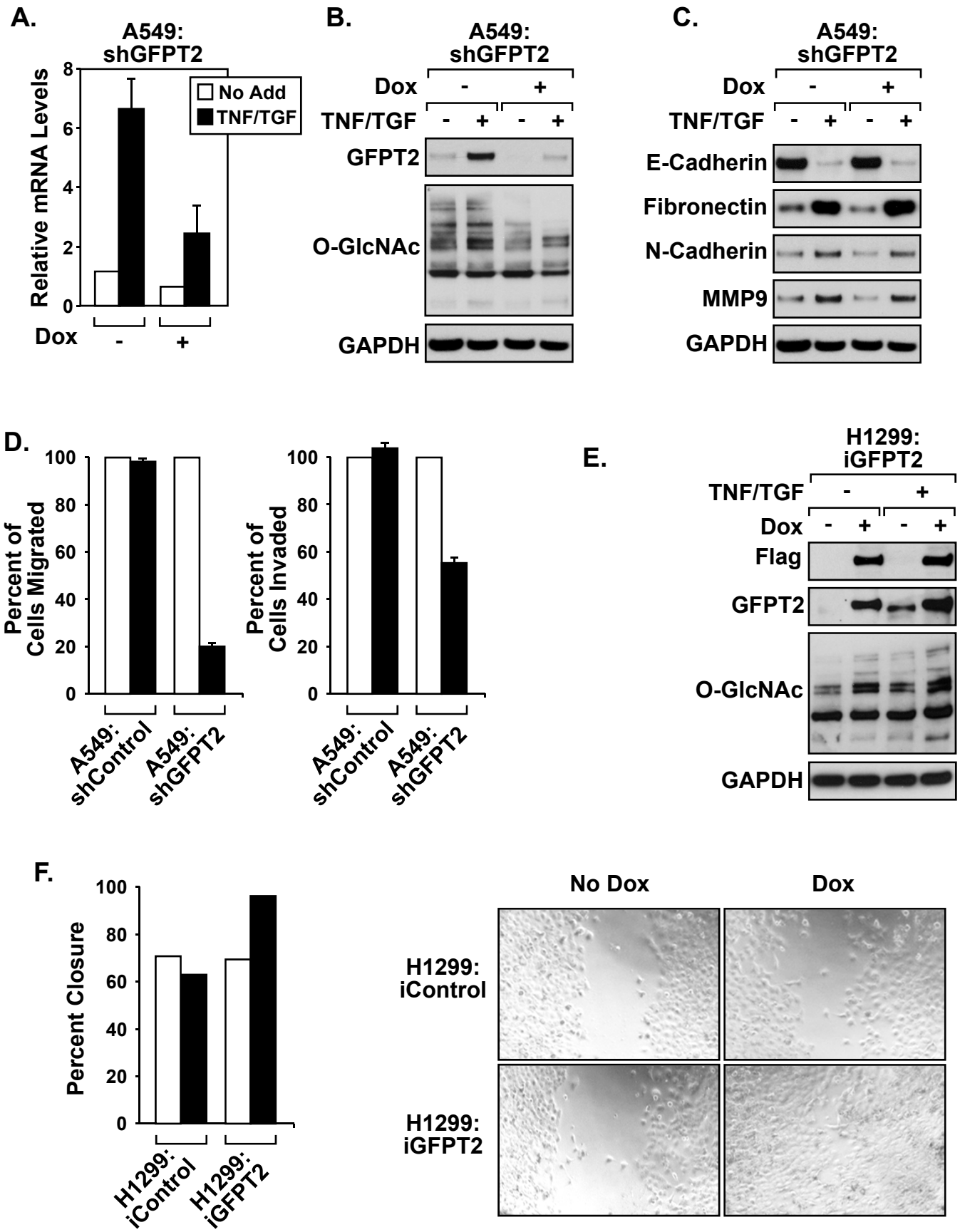
A.
A549: shGFPT2
Relative mRNA Levels
No Add
TNF/TGF
Dox
B.
A549: shGFPT2
Dox
TNF/TGF
GFPT2
O-GlcNAc
GAPDH
C.
A549: shGFPT2
Dox
TNF/TGF
E-Cadherin
Fibronectin
N-Cadherin
MMP9
GAPDH
D.
Percent of Cells Migrated
Percent of Cells Invaded
A549: shControl
A549: shGFPT2
E.
H1299: iGFPT2
TNF/TGF
Dox
Flag
GFPT2
O-GlcNAc
GAPDH
F.
Percent Closure
H1299: iControl
H1299: iGFPT2
No Dox
Dox

Figure 6. GFPT2 regulates migration of mesenchymal NSCLC. Stable A549 cell lines expressing doxycycline-inducible GFPT2 shRNA or scrambled control shRNAs were cultured in tumorspheres without or with the addition of TNF and TGFβ, with or without addition of doxycycline, as indicated. (A) Levels of *GFPT2* transcripts were measured by QRT-PCR in the absence or presence of doxycycline (B) Protein levels of GFAT2 and global O-GlcNAcylation were assessed by immunoblotting. GAPDH served as a protein loading control I immunoblots. (C) Levels of epithelial (E-cadherin) and mesenchymal markers (Fibronectin, N-cadherin, MMP9) were assessed by immunoblotting. GAPDH probing was used as a loading control. (D) 3D spheroids were trypsinized and plated in Boyden-chambers for invasion and migration assays. Numbers of migrated and invaded cells without Doxycycline treatment for each cell line were set as 100%. (E, F). Stable H1299 cell line expressing Doxycycline-inducible V5-tagged *GFPT2* construct or Luciferase control were cultured in 3D spheroids without (-) or with the addition of TNF and TGFβ (+), with or without addition of Doxycycline, as indicated. (E) Protein levels of V5 tag, GFAT2 and global O-GlcNAcylation were assessed by immunoblotting. GAPDH probing was used as a loading control. (F) Spheroid cultures were trypsinized and replated at high density for wound healing assay. A surface of the gap was measured using TScratch software (45).

EMT (Figure 6B and Supplementary S3). To further confirm our results we generated stable H1299 cell line expressing doxycycline-inducible V5-tagged GFPT2 protein or luciferase expressing control using pRetro inducible system (Materials & Methods). In a similar manner, cells were pre-treated with doxycycline for 2 days or left untreated and then induced to undergo EMT in tumorspheres with a combination of TNF/TGFβ. Efficient induction of ectopic *GFPT2* was observed following doxycycline pretreatment by immunoblot analysis for V5 tag (Figure 6D). Importantly ectopic *GFPT2* expression causes elevation in global protein O-GlcNAcylation in both epithelial and mesenchymal cells (Figure 6C). Next we analyzed migration of mesenchymal H1299 using wound-healing assay. Notably ectopic expression of *GFPT2* in mesenchymal cells lead to increased migration measured in wound healing assays (Figure 6F). This effect was not observed in luciferase expressing control cell line (Figure 6F). Thus, experiments shown in Figure 6 indicate that GFPT2 is required and sufficient to induce cell migration, but that GFPT2 is not required for efficient induction of EMT.

DISCUSSION

EMT UDP-N-acetylglucosamine (UDP-GlcNAc), the end-product of the hexosamine biosynthesis pathway (HBP) is utilized in the synthesis of glycans and protein glycosylation, including O-GlcNAcylation of nucleocytoplasmic proteins catalyzed by the enzymes OGT and OGA (11). Increased metabolic flux through HBP and elevated glycan content, have been associated with cancer progression and metastasis. Despite this understanding the mechanisms controlling the transcriptional regulation of HBP in cancer cells is vastly unknown (12-17). NF-κB is a pleiotropic transcription factor implicated in development and progression of lung cancer (30-32). Recently our group showed that NF-κB is required for epithelial to mesenchymal transition in non-small cell lung cancer cells, a process believed to drive cancer metastasis by cancer cells with mesenchymal phenotypes. Mesenchymal cells exhibit unique characteristics including increased migration, invasion, resistance to apoptotic cues and self-renewal capacity (4, 7). Here we utilize our previously described tumorspheres cultures stimulated with TGFβ and TNF to show that global protein O-GlcNAcylation is elevated in mesenchymal NSCLC cells and that siRNA mediated silencing of OGT blocks EMT. Using gene expression microarray confirmed by qPCR we identify a list of metabolic genes up-regulated in mesenchymal cells that can contribute to the increased flux through HBP. Notably, we identify *GFPT2*, glutamine: fructose-6-phposphate aminotransferase 2, the first and rate-limiting enzyme utilized in the HBP, as an inducible gene in

mesenchymal NSCLC. *GFPT2* is an immediate-early gene up-regulated in response to TNF treatment or a combination of TNF and TGFβ, but not TGFβ alone. Importantly we show that *GFPT2* is co-expressed with several well established mesenchymal genes in lung adenocarcinoma (LUAD), including *INHBA. INHBA* encodes for Activin A, a cytokine recently identified by our group as the autocrine maintenance factor of mesenchymal NSCLC cells, which is associated with increased invasiveness and stemness and poor clinical outcome (7). Consistent with this observation, high *GFPT2* expression correlates with poor clinical outcome of LUAD patients. Recently a global analysis of mRNA expression profiles of 1,704 metabolic genes in 978 human cancer cell lines listed *GFPT2* as a metabolic gene associated with mesenchymal gene signatures by unsupervised hierarchical clustering (33). This is the first report showing that GFPT2 is an inducible gene expressed in mesenchymal NSCLC, the expression of which has otherwise been considered to be limited predominantly to the central nervous system (CNS) and that it is marker of mesenchymal state of lung cancer cells (21). Furthermore using a non-degradable mutant of IκB to selectively block NF-κB pathway, we show that GFPT2 is directly regulated by NF-κB both on the basal level and following TNF-mediated stimulation. Using publically available RelA/p65 ChIP-seq dataset in TNF-stimulated A549 cell confirmed by a ChIP-PCR in A549 treated with TNF for 45 and 120 min, we show that p65 directly binds to two distal binding sites located between intron four and six of the *GFPT2* gene, but not in the proximal promoter region. Notably two p65 binding sites overlapped with histone

modifications associated with active enhancers, namely histone H3K4me1 and H3K4me2, and with marks known to correlate with active promoters, H3K4me3, H3K9Ac and H3K27Ac suggesting that they are active enhancers driving NF-κB-dependent *GFPT2* transcription. This is the first report identifying *GFPT2* as a novel NF-κB target, linking NF-κB activation with the flux through HBP. We investigated the role of *GFPT2* in mesenchymal NSCLC cells by inducible silencing of its expression and observed a decrease in global protein O-GlcNAcylation consistent with *GFPT2* role as a rate-limiting enzyme in HBP (11). Moreover, we show that the silencing of *GFPT2* decreases migration and invasion of mesenchymal NSCLC cells. Conversely using doxycycline-inducible ectopic *GFPT2* expression we observe an increase in global protein O-GlcNAcylation and increase migration of mesenchymal cells. These results identify a novel function of *GFPT2* in NSCLC mesenchymal cells in the regulation of cell migration and invasion. Consistent with these results is a recent report showing that silencing of *GFPT1* in human keratinocytes decreased cell migration (34). The mechanism of the effect of *GFPT2* on cell migration requires further investigation. Increased levels of O-GlcNAcylation have been shown to affect migration of breast cancer cells via modification of actin-binding protein cofilin that promotes its localization and invadopodia at the leading edge of migrating cells (35). Silencing of *GFPT2* did not however entirely eradicate O-GlcNAc modification, as compared to silencing of OGT likely due to the basal presence of *GFPT1* isoform sustaining the HBP flux. As a result knockdown of *GFPT2* in mesenchymal cells did not block EMT similar to OGT silencing shown

by us and others (47). This result does not rule out the possibility of GFPT2 involvement in EMT. Indeed *GFPT2* overexpression in A549 cells has been shown to promote TGFβ-induced EMT in monolayer cultures via elevation of expression of oncofetal fibronectin and its mucin-type O-linked glycosylation (12). We did not observe similar effect in H1299 NSCLC cells likely due to differences in experimental system. Given the differences in modes of regulation by UDP-GlcNAc and PKA it is possible that cells in a specific signaling and metabolic context would rely entirely on GFPT2 as the rate-limiting enzyme of HBP due to UDP-GlcNAc feedback inhibition of GFPT1 isoform (36-39). In this environmental context that effect of *GFPT2* on EMT could be more pronounced. Change in a global protein O-GlcNAcylation following manipulation of *GFPT2* expression implies altered flux through the HBP. In addition to protein O-GlcNAcylation, UDP-GlcNAc is required for the synthesis of poly-glycans which have been shown to affect cell migration in multiple cancer types (12-17). It has been shown that increased concentration of UDP-GlcNAc promotes multi-branched N-glycosylation and the synthesis of hyaluronan (48-49). Importantly both hyaluronan and glycosylated proteins including fibronectin and collagens are essential components of tumor ECM (50). Mesenchymal cancer cells are characterized by the increased capacity to secrete ECM (51). Thus it is possible that inducible expression of GFPT2 in mesenchymal cells serves the purpose of elevating UDP-GlcNAc over the basal levels of UDP-GlcNAc produced by GFPT1, specifically for the formation of ECM. Notably, components of ECM serve as ligands for the cell surface receptors, including integrins and CD44 to

promote cancer cell migration and invasion. ECM/integrin engagement activate cellular signaling pathways including stimulation of focal adhesion kinase (FAK) as well as RHO family of small GTPases including RHO, CDC42 and RAC proteins, which can further stimulate ERK via p21-activated kinase (PAK) (52). Additionally CD44 binding to inactive form of matrix metalloproteinases (MMPs) called zymogens, promotes their proteolytic activation (53). Active MMPs are responsible for the digestion of protein components of ECM exposing their Arg-Gly-Asp (RGD) sites that serve as ligands for integrins (54). Increased binding of integrins stimulates membrane translocation of growth factor receptors and the binding of activated growth factors released from degraded ECM (55). Importantly, both integrins and growth factor receptors require N-linked glycosylation for proper membrane localization (56). This sets up a positive signaling feedback-loop resulting in increased cell migration and invasion. Interestingly we do observe interactions of GFPT2 with the small GTPases and components of vesicular transport system suggesting that GFPT2 may have a specific function in the cell distinct from GFPT1 (data not shown). Taken together our results identify *GFPT2* as a novel target of NF-κB pathway and important mesenchymal marker implicated in migration of mesenchymal NSCLC cells. This is the first report showing the regulation of HBP by NF-κB. This observation will most likely hold true in other cellular responses that activate NF-κB, in particular to stress signals, that have also been shown to elevate protein O-GlcNAcylation to act pro-survival and anti-apoptotic both in cancer cells as well as in other biological stress conditions including ischemia-reperfusion injury or diabetes (40-

43). Importantly, despite high amino acid similarity between GFPT1 and GFPT2, the two enzymes show differential regulation by PKA and UDP-GlcNAc, suggesting that they significantly differ in their biological properties, and might be specifically targeted with small molecule inhibitors. Our work presented here shows that GFPT2 isoform is induced in mesenchymal NSCLC cells and is required for migration and invasion. It is in contrast to ubiquitously expressed GFPT1 isoform. Thus GFPT2 constitutes a promising target for therapy aimed at blocking cancer metastasis.

REFERENCES

1. www.cancer.org

2. Bender E. Epidemiology: The dominant malignancy. *Nature.* 2014 Sep 11; 513(7517): S2-3.

3. De Craene B, Berx G. Regulatory networks defining EMT during cancer initiation and progression. *Nat Rev Cancer.* 2013 Feb; 13(2): 97-110.

4. Kumar M, Allison DF, Baranova NN, Wamsley JJ, Katz AJ, Bekiranov S, Jones DR, Mayo MW. NF-kappaB regulates mesenchymal transition for the induction of non-small cell lung cancer initiating cells.*PLoS One.* 2013 Jul 30; 8(7): e68597. PMCID: PMC3728367.

5. Napetschnig J, Wu H. Molecular basis of NF-kappaB signaling. *Annu Rev Biophys.* 2013; 42: 443-468. PMCID: PMC3678348.

6. Huang B, Yang XD, Lamb A, Chen LF. Posttranslational modifications of NF-kappaB: Another layer of regulation for NF-kappaB signaling pathway. *Cell Signal.* 2010 Sep; 22(9): 1282-1290. PMCID: PMC2893268.

7. Wamsley JJ, Kumar M, Allison DF, Clift SH, Holzknecht CM, Szymura SJ, Hoang SA, Xu X, Moskaluk CA, Jones DR, Bekiranov S, Mayo MW. Activin upregulation by NF-kappaB is required to maintain mesenchymal features of cancer stem-like cells in non-small cell lung cancer. *Cancer Res.* 2015 Jan 15; 75(2): 426-435. PMCID: PMC4297542.

8. Hanahan D, Weinberg RA. Hallmarks of cancer: The next generation. *Cell.* 2011 Mar 4; 144(5): 646-674.

9. Vander Heiden MG, Cantley LC, Thompson CB. Understanding the warburg effect: The metabolic requirements of cell proliferation. *Science.* 2009 May 22; 324(5930): 1029-1033. PMCID: PMC2849637.

10. Hensley CT, Wasti AT, DeBerardinis RJ. Glutamine and cancer: Cell biology, physiology, and clinical opportunities. *J Clin Invest.* 2013 Sep; 123(9): 3678-3684. PMCID: PMC3754270.

11. Abdel Rahman AM, Ryczko M, Pawling J, Dennis JW. Probing the hexosamine biosynthetic pathway in human tumor cells by multitargeted tandem mass spectrometry. *ACS Chem Biol.* 2013 Sep 20; 8(9): 2053-2062.

12. Alisson-Silva F, Freire-de-Lima L, Donadio JL, Lucena MC, Penha L, Sa-Diniz JN, Dias WB, Todeschini AR. Increase of O-glycosylated oncofetal fibronectin in high glucose-induced epithelial-mesenchymal transition of cultured human epithelial cells. *PLoS One.* 2013 Apr 12; 8(4): e60471. PMCID: PMC3625189.

13. Xu Q, Isaji T, Lu Y, Gu W, Kondo M, Fukuda T, Du Y, Gu J. Roles of N-acetylglucosaminyltransferase III in epithelial-to-mesenchymal transition induced by transforming growth factor beta1 (TGF-beta1) in epithelial cell lines. *J Biol Chem.* 2012 May 11; 287(20): 16563-16574. PMCID: PMC3351319.

14. Yehezkel G, Cohen L, Kliger A, Manor E, Khalaila I. O-linked beta-N-acetylglucosaminylation (O-GlcNAcylation) in primary and metastatic colorectal cancer clones and effect of N-acetyl-beta-D-glucosaminidase silencing on cell phenotype and transcriptome. *J Biol Chem.* 2012 Aug 17; 287(34): 28755-28769. PMCID: PMC3436545.

15. Lynch TP, Ferrer CM, Jackson SR, Shahriari KS, Vosseller K, Reginato MJ. Critical role of O-linked beta-N-acetylglucosamine transferase in prostate cancer invasion, angiogenesis, and metastasis. *J Biol Chem.* 2012 Mar 30; 287(14): 11070-11081. PMCID: PMC3322861.

16. Park SY, Kim HS, Kim NH, Ji S, Cha SY, Kang JG, Ota I, Shimada K, Konishi N, Nam HW, Hong SW, Yang WH, Roth J, Yook JI, Cho JW. Snail1 is stabilized by O-GlcNAc modification in hyperglycaemic condition. *EMBO J.* 2010 Nov 17; 29(22): 3787-3796. PMCID: PMC2989108.

17. Bond MR, Hanover JA. A little sugar goes a long way: The cell biology of O-GlcNAc. *J Cell Biol.* 2015 Mar 30; 208(7): 869-880. PMCID: PMC4384737.

18. Allison DF, Wamsley JJ, Kumar M, Li D, Gray LG, Hart GW, Jones DR, Mayo MW. Modification of RelA by O-linked N-acetylglucosamine links glucose metabolism to NF-kappaB acetylation and transcription.*Proc Natl Acad Sci U S A.* 2012 Oct 16; 109(42): 16888-16893. PMCID: PMC3479489.

19. Cieslik M, Hoang SA, Baranova N, Chodaparambil S, Kumar M, Allison DF, Xu X, Wamsley JJ, Gray L, Jones DR, Mayo MW, Bekiranov S. Epigenetic coordination of signaling pathways during the epithelial-mesenchymal transition. *Epigenetics Chromatin.* 2013 Sep 2; 6(1): 28-8935-6-28. PMCID: PMC3847279.

20. http://humancyc.org/

21. Oki T, Yamazaki K, Kuromitsu J, Okada M, Tanaka I. cDNA cloning and mapping of a novel subtype of glutamine:Fructose-6-phosphate

amidotransferase (GFAT2) in human and mouse. *Genomics.* 1999 Apr 15; 57(2): 227-234.

22. Gyorffy B, Surowiak P, Budczies J, Lanczky A. Online survival analysis software to assess the prognostic value of biomarkers using transcriptomic data in non-small-cell lung cancer. *PLoS One.* 2013 Dec 18; 8(12): e82241. PMCID: PMC3867325.

23. Kim P, Cheng F, Zhao J, Zhao Z. ccmGDB: A database for cancer cell metabolism genes. *Nucleic Acids Res.* 2016 Jan 4; 44(D1): D959-68. PMCID: PMC4702820.

24. Raskatov JA, Meier JL, Puckett JW, Yang F, Ramakrishnan P, Dervan PB. Modulation of NF-kappaB-dependent gene transcription using programmable DNA minor groove binders. *Proc Natl Acad Sci U S A.* 2012 Jan 24; 109(4): 1023-1028. PMCID: PMC3268328.

25. Van Antwerp DJ, Martin SJ, Kafri T, Green DR, Verma IM. Suppression of TNF-alpha-induced apoptosis by NF-kappaB. *Science.* 1996 Nov 1; 274(5288): 787-789.

26. Okuda H, Kobayashi A, Xia B, Watabe M, Pai SK, Hirota S, Xing F, Liu W, Pandey PR, Fukuda K, Modur V, Ghosh A, Wilber A, Watabe K. Hyaluronan synthase HAS2 promotes tumor progression in bone by stimulating the interaction of breast cancer stem-like cells with macrophages and stromal cells. *Cancer Res.* 2012 Jan 15; 72(2): 537-547. PMCID: PMC3404816.

27. Yan T, Lin Z, Jiang J, Lu S, Chen M, Que H, He X, Que G, Mao J, Xiao J, Zheng Q. MMP14 regulates cell migration and invasion through epithelial-mesenchymal transition in nasopharyngeal carcinoma. *Am J Transl Res.* 2015 May 15; 7(5): 950-958. PMCID: PMC4494146.

28. Baker AM, Bird D, Lang G, Cox TR, Erler JT. Lysyl oxidase enzymatic function increases stiffness to drive colorectal cancer progression through FAK. *Oncogene.* 2013 Apr 4; 32(14): 1863-1868.

29. Meylan E, Dooley AL, Feldser DM, Shen L, Turk E, Ouyang C, Jacks T. Requirement for NF-kappaB signalling in a mouse model of lung adenocarcinoma. *Nature.* 2009 Nov 5; 462(7269): 104-107. PMCID: PMC2780341.

30. Stathopoulos GT, Sherrill TP, Cheng DS, Scoggins RM, Han W, Polosukhin VV, Connelly L, Yull FE, Fingleton B, Blackwell TS. Epithelial NF-kappaB

activation promotes urethane-induced lung carcinogenesis. *Proc Natl Acad Sci U S A.* 2007 Nov 20; 104(47): 18514-18519. PMCID: PMC2141808.

31. Basseres DS, Ebbs A, Levantini E, Baldwin AS. Requirement of the NF-kappaB subunit p65/RelA for K-ras-induced lung tumorigenesis. *Cancer Res.* 2010 May 1; 70(9): 3537-3546. PMCID: PMC2862109.

32. Shaul YD, Freinkman E, Comb WC, Cantor JR, Tam WL, Thiru P, Kim D, Kanarek N, Pacold ME, Chen WW, Bierie B, Possemato R, Reinhardt F, Weinberg RA, Yaffe MB, Sabatini DM. Dihydropyrimidine accumulation is required for the epithelial-mesenchymal transition. *Cell.* 2014 Aug 28; 158(5): 1094-1109. PMCID: PMC4250222.

33. Oikari S, Makkonen K, Deen AJ, Tyni I, Karna R, Tammi RH, Tammi MI. Hexosamine biosynthesis in keratinocytes: Roles of GFAT and GNPDA enzymes in the maintenance of UDP-GlcNAc content and hyaluronan synthesis. *Glycobiology.* 2016 Feb 16.

34. Huang X, Pan Q, Sun D, Chen W, Shen A, Huang M, Ding J, Geng M. O-GlcNAcylation of cofilin promotes breast cancer cell invasion. *J Biol Chem.* 2013 Dec 20; 288(51): 36418-36425. PMCID: PMC3868755.

35. Graack HR, Cinque U, Kress H. Functional regulation of glutamine:Fructose-6-phosphate aminotransferase 1 (GFAT1) of drosophila melanogaster in a UDP-N-acetylglucosamine and cAMP-dependent manner. *Biochem J.* 2001 Dec 1; 360(Pt 2): 401-412. PMCID: PMC1222241.

36. Eguchi S, Oshiro N, Miyamoto T, Yoshino K, Okamoto S, Ono T, Kikkawa U, Yonezawa K. AMP-activated protein kinase phosphorylates glutamine : Fructose-6-phosphate amidotransferase 1 at Ser243 to modulate its enzymatic activity. *Genes Cells.* 2009 Feb; 14(2): 179-189

37. Hu Y, Riesland L, Paterson AJ, Kudlow JE. Phosphorylation of mouse glutamine-fructose-6-phosphate amidotransferase 2 (GFAT2) by cAMP-dependent protein kinase increases the enzyme activity. *J Biol Chem.* 2004 Jul 16; 279(29): 29988-29993.

38. Broschat KO, Gorka C, Page JD, Martin-Berger CL, Davies MS, Huang Hc HC, Gulve EA, Salsgiver WJ, Kasten TP. Kinetic characterization of human glutamine-fructose-6-phosphate amidotransferase I: Potent feedback inhibition by glucosamine 6-phosphate. *J Biol Chem.* 2002 Apr 26; 277(17): 14764-14770.

39. Chang Q, Su K, Baker JR, Yang X, Paterson AJ, Kudlow JE. Phosphorylation of human glutamine:Fructose-6-phosphate amidotransferase by cAMP-

dependent protein kinase at serine 205 blocks the enzyme activity. *J Biol Chem.* 2000 Jul 21; 275(29): 21981-21987.

40. Janssens S, Tschopp J. Signals from within: The DNA-damage-induced NF-kappaB response. *Cell Death Differ.* 2006 May; 13(5): 773-784.

41. Zachara NE, Molina H, Wong KY, Pandey A, Hart GW. The dynamic stress-induced "O-GlcNAc-ome" highlights functions for O-GlcNAc in regulating DNA damage/repair and other cellular pathways.*Amino Acids.* 2011 Mar; 40(3): 793-808. PMCID: PMC3329784.

42. Chatham JC, Not LG, Fulop N, Marchase RB. Hexosamine biosynthesis and protein O-glycosylation: The first line of defense against stress, ischemia, and trauma. *Shock.* 2008 Apr; 29(4): 431-440.

43. Ma J, Hart GW. Protein O-GlcNAcylation in diabetes and diabetic complications. *Expert Rev Proteomics.* 2013 Aug; 10(4): 365-380. PMCID: PMC3985334.

44. Zachara NE, O'Donnell N, Cheung WD, Mercer JJ, Marth JD, Hart GW. Dynamic O-GlcNAc modification of nucleocytoplasmic proteins in response to stress. A survival response of mammalian cells. *J Biol Chem.* 2004 Jul 16; 279(29): 30133-30142.

45. Geback T, Schulz MM, Koumoutsakos P, Detmar M. TScratch: A novel and simple software tool for automated analysis of monolayer wound healing assays. *BioTechniques.* 2009 Apr; 46(4): 265-274.

46. Yamazaki K, Mizui Y, Oki T, Okada M, Tanaka I. Cloning and characterization of mouse glutamine:Fructose-6-phosphate amidotransferase 2 gene promoter. *Gene.* 2000 Dec 31; 261(2): 329-336.

47. Lucena MC, Carvalho-Cruz P, Donadio JL, Oliveira IA, de Queiroz RM, Marinho-Carvalho MM, de Paula IF, Gondim KC, McComb ME, Costello CE, Whelan SA, Todeschini AR, Dias WB. Epithelial mesenchymal transition induces aberrant glycosylation through hexosamine biosynthetic pathway activation. *J Biol Chem.* 2016 Apr 18.

48. Rilla K, Oikari S, Jokela TA, Hyttinen JM, Karna R, Tammi RH, Tammi MI. Hyaluronan synthase 1 (HAS1) requires higher cellular UDP-GlcNAc concentration than HAS2 and HAS3. *J Biol Chem.* 2013 Feb 22; 288(8): 5973-5983. PMCID: PMC3581382.

49. Sasai K, Ikeda Y, Fujii T, Tsuda T, Taniguchi N. UDP-GlcNAc concentration is an important factor in the biosynthesis of beta1,6-branched oligosaccharides: Regulation based on the kinetic properties of N-acetylglucosaminyltransferase V. *Glycobiology.* 2002 Feb; 12(2): 119-127.

50. Bonnans C, Chou J, Werb Z. Remodelling the extracellular matrix in development and disease. *Nat Rev Mol Cell Biol.* 2014 Dec; 15(12): 786-801. PMCID: PMC4316204.

51. O'Connor JW, Gomez EW. Biomechanics of TGFbeta-induced epithelial-mesenchymal transition: Implications for fibrosis and cancer. *Clin Transl Med.* 2014 Jul 15; 3: 23-1326-3-23. eCollection 2014. PMCID: PMC4114144.

52. Hood JD, Cheresh DA. Role of integrins in cell invasion and migration. *Nat Rev Cancer.* 2002 Feb; 2(2): 91-100.

53. Yu Q, Stamenkovic I. Localization of matrix metalloproteinase 9 to the cell surface provides a mechanism for CD44-mediated tumor invasion. *Genes Dev.* 1999 Jan 1; 13(1): 35-48. PMCID: PMC316376.

54. Rozario T, DeSimone DW. The extracellular matrix in development and morphogenesis: A dynamic view. *Dev Biol.* 2010 May 1; 341(1): 126-140. PMCID: PMC2854274.

55. Ju L, Zhou C. Association of integrin beta1 and c-MET in mediating EGFR TKI gefitinib resistance in non-small cell lung cancer. *Cancer Cell Int.* 2013 Feb 13; 13(1): 15-2867-13-15. PMCID: PMC3583715.

56. Lau KS, Dennis JW. N-glycans in cancer progression. *Glycobiology.* 2008 Oct; 18(10): 750-760.

57. Robinson JT, Thorvaldsdottir H, Winckler W, Guttman M, Lander ES, Getz G, Mesirov JP. Integrative genomics viewer. *Nat Biotechnol.* 2011 Jan; 29(1): 24-26. PMCID: PMC3346182.

58. Thorvaldsdottir H, Robinson JT, Mesirov JP. Integrative genomics viewer (IGV): High-performance genomics data visualization and exploration. *Brief Bioinform.* 2013 Mar; 14(2): 178-192. PMCID: PMC3603213.

Supplementary Figures

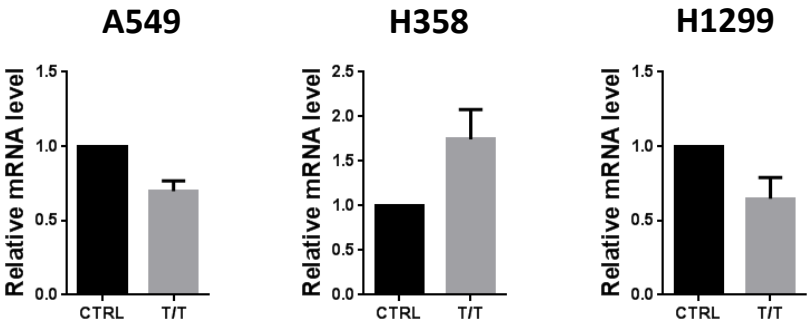
A549
H358
H1299
Relative mRNA level
1.5
1.0
0.5
0.0
2.5
2.0
CTRL
T/T

Supplementary Figure S1. Expression of *GFPT1* in mesenchymal NSCLCs. NSCLC cell lines A549, H358 and H1299 were grown in tumorspheres stimulated with TNF/TGFβ (T/T) or left untreated (CTRL), as described in materials and methods. QRT-PCR analysis was performed for *GFPT1*. Transcription levels were normalized to *HPRT* control and expressed as a fold-induction over unstimulated control cells.

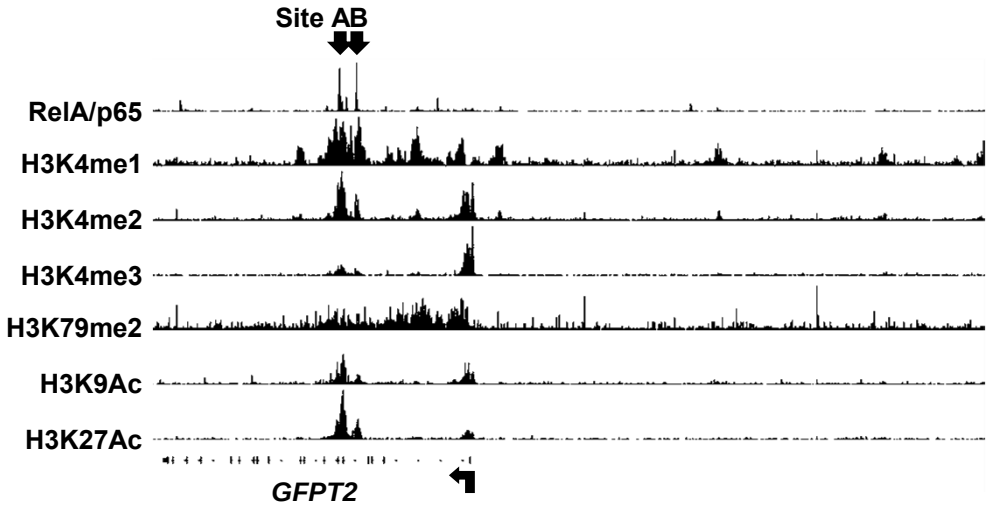
Site AB
RelA/p65
H3K4me1
H3K4me2
H3K4me3
H3K79me2
H3K9Ac
H3K27Ac
GFPT2

Supplementary Figure S2. Epigenetic landscape of the proximal promoter of *GFPT2* confirms the location of the NF-κB enhancer within the body of the gene locus. ChIP-seq data for histone marks in A549 was retrieved from ENCODE database (https://genome.ucsc.edu/ENCODE/). ChIP-seq for p65 was obtained from Roskov. et. al. (24). Signals were overlaid and visualized using Integrated Genome Viewer (IGV) software (57-58). An arrow underneath ChIP-seq data indicated transcription start site and direction of *GFPT2* gene from right to left.

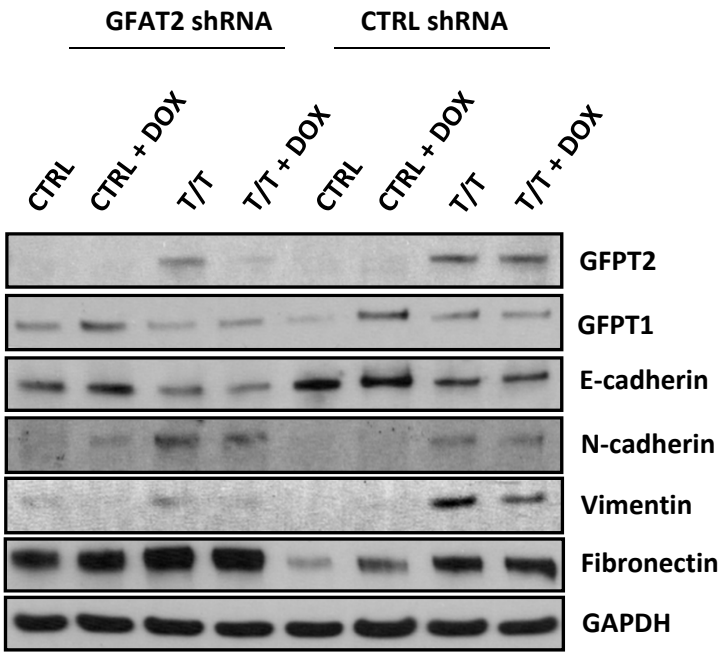
GFAT2 shRNA
CTRL shRNA
CTRL
CTRL + DOX
T/T
T/T + DOX
CTRL
CTRL + DOX
T/T
T/T + DOX
GFPT2
GFPT1
E-cadherin
N-cadherin
Vimentin
Fibronectin
GAPDH

Supplementary Figure S3. *GFPT2* knockdown does not block the induction of EMT markers. Stable A549 cell lines expressing doxycycline-inducible GFPT2 shRNA or control constitutive scrambled shRNAs were generated as described in materials and methods and were treated without or with doxycycline (+DOX) during formation of tumorspheres and during subsequent culturing in tumorspheres stimulated with TNF/TGFβ (T/T) or without stimulation (CTRL). Immunoblot analysis was performed using primary antibodies that detect GFPT1, GFPT2 and the epithelial marker E-cadherin and mesenchymal markers (Fibronectin, N-cadherin and Vimentin). GAPDH was used as a loading control.

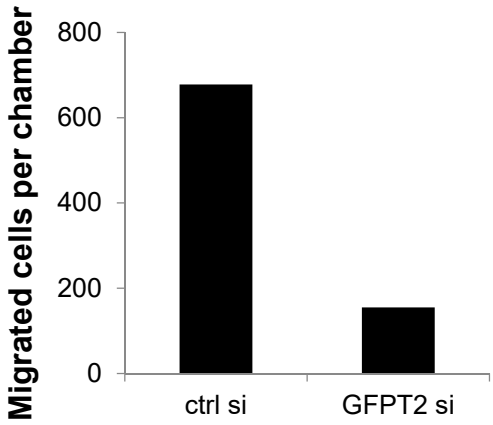
Migrated cells per chamber
800
600
400
200
0
ctrl si
GFPT2 si

Supplementary Figure S4. siRNA-mediated silencing of *GFPT2* reduces migration of H1299 NSCLC cells. H1299 cells were transfected with control siRNA (CTRLsi) or GFPT2 siRNA (GFPT2si) and cultured in tumorspheres with addition of TNF/TGFβ as described in materials and methods. Cells were trypsinized and plated into Boyden migration chambers and incubated for 15h followed by fixation in methanol and staining with crystal violet. Cell migration was quantified as described in materials and methods.

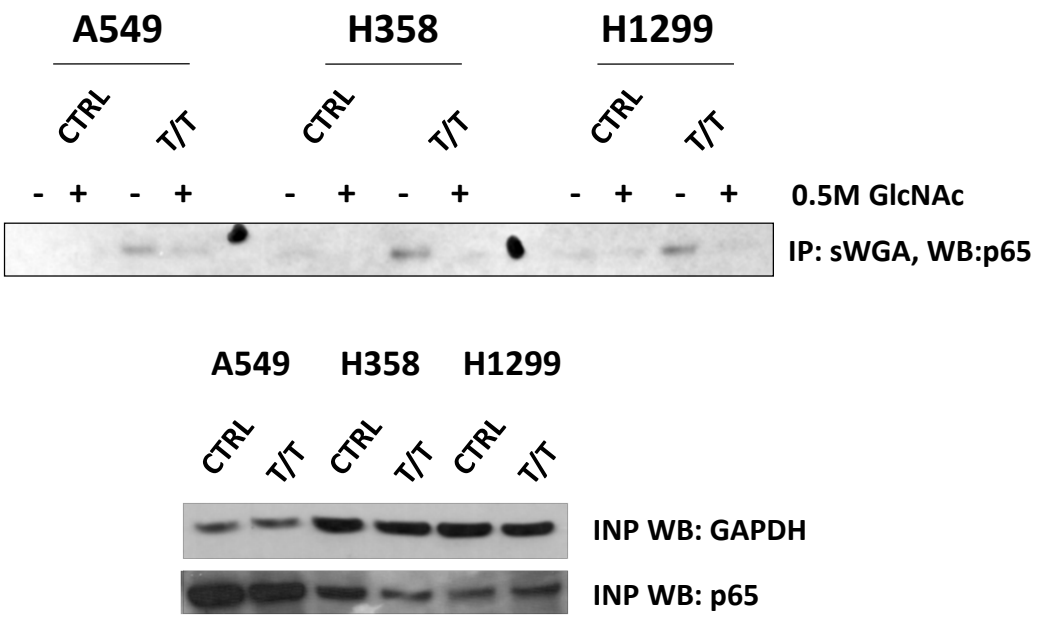
A549
H358
H1299
CTRL
T/T
- + - + - + - + - + - +
0.5M GlcNAc
IP: sWGA, WB:p65
A549
H358
H1299
CTRL
T/T
INP WB: GAPDH
INP WB: p65

Supplementary Figure S5. O-GlcNAcylation of RelA/p65 is elevated in mesenchymal NSCLC cells. NSCLC cell lines A549, H358 and H1299 were cultured as tumorspheres without (CTRL) or with the addition of TNF/TGFβ (T/T). Cells were lysed and subjected to pull-down assay using succinylated Wheat Germ Agglutinin (sWGA) lectin in the absence (-) or presence (+) of competitive inhibitor N-acetyl-glucosamine (GlcNAc). Immunoblot analysis of inputs and pull-down samples for a known O-GlcNAcylated protein target RelA/p65. GAPDH was used as a loading control.

CHAPTER IV

NF-kappaB and hexosamine biosynthesis pathway (HBP) activation promote resistance to MEK inhibition in *KRAS*-mutant Non-Small Cell Lung Cancer

ABSTRACT

KRAS is the most commonly mutated proto-oncogene in non-small cell lung cancer occurring in thirty five percent of adenocarcinomas. Inhibition of a Ras downstream effector kinase MEK shows limited efficacy due to the activation of compensatory survival mechanisms. Here we show that nuclear factor kappa-B (NF-κB), a key anti-apoptotic signaling pathway in the cell, is activated in response to MEK inhibition in *KRAS*-mutant NSCLC and is required for the cell survival. Furthermore a recently identified target of NF-κB, *GFPT2* is induced by MEK inhibition in NSCLC. GFPT2 is the first and rate-limiting enzyme in the hexosamine biosynthesis pathway (HBP) that generates UDP-GlcNAc precursor molecule for O-GlcNAcylation of nucleocytoplasmic proteins. O-GlcNAcylation is induced by variety of stress stimuli and promotes survival and prevents apoptosis by directly modifying the p65 subunit of NF-κB to sustain its transcriptional activity. Here we show that protein O-GlcNAcylation is induced by MEK inhibition in NSCLC. Furthermore, silencing of *GFPT2* in combination with MEK inhibition results in decreased cell survival and GFPT2 promotes O-GlcNAcylation and NF-κB signaling. Our results suggest a potential benefit of combinatorial targeting MEK and the HBP NSCLC carrying mutations in the Kras proto-oncogene.

INTRODUCTION

Lung cancer is one of the most prevalent cancer types and the leading cause of cancer-related mortality in the world (1). About 85% of lung cancers belong to non-small cell lung cancer (NSCLC) type of which close to 50% are adenocarcinomas (ADC) (2). Majority of diagnosed NSCLC are late stage cancers for which standard treatment with cisplatin-based chemotherapy shows only limited efficacy (3).

KRAS is the most commonly mutated proto-oncogene in NSCLC and occurs in 35% of ADC (4). Activated Ras signals to the downstream effectors, including Raf/MEK/ERK and PI3K/Akt pathways to promote proliferation, survival and metastasis (5). *KRAS* mutant cancers show oncogene addiction to Ras, thus creating a window of opportunity for targeted therapy (5). However initial promise of targeting Kras in cancers has been hindered by its low druggability shifting efforts towards targeting downstream pathways activated by Ras (5).

Targeting mitogen activated protein kinase kinase (MEK) with small molecule inhibitors has recently proven successful in treatment of BRAF mutant melanoma and several other cancers including NSCLC (5-6). However the resistance of cancer cells to MEK inhibitors has emerged due to compensatory activation of alternative Ras downstream effectors. This highlights the need for combinatorial inhibition of multiple Ras downstream pathways such as MEK and Akt, which have proven to be more effective (7-10).

Nuclear factor kappa B (NF-κB) is an important anti-apoptotic transcription factor activated by a variety of extra- and intracellular stimuli including pro-

inflammatory cytokines, growth factors and DNA damage (11). NF-κB activation proceeds through IκB kinase (IKK)-mediated phosphorylation of IκB complex that binds inactive NF-κB in the cytoplasm (11). IκB phosphorylation leads to its poly-ubiquitination and proteasomal degradation to allow NF-κB nuclear translocation, of DNA binding within gene promoters and enhancers, to actively stimulate transcription (11). NF-κB undergoes several posttranslational modifications including phosphorylation by cAMP-dependent protein kinase A (PKA) and acetylation by p300 (12). Importantly NF-κB activity is required for lung tumor formation *in vivo* and for a survival of *KRAS* mutant lung cancer cells (13-16).

Hexosamine biosynthesis pathway (HBP) utilizes fructose-6-phosphate, an intermediate metabolite of the glycolysis, glutamine, acetyl-CoA and UTP to generate UDP-GlcNAc amino sugar moiety, an essential precursor molecule for all glycosylation processes and the synthesis of poly-glycans (17). The first and rate-limiting step in HBP is catalyzed by the enzyme glutamine: fructose-6-phosphate transaminase (GFPT) that converts fructose-6-phpsphate and glutamine into glucosamine-6-phosphate and glutamate (17). Glucosamine-6-phospate is further converted into UDP-GlcNAc is three enzymatic steps (17). A particular form of O-linked glycosylation occurring on the nucleocytoplasmic proteins is called O-GlcNAcylation, and relies on a dynamic addition of a single UDP-GlcNAc molecule onto the hydroxyl groups of serine or threonine of target proteins by the enzyme O-GlcNAc transferase (OGT) and its removal by the enzyme O-GlcNAcase (OGA) (18). O-GlcNAcylation is induced by cellular stresses such as DNA damage, heat shock, unfolded protein response (UPR)

and starvation and is implicated in a regulation of a multitude of cellular processes including signaling and cell survival (19-22). O-GlcNAc modification has been shown to prevent protein aggregation and acts as a recognition site for the heat shock proteins that possess lectin-like binding capacity towards O-GlcNAc peptides (23-24). Elevation of HBP and protein O-GlcNAcylation has recently been shown to prolong life and protect from proteotoxic stress (25-26). Importantly, the Mayo laboratory has shown that O-GlcNAcylation of NF-κB at threonine 305 is required for its subsequent acetylation on lysine 310 by p300 and its full transcriptional activation (27). Consistently O-GlcNAcylation sustains NF-κB signaling and promotes cell survival by upregulating anti-apoptotic gene products (27-30). Here we show that NF-κB pathway is induced in *KRAS*-mutant NSCLC adenocarcinoma in response to MEK inhibition and show that NF-κB activation is required for cell survival. This observation is consistent with previous reports in other cancer types (31-32). We further describe an induction of a novel NF-κB target gene *GFPT2* and concomitant elevation of global protein O-GlcNAcylation in response to MEK inhibition. Furthermore we show that silencing of GFPT2 induces cell death in response to MEK inhibition. Our work supports the existence of a positive feedback loop by which NF-κB signaling pathway via HBP, *GFPT2* and O-GlcNAcylation promotes a survival advantage, suggesting a potential benefit of combinatorial targeting of MEK and HBP in *KRAS*-mutant NSCLC.

RESULTS

MEK inhibition activates Akt and NF-κB pathways in *KRAS*-mutant NSCLC cells

MEK inhibition has proven effective in decreasing tumor growth of *KRAS*-driven transgenic mouse model of lung adenocarcinoma however a rapid regrowth of tumors is observed after cessation of MEK inhibitor treatment suggesting that a subset of lung adenocarcinoma cells are able of withstanding growth inhibitory effect of MEK inhibition (6). Indeed activation of several compensatory pathways following MEK inhibition has been observed; notably activation of PI3K/Akt has been described in several cancer types including prostate and lung (7-10). For these reasons a combination of MEK and Akt inhibition is more effective than MEK inhibitor alone in decreasing tumor growth (7-10). Interestingly, activation of the components of NF-κB pathway has been observed following MEK inhibition in prostate cancer. Similarly, pharmacological inhibition of MEK and NF-kB target cyclooxygenase (COX) synergize in targeting melanoma (31, 33).

To further investigate NF-κB activation following MEK inhibition in *KRAS*-mutant NSCLC adenocarcinomas we performed a time-course experiment of MEK inhibitor (PD0325901) treatment of A549 cell line. MEK inhibitor treatment did not cause visible cell death in standard 2D culture conditions but instead decreased proliferation rates and induced cell morphology changes (data not shown). Immunoblotting analysis of the time course experiment shows that

MEK inhibitor rapidly blocked phosphorylation of ERK, which was sustained thorough 48hrs of experiment (Figure 7A). Concomitant induction of phosphorylation of Akt was observed indicating compensatory activation of PI3K pathway (Figure 7A). Interestingly, we observed an induction of phosphorylation of components of NF-κB pathway; IKK and IκB following MEK inhibitor treatment (Figure 7A). To determine whether a phosphorylation of the NF-κB pathway correlates with an induction of its transcriptional activity, we performed a similar MEK inhibitor treatment time course in A549 cells and analyzed the expression of known NF-κB-regulated genes (Figure 7B). We observe an induction of transcription of NF-κB target genes including *TNFAIP3*/A20 and *BIRC3*/cIAP-2 (Figure 7B). These results indicate that NF-κB pathway is induced following MEK inhibition in *KRAS*-mutant lung adenocarcinoma possibly as a compensatory survival mechanism consistently with similar observations in prostate cancer (31).

Inhibition of NF-κB promotes apoptosis following MEK inhibition in *KRAS*-mutant LUAD cells

NF-κB pathway has been shown to inhibit apoptosis through transcriptional regulation of a several anti-apoptotic proteins including Bcl-2 and Bcl-xl (11). NF-κB signaling has been shown to be required for survival of *KRAS*-mutant lung adenocarcinoma (12-16). Inhibition of IKK in combination with the treatment with MEK inhibitor resulted in decreased cell survival of *KRAS*-mutant

A.

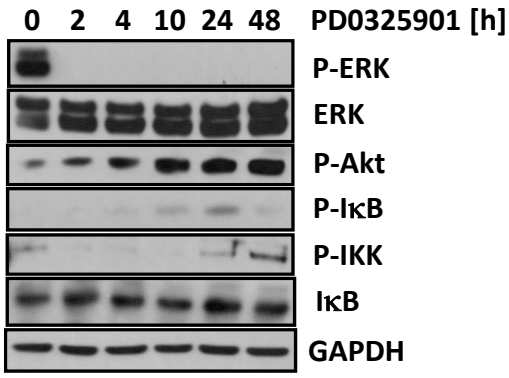
0 2 4 10 24 48 PD0325901 [h]
P-ERK
ERK
P-Akt
P-IκB
P-IKK
IκB
GAPDH

B.

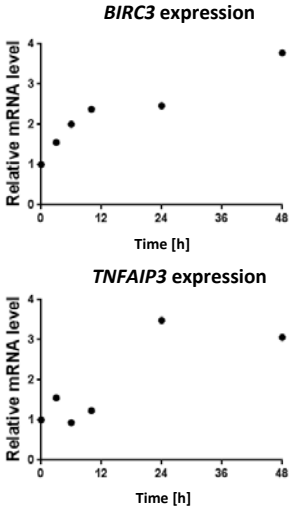
BIRC3 expression
Relative mRNA level
Time [h]
TNFAIP3 expression
Relative mRNA level
Time [h]

Figure 7. MEK inhibition activates Akt and NF-κB pathways in *KRAS*-mutant NSCLC. A549 cells were treated with the MEK inhibitor PD0325901 for the indicated time points. A. Immunoblot analysis was performed using phosphorylated ERK (P-ERK), pan-ERK, phosphorylated Akt (P-Akt), phosphorylated IκB (P-IκB), phosphorylated IKK (P-IKK) and IκB. GAPDH was used as a loading control. B. QRT-PCR analysis of the expression of NF-κB targets *BIRC3*/cIAP-2 and *TNFAIP3*/A20 following time-course treatment with MEK inhibitor. Values were normalized to mRNA levels of HPRT.

prostate cancer cells (31). To determine whether NF-κB induction is required for the survival of A549 cells, following MEK inhibition, we blocked NF-κB pathway in by siRNA-mediated silencing of RelA/p65, a main subunit of transcriptionally competent NF-κB heterodimers. Importantly we observe that inhibition of NF-κB pathway by siRNA-mediated silencing of RelA/p65 resulted in an induction of apoptosis of A549 lung adenocarcinoma cells following MEK inhibition as determined by immunoblotting for cleaved caspase 3, a marker of activated apoptotic pathway (Figure 8). Cleaved caspase 3 was not detectable in A549 cells treated with DMSO or transfected with the control scrambled siRNA during the 48h time course of the experiment (Figure 8). These observations indicate a potential benefit of the combinatorial targeting MEK and NF-κB pathway in *KRAS*-mutant NSCLC.

MEK inhibition induces protein O-GlcNAcylation and upregulates the expression of *GFPT2*

Protein O-GlcNAcylation is induced by a number of stress signals including DNA damage, hypoxia, heat shock and ER stress and has been shown to regulate protein homeostasis and promote cell survival (19-22). O-GlcNAcylation relies on an addition of a single UDP-N-acetylglucosamine (UDP-GlcNAc) moiety onto hydroxyl groups of serine and threonine of target proteins by enzymes OGT and its removal by enzyme OGA (18). Recently the Mayo laboratory identified glutamine: fructose-6-phpsphate aminotransferase 2 (GFPT2), an isoform of the first and rate-limiting step in the hexosamine

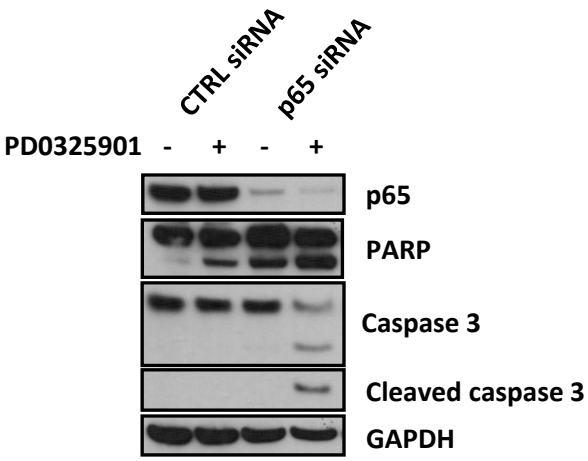
CTRL siRNA
p65 siRNA
PD0325901 - + - +
p65
PARP
Caspase 3
Cleaved caspase 3
GAPDH

Figure 8. NF-κB activation is required for the survival of *KRAS*-mutant NSCLC cells following MEK inhibition. A549 cells were transfected with control (CTRL) or RelA/p65 (p65) siRNAs and left untreated (-) or treated with MEK inhibitor (+) PD0325901 for 48h. Immunoblot analysis was performed using RelA/p65, caspase 3 and PARP specific antibodies. GAPDH was used as a loading control.

biosynthesis pathway (HBP) as a novel inducible NF-κB regulated gene in NSCLC (manuscript in preparation). Notably, we showed that *GFPT2* induction elevates protein O-GlcNAcylation in mesenchymal NSCLC cells. Given the observed activation of NF-κB pathway following MEK inhibition in *KRAS*-mutant NSCLC and recently described the relationship between NF-κB activation and HBP, we decided to investigate the levels of protein O-GlcNAcylation in A549 cells in response to MEK inhibition. We performed a time-course experiment of MEK inhibitor treatment in A549 cells and analyzed global levels of O-GlcNAcylation by immunoblotting. Global elevation of basal O-GlcNAcylation was observed following MEK inhibition (Figure 9A). Concomitantly we observe a gradual accumulation of GFPT2 protein levels. The elevation in O-GlcNAcylation was not attributed to observable changes in the levels of GFPT1, OGT or OGA enzymes (Figure 9A). Consistent with these results we observe an induction of *GFPT2* mRNA, but not *GFPT1*, *OGT* or *OGA* transcripts by QRT-PCR following a 48h time course analysis post-MEK inhibitor treatment (Figure 9B). These results indicate that elevated protein O-GlcNAcylation is attributed to the increase in the flux through hexosamine biosynthetic pathway, which is associated with GFPT2. Additionally the kinetics of *GFPT2* induction resembled that of other NF-κB regulated genes including *TNFAIP3* and *BIRC3* (Figure 7B) suggesting that *GFPT2* is most likely upregulated by NF-κB following inhibition of MEK.

A.

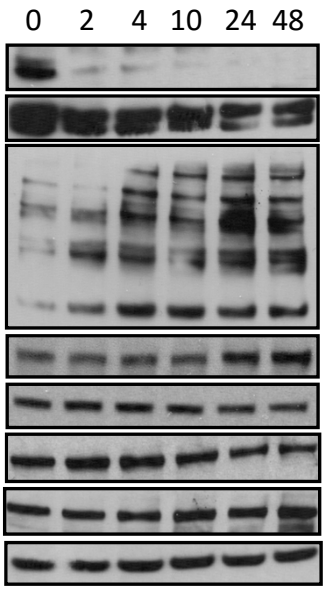
0 2 4 10 24 48 PD0325901 [h]
P-ERK
ERK
O-GlcNAc
GFPT2
GFPT1
OGT
OGA
GAPDH

B.

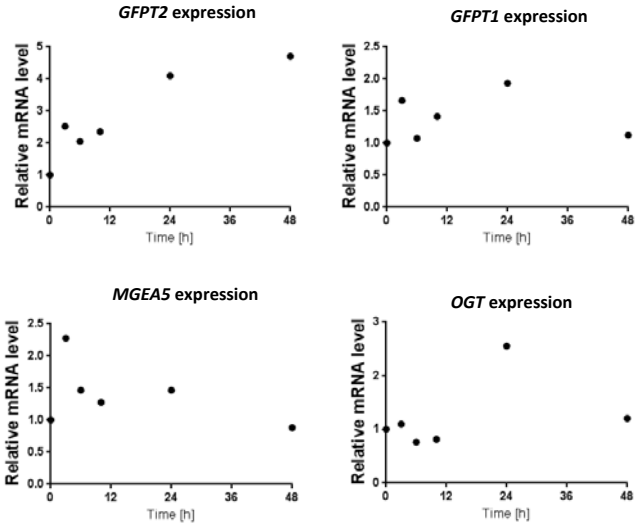
GFPT2 expression
GFPT1 expression
MGEA5 expression
OGT expression
Relative mRNA level
Time [h]

Figure 9. MEK inhibition induces protein O-GlcNAcylation and *GFPT2* expression. A549 cells were treated with MEK inhibitor PD0325901 for indicated times. A. Immunoblot analysis was performed using phosphorylated ERK (P-ERK), ERK as well as GFPT1, GFPT2, OGA, OGT and the modification-specific O-GlcNAc antibody. GAPDH was used as a loading control. B. QRT-PCR analysis of enzymes involved in protein O-GlcNAcylation, OGT, OGA, GFPT1 and GFPT2 during the time-course treatment with MEK inhibitor.

GFPT2 elevates protein O-GlcNAcylation and sustains NF-κB signaling

O-GlcNAcylation has been shown to act in an anti-apoptotic manner by sustaining the signaling of NF-κB (27-30). Recently the Mayo laboratory and others have shown that several components of NF-κB pathway are modified with O-GlcNAc and are required for its transcriptional activation and anti-apoptotic signaling (27-30). We sought to determine whether *GFPT2* expression might potentiate NF-κB signaling via elevated flux through HBP and increased protein O-GlcNAcylation to promote NF-κB-dependent transcription. To test this we transfected HEK293T cells with an empty plasmid or a vector encoding V5-tagged GFPT2 and analyzed the levels of protein O-GlcNAcylation by immunoblotting. We observe an elevation in global protein O-GlcNAcylation following ectopic expression of GFPT2 (Figure 10A) consistent with our previous results in mesenchymal NSCLC (manuscript in preparation). Next we asked whether the expression of *GFPT2* affects NF-κB signaling. To address this we transfected HEK293T cells with empty vector or *GFPT2* construct and stimulated the cells with TNF for 2h. As a measure of activated NF-κB pathway we determined the levels of phosphorylated IKK and IκB by immunoblotting. Importantly, *GFPT2* overexpression led to an increase in both basal and inducible phosphorylation of IKK and IκB suggesting increased signaling through NF-κB pathway (Figure 10B). To assess the effect of *GFPT2* expression on NF-κB-mediated transcription we utilized NF-κB responsive luciferase reporter 3x κB-luc (35). We transfected HEK293T cells with 3x κB-luc reporter construct

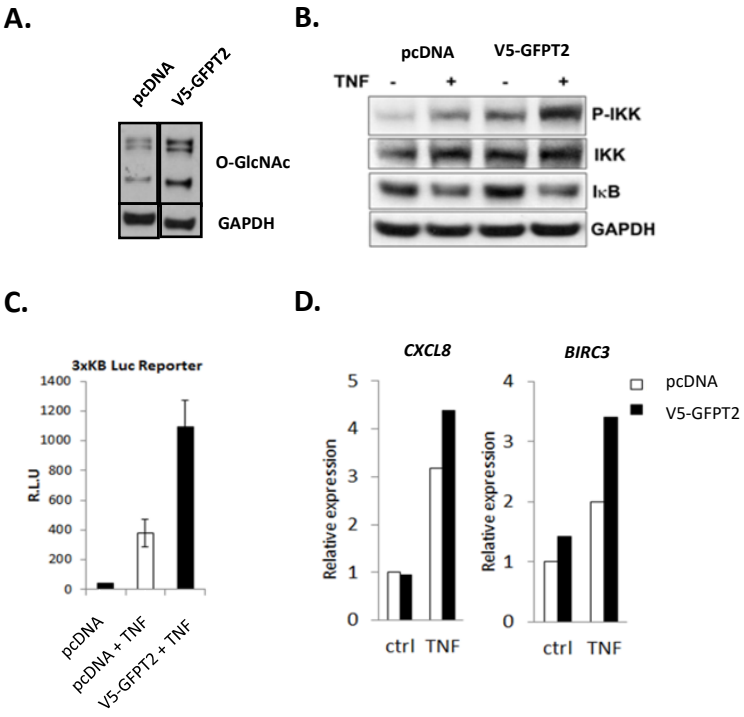
A.
pcDNA
V5-GFPT2
O-GlcNAc
GAPDH
B.
pcDNA
V5-GFPT2
TNF - + - +
P-IKK
IKK
IκB
GAPDH
C.
3xKB Luc Reporter
R.L.U
1400
1200
1000
800
600
400
200
0
pcDNA
pcDNA + TNF
V5-GFPT2 + TNF
D.
CXCL8
BIRC3
pcDNA
V5-GFPT2
Relative expression
5
4
3
2
1
0
ctrl TNF
ctrl TNF

Figure 10. GFPT2 potentiates NF-κB signaling *in vitro.* A. HEK293T cells were transfected with pcDNA vector control or V5-GFPT2 and analyzed by immunoblot for global O-GlcNAcylation. GAPDH was used as a loading control. B. HEK293T cells were transfected with pcDNA or V5-GFPT2 ad stimulated with TNF for 30 minutes followed by immunoblot analysis for phosphorylated IKK and IκB. GAPDH was used as a loading control. C. HEK293T cells were transfected with 3x κB luciferase reported construct alone or in a combination with V5-GFPT2 and either left untreated or stimulated with TNF. Cells were lysed and analyzed for luciferase activity as described in materials and methods. D. HEK293T cells were transfected with pcDNA vector control or V5-GFPT2 and either left untreated (ctrl) or stimulated with TNF (TNF). QRT-PCR analysis was performed for NF-κB targets *CXCL8* and *BIRC3*.

together with a control plasmid or a vector encoding *GFPT2*, and stimulated the cells with TNF for 2h. We analyzed activity or the 3x κB-luc promoter with luciferase assay. Interestingly, we observed that ectopic expression of *GFPT2* increased 3x κB-luc reporter activity in response to TNF suggesting an increase in NF-κB transcriptional activity (Figure 10C). Finally we determined the expression of endogenous targets of NF-κB in HEK293T transfected with empty vector control or *GFPT2* construct and stimulated with TNF (Figure 10D). We observe an increase in TNF-induced expression of NF-κB targets *BIRC3* and CXCL8 in cells transfected with *GFPT2* construct as compared to control cells (Figure 10D). Together these results indicate that a unique axis between NF-κB and GFPT2 such that GFPT2 increased synthesis of UDP-GlcNAc feedback to heighten NF-κB signaling and transcription.

Silencing of *GFPT2* promotes cell death following MEK inhibition in *KRAS*-mutant LUAD cells

Protein O-GlcNAcylation is induced by a number of stress signals to promote cell survival (19-22). Importantly ectopic expression of *GFPT2* has been shown to protect neuronal cells from hydrogen peroxide-induced oxidative stress whereas expression of GFPT protects *Saccharomyces cerevisiae* from methylmercury cytotoxicity (33-37). This indicates potential role of *GFPT2* in pro-survival signaling. We hypothesized that *GFPT2* may promote survival following MEK treatment of *KRAS*-mutant NSCLC cells possibly via elevation of hexosamine biosynthetic pathway and an increase in protein O-GlcNAcylation.

Indeed glucose starvation has been shown to induce cell death of *KRAS*-mutant cancer cells by affecting HBP and inducing ER stress whereas glucosamine supplementation or *GFPT1* overexpression protects cells from proteotoxic stress (25-26, 38). Notably, we observe an elevated cell death following MEK inhibitor treatment of A549 in a low glucose condition which is not observed in a high glucose media (data not shown). To test whether induction of *GFPT2* is required for the cell survival following MEK inhibition we utilized a stable A549 cell line expressing doxycycline-inducible shRNA targeting *GFPT2*. Cells were pre-treated for 2d with doxycycline or left untreated following treatment with MEK inhibitor for additional 48h. We confirmed *GFPT2* silencing following doxycycline pre-treatment by measuring mRNA levels of *GFPT2* product by QRT-PCR (Figure 11A). Next, we determined cell survival following MEK inhibition by trypan blue cell counting. A decrease in cell viability in MEK treated cells was observed following silencing of *GFPT2* by doxycycline pre-treatment, compared to cells without doxycycline pretreatment (Figure 11B). Our results indicate that increase in *GFPT2* expression in response to MEK inhibitors is critical for cell viability.

A.

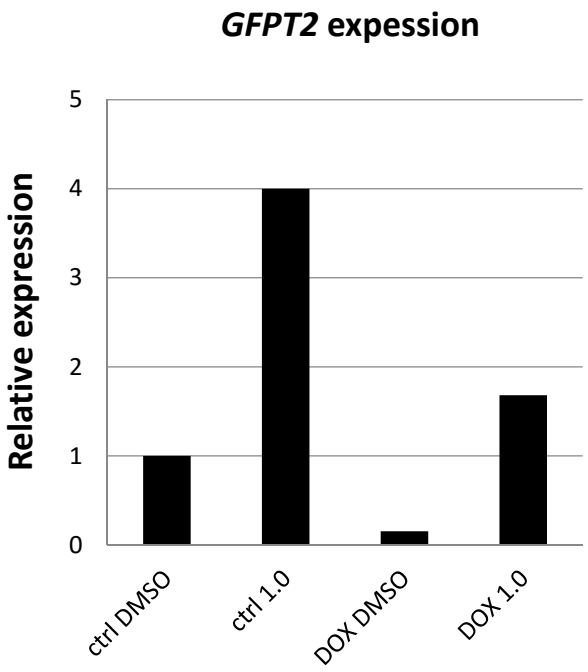
GFPT2 expession
Relative expression
5
4
3
2
1
0
ctrl DMSO
ctrl 1.0
DOX DMSO
DOX 1.0

B.

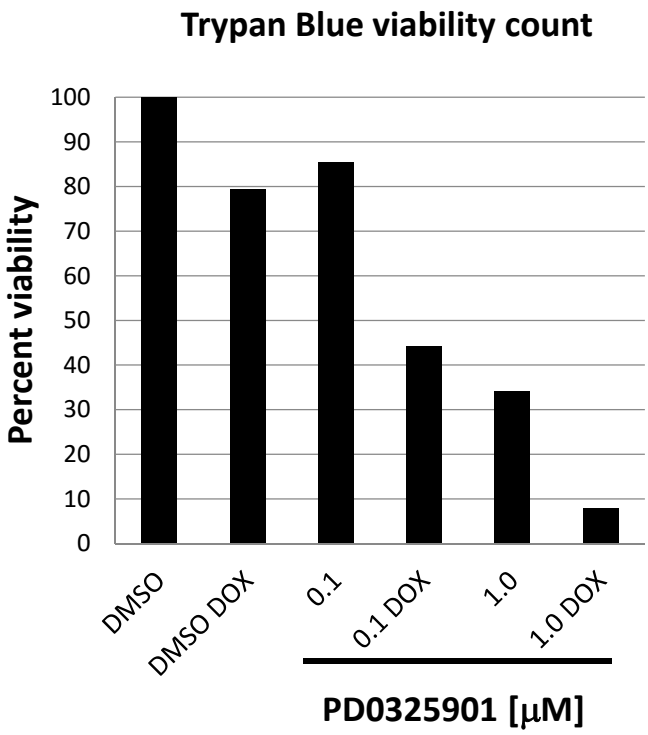
Trypan Blue viability count
Percent viability
100
90
80
70
60
50
40
30
20
10
0
DMSO
DMSO DOX
0.1
0.1 DOX
1.0
1.0 DOX
PD0325901 [μM]

Figure 11. *GFPT2* is required for the survival of *KRAS*-mutant NSCLC following MEK inhibition. Stable A549 cell line expressing doxycycline-inducible *GFPT2* shRNA was generated as described in materials and methods. Cells were pre-treated with doxycycline for 3 days following by treatment with MEK inhibitor for an additional 60h in low glucose (5mM) and reduced serum (2%) media. A. QRT-PCR analysis of *GFPT2* expression cells without (ctrl) or with doxycycline (DOX) pre-treatment in cells treated with DMSO compared to treatment with MEK inhibitor at concentration of 1.0 μM. B. A549 *GFPT2* shRNA cell line was either left untreated or pre-treated with doxycycline (DOX) followed by treatment with increasing concentrations of MEK inhibitor at 0.1 μM and 1.0 μM, respectively. Cells were trypsinized and counted with trypan blue using hemocytometer.

DISCUSSION

KRAS proto-oncogene is mutated in 35 percent of lung adenocarcinomas however because drug inhibitors have been unsuccessful, efforts have focused on targeting downstream Kras effectors such as the mitogen activated protein kinase kinase (MEK) (5). MEK kinase is activated by Raf and phosphorylates ERK to promote cancer proliferation and survival (5). Initial promise of targeting MEK in cancer showed limited success due to the activation of compensatory survival mechanisms leading to drug resistance (7-10). Phosphoinositide 3-kinase (PI3K) pathway has been shown to be activated in response to MEK inhibition and combinatorial targeting of MEK and PI3K has proven more effective than targeting either of the pathways alone in NSCLC (7-8). Here we show that NF-κB, a key anti-apoptotic pathway in the cell, is activated in response to MEK inhibition in *KRAS*-mutant NSCLC. This is consistent with previous observations in melanoma and prostate cancer (31, 33). Importantly blocking NF-κB in combination with MEK inhibition induces apoptosis in NSCLC. The mechanism of NF-κB activation in response to MEK inhibition remains to be determined however given that Akt has been shown to activate NF-κB, it is plausible to speculate that compensatory activation of Akt in response to MEK inhibition is responsible for induction of NF-κB (35). Indeed we observe an activation of Akt pathway in *KRAS*-mutant NSCLC in response to MEK inhibition, consistent with previous reports (7-8).

Furthermore we observe an induction of a novel NF-κB target *GFPT2* in response to MEK inhibition in NSCLC. *GFPT2* encodes for the neuron-specific isoform of the first and rate-limiting enzyme of the hexosamine biosynthesis pathway (HBP) that utilizes glucose and glutamine to generate UDP-N-acetylglucosamine (UDP-GlcNAc) precursor molecule for the synthesis of poly-glycans and O-GlcNAcylation of nucleocytoplasmic proteins (17). Indeed concomitantly with the induction of *GFPT2* we observe an elevation in global protein O-GlcNAcylation in response to MEK inhibition. It remains to be determined whether this elevation of O-GlcNAcylation is dependent on NF-κB induction and *GFPT2* expression and whether *GFPT2* is regulated by NF-κB in this setting. Our previous report indicates that GFPT2 is directly regulated by NF-κB in mesenchymal NSCLC cells.

Importantly protein O-GlcNAcylation has been shown to be induced by a variety of stress stimuli including heat shock, starvation and proteotoxic stress, to promote cell survival and inhibit apoptosis by directly modulating RelA/p65 and IKK to promote NF-κB signaling (17-22, 27-30). Recently our laboratory has shown that RelA/p65 is directly O-GlcNAcylated at threonine 305 which is required for its subsequent acetylation at lysine 310 by p300 and the full transcriptional activation (27). Using HEK293T we show that expression of GFPT2 promotes protein O-GlcNAcylation and NF-κB signaling. The mechanism by which ectopic expression of GFPT2 promotes NF-κB transcription remains to be determined but may involve direct O-GlcNAcylation of RelA/p65, thus

establishing a HBP-dependent positive feedback-loop to NF-κB signaling and transcription.

Our work demonstrates that silencing of *GFPT2* in cells treated with MEK inhibitor results in decreased cell survival. This is consistent with previous reports indicating that expression of *GFPT2* protects neuronal cell line HT-22 from oxidative stress induced by hydrogen peroxide (36). It remains to be determined whether this reduction in cell survival is a result of an induction of apoptosis, or whether GFPT2 exerts its cytoprotective effect via elevated HBP, protein O-GlcNAcylation and/or modulation of NF-κB signaling pathways.

This is the first report indicating an induction of NF-κB and protein O-GlcNAcylation in response to MEK inhibition in *KRAS*-mutant NSCLC. This study further supports our previous observations indicating that *GFPT2* is an inducible gene expressed in NSCLC and that it is required for the cell survival following MEK inhibition. Thus our results point out a potential benefit of combinatorial targeting MEK and GFPT2 in *KRAS*-mutant NSCLC.

REFERENCES

1. www.cancer.org

2. Bender E. Epidemiology: The dominant malignancy. *Nature.* 2014 Sep 11; 513(7517): S2-3.

3. Thomas A, Liu SV, Subramaniam DS, Giaccone G. Refining the treatment of NSCLC according to histological and molecular subtypes. *Nat Rev Clin Oncol.* 2015 Sep; 12(9): 511-526.

4. Cancer Genome Atlas Research Network. Comprehensive molecular profiling of lung adenocarcinoma. *Nature.* 2014 Jul 31; 511(7511): 543-550. PMCID: PMC4231481.

5. Zhao Y, Adjei AA. The clinical development of MEK inhibitors. *Nat Rev Clin Oncol.* 2014 Jul; 11(7): 385-400.

6. Trejo CL, Juan J, Vicent S, Sweet-Cordero A, McMahon M. MEK1/2 inhibition elicits regression of autochthonous lung tumors induced by KRASG12D or BRAFV600E. *Cancer Res.* 2012 Jun 15; 72(12): 3048-3059. PMCID: PMC3393094.

7. Sos ML, Fischer S, Ullrich R, Peifer M, Heuckmann JM, Koker M, Heynck S, Stuckrath I, Weiss J, Fischer F, Michel K, Goel A, Regales L, Politi KA, Perera S, Getlik M, Heukamp LC, Ansen S, Zander T, Beroukhim R, Kashkar H, Shokat KM, Sellers WR, Rauh D, Orr C, Hoeflich KP, Friedman L, Wong KK, Pao W, Thomas RK. Identifying genotype-dependent efficacy of single and combined PI3K- and MAPK-pathway inhibition in cancer. *Proc Natl Acad Sci U S A.* 2009 Oct 27; 106(43): 18351-18356. PMCID: PMC2757399.

8. Meng J, Dai B, Fang B, Bekele BN, Bornmann WG, Sun D, Peng Z, Herbst RS, Papadimitrakopoulou V, Minna JD, Peyton M, Roth JA. Combination treatment with MEK and AKT inhibitors is more effective than each drug alone in human non-small cell lung cancer in vitro and in vivo. *PLoS One.* 2010 Nov 29; 5(11): e14124. PMCID: PMC2993951.

9. Turke AB, Song Y, Costa C, Cook R, Arteaga CL, Asara JM, Engelman JA. MEK inhibition leads to PI3K/AKT activation by relieving a negative feedback on ERBB receptors. *Cancer Res.* 2012 Jul 1; 72(13): 3228-3237. PMCID: PMC3515079.

10. Yoon YK, Kim HP, Han SW, Oh do Y, Im SA, Bang YJ, Kim TY. KRAS mutant lung cancer cells are differentially responsive to MEK inhibitor due to AKT or STAT3 activation: Implication for combinatorial approach. *Mol Carcinog.* 2010 Apr; 49(4): 353-362.

11. Napetschnig J, Wu H. Molecular basis of NF-kappaB signaling. *Annu Rev Biophys.* 2013; 42: 443-468. PMCID: PMC3678348.

12. Huang B, Yang XD, Lamb A, Chen LF. Posttranslational modifications of NF-kappaB: Another layer of regulation for NF-kappaB signaling pathway. *Cell Signal.* 2010 Sep; 22(9): 1282-1290. PMCID: PMC2893268.

13. Meylan E, Dooley AL, Feldser DM, Shen L, Turk E, Ouyang C, Jacks T. Requirement for NF-kappaB signalling in a mouse model of lung adenocarcinoma. *Nature.* 2009 Nov 5; 462(7269): 104-107. PMCID: PMC2780341.

14. Stathopoulos GT, Sherrill TP, Cheng DS, Scoggins RM, Han W, Polosukhin VV, Connelly L, Yull FE, Fingleton B, Blackwell TS. Epithelial NF-kappaB activation promotes urethane-induced lung carcinogenesis. *Proc Natl Acad Sci U S A.* 2007 Nov 20; 104(47): 18514-18519. PMCID: PMC2141808.

15. Basseres DS, Ebbs A, Levantini E, Baldwin AS. Requirement of the NF-kappaB subunit p65/RelA for K-ras-induced lung tumorigenesis. *Cancer Res.* 2010 May 1; 70(9): 3537-3546. PMCID: PMC2862109.

16. Xia Y, Yeddula N, Leblanc M, Ke E, Zhang Y, Oldfield E, Shaw RJ, Verma IM. Reduced cell proliferation by IKK2 depletion in a mouse lung-cancer model. *Nat Cell Biol.* 2012 Feb 12; 14(3): 257-265. PMCID: PMC3290728.

17. Abdel Rahman AM, Ryczko M, Pawling J, Dennis JW. Probing the hexosamine biosynthetic pathway in human tumor cells by multitargeted tandem mass spectrometry. *ACS Chem Biol.* 2013 Sep 20; 8(9): 2053-2062.

18. Bond MR, Hanover JA. A little sugar goes a long way: The cell biology of O-GlcNAc. *J Cell Biol.* 2015 Mar 30; 208(7): 869-880. PMCID: PMC4384737.

19. Zachara NE, Molina H, Wong KY, Pandey A, Hart GW. The dynamic stress-induced "O-GlcNAc-ome" highlights functions for O-GlcNAc in regulating DNA damage/repair and other cellular pathways.*Amino Acids.* 2011 Mar; 40(3): 793-808. PMCID: PMC3329784.

20. Chatham JC, Not LG, Fulop N, Marchase RB. Hexosamine biosynthesis and protein O-glycosylation: The first line of defense against stress, ischemia, and trauma. *Shock.* 2008 Apr; 29(4): 431-440.

21. Zachara NE, O'Donnell N, Cheung WD, Mercer JJ, Marth JD, Hart GW. Dynamic O-GlcNAc modification of nucleocytoplasmic proteins in response to stress. A survival response of mammalian cells. *J Biol Chem.* 2004 Jul 16; 279(29): 30133-30142.

22. Kang JG, Park SY, Ji S, Jang I, Park S, Kim HS, Kim SM, Yook JI, Park YI, Roth J, Cho JW. O-GlcNAc protein modification in cancer cells increases in response to glucose deprivation through glycogen degradation. *J Biol Chem.* 2009 Dec 11; 284(50): 34777-34784. PMCID: PMC2787340.

23. Lefebvre T, Cieniewski C, Lemoine J, Guerardel Y, Leroy Y, Zanetta JP, Michalski JC. Identification of N-acetyl-d-glucosamine-specific lectins from rat liver cytosolic and nuclear compartments as heat-shock proteins. *Biochem J.* 2001 Nov 15; 360(Pt 1): 179-188. PMCID: PMC1222216.

24. Marotta NP, Lin YH, Lewis YE, Ambroso MR, Zaro BW, Roth MT, Arnold DB, Langen R, Pratt MR. O-GlcNAc modification blocks the aggregation and toxicity of the protein alpha-synuclein associated with parkinson's disease. *Nat Chem.* 2015 Nov; 7(11): 913-920. PMCID: PMC4618406.

25. Denzel MS, Storm NJ, Gutschmidt A, Baddi R, Hinze Y, Jarosch E, Sommer T, Hoppe T, Antebi A. Hexosamine pathway metabolites enhance protein quality control and prolong life. *Cell.* 2014 Mar 13; 156(6): 1167-1178.

26. Wang ZV, Deng Y, Gao N, Pedrozo Z, Li DL, Morales CR, Criollo A, Luo X, Tan W, Jiang N, Lehrman MA, Rothermel BA, Lee AH, Lavandero S, Mammen PP, Ferdous A, Gillette TG, Scherer PE, Hill JA. Spliced X-box binding protein 1 couples the unfolded protein response to hexosamine biosynthetic pathway. *Cell.* 2014 Mar 13; 156(6): 1179-1192. PMCID: PMC3959665.

27. Allison DF, Wamsley JJ, Kumar M, Li D, Gray LG, Hart GW, Jones DR, Mayo MW. Modification of RelA by O-linked N-acetylglucosamine links glucose metabolism to NF-kappaB acetylation and transcription.*Proc Natl Acad Sci U S A.* 2012 Oct 16; 109(42): 16888-16893. PMCID: PMC3479489.

28. Ma Z, Vocadlo DJ, Vosseller K. Hyper-O-GlcNAcylation is anti-apoptotic and maintains constitutive NF-kappaB activity in pancreatic cancer cells. *J Biol Chem.* 2013 May 24; 288(21): 15121-15130. PMCID: PMC3663532.

29. Kawauchi K, Araki K, Tobiume K, Tanaka N. Loss of p53 enhances catalytic activity of IKKbeta through O-linked beta-N-acetyl glucosamine modification. *Proc Natl Acad Sci U S A.* 2009 Mar 3; 106(9): 3431-3436. PMCID: PMC2651314.

30. Yang WH, Park SY, Nam HW, Kim do H, Kang JG, Kang ES, Kim YS, Lee HC, Kim KS, Cho JW. NFkappaB activation is associated with its O-GlcNAcylation state under hyperglycemic conditions. *Proc Natl Acad Sci U S A.* 2008 Nov 11; 105(45): 17345-17350. PMCID: PMC2582288.

31. Gioeli D, Wunderlich W, Sebolt-Leopold J, Bekiranov S, Wulfkuhle JD, Petricoin EF,3rd, Conaway M, Weber MJ. Compensatory pathways induced by MEK inhibition are effective drug targets for combination therapy against

castration-resistant prostate cancer. *Mol Cancer Ther.* 2011 Sep; 10(9): 1581-1590. PMCID: PMC3315368.

32. Barbie DA, Tamayo P, Boehm JS, Kim SY, Moody SE, Dunn IF, Schinzel AC, Sandy P, Meylan E, Scholl C, Frohling S, Chan EM, Sos ML, Michel K, Mermel C, Silver SJ, Weir BA, Reiling JH, Sheng Q, Gupta PB, Wadlow RC, Le H, Hoersch S, Wittner BS, Ramaswamy S, Livingston DM, Sabatini DM, Meyerson M, Thomas RK, Lander ES, Mesirov JP, Root DE, Gilliland DG, Jacks T, Hahn WC. Systematic RNA interference reveals that oncogenic KRAS-driven cancers require TBK1. *Nature.* 2009 Nov 5; 462(7269): 108-112. PMCID: PMC2783335.

33. Roller DG, Axelrod M, Capaldo BJ, Jensen K, Mackey A, Weber MJ, Gioeli D. Synthetic lethal screening with small-molecule inhibitors provides a pathway to rational combination therapies for melanoma. *Mol Cancer Ther.* 2012 Nov; 11(11): 2505-2515. PMCID: PMC3496043.

34. http://www.bu.edu/nf-kb/gene-resources/target-genes/

35. Madrid LV, Wang CY, Guttridge DC, Schottelius AJ, Baldwin AS,Jr, Mayo MW. Akt suppresses apoptosis by stimulating the transactivation potential of the RelA/p65 subunit of NF-kappaB. *Mol Cell Biol.*2000 Mar; 20(5): 1626-1638. PMCID: PMC85346.

36. Zitzler J, Link D, Schafer R, Liebetrau W, Kazinski M, Bonin-Debs A, Behl C, Buckel P, Brinkmann U. High-throughput functional genomics identifies genes that ameliorate toxicity due to oxidative stress in neuronal HT-22 cells: GFPT2 protects cells against peroxide. *Mol Cell Proteomics.* 2004 Aug; 3(8): 834-840.

37. Miura N, Kaneko S, Hosoya S, Furuchi T, Miura K, Kuge S, Naganuma A. Overexpression of L-glutamine:D-fructose-6-phosphate amidotransferase provides resistance to methylmercury in saccharomyces cerevisiae. *FEBS Lett.* 1999 Sep 17; 458(2): 215-218.

38. Palorini R, Cammarata FP, Balestrieri C, Monestiroli A, Vasso M, Gelfi C, Alberghina L, Chiaradonna F. Glucose starvation induces cell death in K-ras-transformed cells by interfering with the hexosamine biosynthesis pathway and activating the unfolded protein response. *Cell Death Dis.* 2013 Jul 18; 4: e732. PMCID: PMC3730427.

CHAPTER V

Summary and Future Directions

SUMMARY

Hexosamine biosynthesis pathway (HBP) generates UDP-N-acetylglucosamine (UDP-GlcNAc), a precursor molecule for the synthesis of majority of glycans in the cell, including protein N- and O-glycosylation, O-GlcNAcylation, and the synthesis of glycosaminoglycans (1). For many years it has been recognized that cancer cells show increased levels of glycan content, however how HBP is regulated in cancer cells has remained poorly understood (2-9). Here we identify glutamine: fructose-6-phosphate aminotransferase (GFPT2), the first and rate-limiting enzyme in the HBP, as a novel target of NF-κB in non-small cell lung cancer (NSCLC). We show that chronic activation of NF-κB pathway by tumor necrosis factor (TNF) during epithelial to mesenchymal transition or by MEK inhibitor elevates *GFPT2* expression in NSCLC cells resulting in increased protein O-GlcNAcylation. We further show that *GFPT2* is co-expressed with mesenchymal marker genes in lung adenocarcinoma patients and correlates with poor clinical outcome, indicating that it is an important marker of mesenchymal state in lung cancer. Elevated protein O-GlcNAcylation has been associated with cancer progression, metastasis and cancer cell survival (6-9). Here we show that protein O-GlcNAcylation is elevated in NSCLC cells following TGFβ and TNF-induced epithelial to mesenchymal transition and that OGT and protein O-GlcNAcylation is required for efficient EMT. Silencing of *GFPT2* in mesenchymal NSCLC cells decreases levels of global protein O-GlcNAcylation and affects migration and invasion of mesenchymal NSCLC cells.

The mechanism by which GFPT2 is required for mesenchymal cell migration and invasion requires further investigation. Furthermore we show that NF-κB pathway is activated in *KRAS*-mutant NSCLC in response to treatment with MEK inhibitor and that NF-κB activation is required for the cell survival following drug treatment. MEK inhibition causes induction of *GFPT2* and elevation of protein O-GlcNAcylation whereas silencing of *GFPT2* decreases cell survival following treatment with MEK inhibitor. This is the first report indicating that NF-κB directly regulated *GFPT2* in variety of biological settings. Interestingly, we also observed *GFPT2* induction by TNF in adipocytes suggesting that *GFPT2* is a general target of NF-κB in many cell types and may have interesting implications in variety of pathophysiological processes that involve inflammatory NF-κB activation including the development of insulin resistance in type 2 diabetes (T2D).

FUTURE DIRECTIONS

Determine the mechanisms by which GFPT2 promotes migration in mesenchymal NSCLC cells

Here we show that *GFPT2* is a novel NF-κB target required for the migration of mesenchymal NSCLC cells. Silencing of *GFPT2* with either doxycycline-inducible shRNA or siRNA transfection decreased migration of A549 cells measured using Boyden chamber assay (Figure 6 and 11). Similarly ectopic expression of doxycycline-inducible *GFPT2* construct elevated migration of H1299 cell line as measured by the wound healing assay (Figure 6). *GFPT2* is the first and rate-limiting enzyme in the HBP that generates UDP-GlcNAc precursor molecule for protein O- and N-linked glycosylation and the synthesis of glycosaminoglycans including hyaluronan (1). Silencing of *GFPT2* results in decreased, but not entirely eradicated, global protein O-GlcNAcylation whereas *GFPT2* overexpression elevates protein O-GlcNAcylation in both epithelial and mesenchymal cells (Figure 6B and D). These results suggest that *GFPT2* may contribute to the flux through HBP to potentially increase the levels of glycosylated products.

Notably both O- and N-linked glycosylation of transmembrane and extracellular proteins as well as the synthesis of proteoglycans have been shown to affect cell migration and are implicated in cancer progression and metastasis in multiple malignancies (2-9). Proteoglycans and glycosylated proteins including fibronectin and laminin are the main components of the extracellular matrix

(ECM) that constitutes both a physical substrate for adhesion and pro-migratory signaling in migrating cells as well as the reservoir of ECM-bound pro-survival growth factors and cytokines (10). Integrins are glycosylated transmembrane receptors that mediate adhesion and signaling following binding to various components of ECM and promote the assembly of focal adhesions, formation of actin stress fibers, filopodia and membrane ruffling at the leading edge of migrating cell to promote cell motility (11). Downstream effectors of integrin receptors include the focal adhesion kinase (FAK) which activates RAS via growth-factor-receptor-bound protein 2 (GRB2) and SRC kinase-dependent phosphorylation of SHC adaptor proteins. This cascade then stimulates the RHO family of small GTPases including RHO, CDC42 and RAC proteins, which further activate ERK via p21-activated kinase (PAK) (11). Similarly CD44 receptor bound to the hyaluronan (HA) component of ECM can stimulate cell migration via activation of RAC (12). Additionally O-GlcNAcylation of cofilin, protein that promotes actin cytoskeleton rearrangements and cell motility has been shown to promote its activity and stimulates cell migration through intracellular mechanisms (13). Thus, several potential mechanisms of *GFPT2* involvement in the cell migration require further investigation.

To further confirm the role of *GFPT2* in the regulation of cell motility we will ectopically express a shRNA resistant GFPT2 to determine whether these cells displayed restored migration follow knockdown of endogenous GFPT2. Tumorspheres will be disaggregated following 96h culture time and seeded at the bottom of Boyden chamber to measure migration and invasion. We expect that

overexpression of shRNA-resistant V5-tagged GFPT2 following knockdown of endogenous GFPT2 will rescue migratory potential of A549 cells. This experiment is feasible in our A549 GFPT2 *shRNA* cell line as pTripZ vector targets 3'UTR region of endogenous *GFPT2* absent in cDNA of *GFPT2* vector. To further characterize the change in the flux via HBP during EMT and the effect of silencing of *GFPT2* on the rate of UDP-GlcNAc synthesis we will conduct measurements of UDP-GlcNAc levels in cellular extracts of epithelial and mesenchymal A549 cells expressing either control or *GFPT2* shRNA using liquid chromatography−tandem mass spectrometry method (14). We expect to observe an elevation in UDP-GlcNAc concentrations in mesenchymal as compared to epithelial cells, consistent with up-regulation of enzymes contributing to HBP flux (Figure 2). Furthermore we expect that knockdown of GFPT2 will result in a decrease in UDP-GlcNAc concentration of doxycycline pre-treated *GFPT2* shRNA mesenchymal A549 as compared to a control cell line. To determine whether the end-product of HBP, UDP-GlcNAc is involved in the mechanism of the regulation of cell migration by *GFPT2*, a similar rescue experiment will be performed in *GFPT2* shRNA A549 cell line with or without glucosamine supplementation in the culture media. Glucosamine added to the culture media is transported into the cell and bypasses GFPT step to directly feed into the following reaction of HBP thus elevating UDP-GlcNAc (15). We expect that glucosamine supplementation of doxycycline pre-treated A549 *GFPT2* shRNA cell line will restore its migratory properties and further increase migration of a control shRNA A549 cell line. Similarly a enzyme-dead V5-tagged *GFPT2*

construct will be used to further show that enzymatic activity of *GFPT2* is required for its effect on cell migration. To accomplish this *GFPT2* enzyme-dead will be generated that lacks N-terminal cysteine residue required for the enzymatic activity of glutaminase domain (16). *GFPT2* shRNA A549 cell line will be transfected with enzyme-dead V5-GFPT2, wild-type GFPT2 or empty vector followed by induction of EMT in tumorspheres with TNF/TGFβ with or without doxycycline pre-treatment. We expect that enzyme-dead GFPT2 will not be able to restore migratory properties of doxycycline pre-treated A549 *GFPT2* shRNA cell line as compared to cells expressing wild-type GFPT2. Additionally it is possible that enzyme-domain will further decrease cell migration in both *GFPT2* shRNA and control cell line given the ability of GFPT2 to form tetramers and potential of acting as a dominant negative (16). This becomes especially important since our preliminary data indicates that GFPT2 physically interact with GFPT1. For this reason an enzyme-dead GFPT2 may block both GFPT1 and GFPT2 activities significantly dampening the HBP. Experiments described above will validate whether *GFPT2* acts via HBP to regulate cell migration. It is possible that the enzymatic activity of GFPT2 is dispensable for its role in the regulation of cell migration and instead GFPT2 has more structural role during migration. In this case glucosamine supplementation would not rescue cell migration and the expression of both wild-type and enzyme-dead GFPT2 would yield similar rescue of cell migration. In this unlikely scenario, alternative mechanistic role of *GFPT2* in cell migration is proposed in following paragraph.

To determine which of the UDP-GlcNAc products is involved in GFPT2-dependent effect on cell migration, A549 cells expressing *GFPT2* shRNA and control cells will be stimulated to undergo EMT with TNF/TGFβ. Tumorsphere cultures will be harvested and analyzed by immunoblot for global N-linked glycosylated proteins using lectin probes; phytohemagglutinin-L (PHA-L), Datura Stramonium Lectin (DSL) and concavalin A (ConA). Our preliminary data using lectin probes indicate that protein glycosylation changes during EMT in several NSCLC cell lines and that tetraantenary oligosascharides detected by PHA-L and DSL are upregulated in 3D A549 mesenchymal cells, consistent with the induction of *MGAT5* along with several other glycosyltransferases as detected by gene expression microarray (Figure 12). Additionally lectin probes will be used to pull-down N-glycosylated proteins from control and *GFPT2* shRNA A549 mesenchymal cells and samples will be analyzed by immunoblotting in a biased approach. Among our top candidates are integrin receptors that are key players in cell migration (11). As the majority of secreted proteins, including components of ECM and growth factors and cytokines require N-glycosylation for the proper secretion we will also analyze the change in N-glycosylation of secreted proteins by immunoblot analysis of trichloroacetic acid-precipitated proteins from culture media from control and *GFPT2* shRNA A549 mesenchymal cells (17). An additional unbiased approach would be to quantify global levels of differentially O- and N-glycosylated proteins using $^{13}C/^{12}C$ isotopic labeling followed by mass spectrometry analysis (18). This approach will further expand our initial lectin pull-down analysis and identify

differentially secreted O-glycosylated proteoglycans, important components of ECM as well as O-GlcNAcylated nucleocytoplasmic proteins (18). We will quantitate changes in levels of N-glycosylation of secretome as well as the levels of differentially O- and N-glycosylated cellular proteins using extracts from cell lysates of control and *GFPT2* knock-down A549 cells followed by mass spectrometry analysis (18). Additionally, we will determine the levels and types of oligosaccharide branching in control and *GFPT2* knockdown A549 cells by mass spectrometry analysis on permethylated glycans (18). Our data indicates that O-GlcNAcylation is affected by manipulation of *GFPT2* expression in mesenchymal NSCLC cells (Figure 6 and 17). O-GlcNAcylation of actin-binding protein, cofilin, has been shown to promote migration of breast cancer cells through mechanism involving regulation of actin fibers dynamics (13). To determine whether *GFPT2* affects cell migration via protein O-GlcNAcylation we will perform a rescue experiment using *GFPT2* shRNA and control A549 cell lines transfected with OGT cDNA or empty vector control. If O-GlcNAcylation is responsible for the *GFPT2* effect on cell migration we expect to see a rescue of migratory properties of *GFPT2* shRNA A549 cell line by either one or in response to all of the proposed treatments. If this hypothesis is correct a global approach of the identification of O-GlcNAcylated proteins could be undertaken in which sWGA beads will be used for pull-down O-GlcNAcylated proteins followed by the mass spectrometry analysis of peptides. Finally the synthesis and secretion of hyaluronan (HA) will be tested in *GFPT2* shRNA or control A549 cell lines. Supernatants from tumorsphere cultures stimulated with TNF/TGFβ will be

collected and HA concentration will be determined using HA specific ELISA kit (R&D Systems). Subsequently, tumorspheres will be trypsinized and replated on cover slips and stained with fluorescently labeled hyaluronan binding protein (HBP) to visualize secretion of the HA coat on tumorspheres (19). Using these approaches we expect to identify protein targets, including components of ECM, transmembrane receptors, adhesion molecules, and nucleocytoplasmic proteins, would be predicted to be altered following silencing of *GFPT2* in mesenchymal A549 cells. We also expect to observe a shift in the structure of oligosaccharides of N-glycans towards non-bisecting type in mesenchymal cells expressing *GFPT2* shRNA (20). Additionally we expect that both secreted HA levels determined by ELISA and HA coating will be decreased in *GFPT2* knockdown as compared to the control A549 cells. This notion is consistent with the fact that HA synthesis has been shown to depend on UDP-GlcNAc concentration and be regulated by O-GlcNAc. Moreover, our gene expression microarray analysis demonstrates elevated expression of hyaluronan synthase 2 (HAS2) in mesenchymal A549 cells (Figure 12, 21).

Decreased secretion of the components of the ECM or changes in the glycosylation pattern of transmembrane receptors and adhesion molecules may affect cell migration by both altering a physical properties of cell environment and by affecting signaling pathways promoting migration (10). Among the potential signaling pathways affected by decreased synthesis of glycans are downstream effectors of integrin receptors including FAK/RAS/Raf/MEK/ERK cascade and RHO family; RHO, CDC42 and RAC (11). Similarly RAC is an effector of CD44

receptor of hyaluronan (12). To determine whether signaling downstream of integrin receptors and CD44 is affected, *GFPT2* shRNA expressing A549 and control cell line will be cultured in tumorspheres and stimulated with TNF/TGFβ. Immunoblot analysis will be performed to examine phosphorylated molecules, namely of FAK, SHC, MEK, ERK, CRK-associated substrate (CAS), myosin-light-chain-kinase (MLCK), and myosin II. We predict that levels of phosphorylated proteins will be decreased in *GFPT2* knockdown A549 cells, compared to control cells. In support of these experiments we identified an interaction of GFPT2 with several small GTPases including those involved in cell migration, RhoG, Cdc42 and others, Rheb and RRAS2 *in vitro* (Figure 13). Additionally, we observe and interaction of GFPT2 with several Rab proteins, components of vesicular transport system, including Rab5C, Rab11A, Rab6C and Rab2A (Figu13). Vesicular transport is known to play a pivotal role in cell migration by facilitating endocytosis and recycling of integrins and other adhesion molecules at the leading edge of migrating cell (22). Consistent with this notion, immunofluorescence staining of endogenous GFPT2 in A549 cells shows vesicular localization of this protein (23). We will perform GFPT1 and GFPT2 staining in mesenchymal A549 cells to further confirm cellular localization of these two different isoforms. It is possible that GFPT2 plays a structural role in vesicular transport that is independent of its enzymatic activity. This mechanism will be examined experimentally the in preceding paragraph. In addition to immunoblotting analysis, we will perform a global analysis of phosphoproteomics in mesenchymal control and *GFPT2* shRNA A549 cells (24). Lysates will be

analyzed for global changes in protein phosphorylation levels by mass spectrometry to identify potential affected signaling pathways (24). Similarly a global RNA-seq analysis of transcripts in *GFPT2* shRNA and control cells will enable the identification of GFPT2-dependent target genes that may be differentially regulated (25).

Determine the relevance of the *GFPT2* induction in mesenchymal NSCLC cells *in vivo*

Although our work implicates GFPT2 in NSCLC migration and invasion it remains to be determined whether GFPT2 impacts metastasis *in vivo*. To confirm that *GFPT2* is induced *in vivo* in NSCLC patients LCC tissue microarrays (TMA) will be purchased (LC121a, US Biomax). Immunohistochemistry (IHC) will be performed using GFPT2 antibody available via Human Protein Atlas. Similar staining will be performed for GFPT1 to distinguish differential expression of the two GFPT isoforms. Furthermore we will perform IHC staining for NF-κB and Activin A, a recently described marker of mesenchymal phenotype in NSCLC. Such experiment will determine whether NF-κB is active and localized in nuclei in NSCLC tumors and whether the NF-κB activation is correlated with the expression of GFPT2. Additionally, it will determine whether GFPT2 expression is elevated specifically in mesenchymal NSCLC *in vivo*. We expect an elevated GFPT2 staining in cancer samples, compared to adjacent normal tissue. We predict GFPT2 expression to coincide with activated NF-κB and Activin A consistent with our observations *in vitro* and the analysis of gene co-expression

in LUAD patients. However we do not anticipate changes in the GFPT1 isoform, which is predicted to remain unaltered in tissue samples, compared to adjacent tissue. Additionally, we will perform IHC stainings with trichrome and hyaluronan binding protein (HBP) to determine whether the levels of GFPT2 protein in tumor samples correlate with the amount of ECM. We predict that cancer samples with high GFPT2 levels will also have increased amount of ECM.

To determine the role of *GFPT2* in mesenchymal cells *in vivo* five 4- to 5-week-old female outbred Crl:NU/NU nude mice (Jackson Laboratories) will be kept on doxycycline-containing water for two weeks followed by subcutaneous injection with $1x10^6$ cells/site cells from disaggregated tumorsphere cultures of *GFPT2* shRNA or control A549 cell lines stimulated with TNF/TGFβ and pre-treated with doxycycline. Mice will stay on doxycycline for additional 40 days, after which animals will be euthanized following approved procedures by the University of Virginia (UVA; Charlottesville, VA) ACUC (26). Primary subcutaneous tumors (SC) will be removed and weighed. Additionally, the lungs will be removed, fixed in formalin, and surface lung metastases will be counted using a dissecting scope. To quantify the amount of total tumor burden in the formalin fixed lung tissue, genomic DNA will be extracted and assayed for the presence of human genomic DNA by quantitative real time PCR (QRT-PCR) primers specific to human endogenous retrovirus-3 (ERV3) (26). We predict fewer lung metastases in *GFPT2* shRNA A549 compared to the control cells. The effect of *GFPT2* silencing on the primary SC remains to be determined. It is possible that potentially decreased synthesis of ECM in *GFPT2* shRNA A549 cell

line will adversely affect the formation and survival of the primary tumors due to decreased formation of tumor promoting microenvironment (27).

Next we will determine whether ECM components are affected by *GFPT2* silencing in A549-derived tumor *in vivo*. To accomplish that both dissected primary subcutaneous tumors lung metastases from mice injected with *GFPT2* shRNA and control shRNA A549 cell lines will be paraffin embedded and tissue slices will be prepared for IHC staining. We will perform staining use HRP-conjugated hyaluronan binding protein (HBP) and trichrome staining. This approach will determine the amount of secreted hyaluronan and the components of ECM including collagen and fibronectin. We will also perform staining using PHA-L and DSL lectins for tetraantenary oligosaccharide structures which will reveal changes in the level of glycans and the content of glycosylated components of ECM. Next we will perform IHC staining using O-GlcNAc antibody to determine the amount of global O-GlcNAcylated proteins. We expect to observe a decrease in the amount of protein modification by O-GlcNAcylation in cells with silenced *GFPT2* consistent with our results *in vitro*. We predict that the levels on other products of UDP-GlcNAc including hyaluronan and glycosylated components of ECM will also be decreased which would affect a global secretion and structure of ECM as visualized by trichrome stain. Notably, the synthesis and functioning of cancer ECM would have much more profound effect on the formation of tumors *in vivo* than it has *in vitro* due to the involvement of ECM in pro-tumor interactions with other cell types including activated fibroblasts, endothelial cells, tumor associated macrophages (TAMs) and tumor associated

neutrophils (TAN). Together this population of cells is known to promote cancer cell proliferation, invasion and angiogenesis (27). The presence of those cellular components of tumor microenvironment may be visualized using cell-type specific antibody IHC stainings (28). Thus silencing of *GFPT2* in mesenchymal cancer cells may result in significant reduction of tumor growth and metastasis *in vivo*. Notably given the opposite regulation of enzymatic activity of the two GFPT isoforms by UDP-GlcNAc, glucosamine-6-phpsphate and PKA it is possible that certain cellular setting may favor the activity of one GFPT isoform and block activity of the other. GFPT1 activity is blocked by PKA-dependent phosphorylation and UDP-GlcNAc and glucosamine-6-phposphate (29-31). On the contrary GFPT2 is not feedback-inhibited by the metabolites of HBP and its enzymatic activity is stimulated by PKA phosphorylation (32). These results suggest that metabolically active cells that receive variety of extra-cellular stimuli would rely predominantly of *GFPT2* isoform. Thus, it is possible that *in vivo* the tumor microenvironment would further exacerbate the effect of *GFPT2* silencing to affect not only migration and invasion but other biological processes including proliferation and EMT. Recently a homozygous GFPT2 knockdown mouse was generated (47). These animals are mostly viable but show significant alterations in functioning of neuronal cells and altered glucose homeostasis and adipocyte function indicating that *GFPT2* plays specific and distinct role in the organism as compared to constitutive and essential *GFPT1* isoform (47). Future experiment could be undertaken to test whether GFPT2 is required for lung cancer formation and metastasis. To accomplish this, one could will utilize urethane chemical

carcinogen to induce spontaneous formation of NSCLC in mice (48). Wild-type of *GFPT2* knock-out mice will be injected with urethane and monitored for tumor formation by CT/FDG-PET scan. In our hands urethane induces lung adenocarcinoma formation within 9 months post-urethane injection. Following this time mice will be sacrificed and lung tumors will be dissected and analyzed as described above. Select tumor tissue samples will be digested with collagenase and primary tumor cells will be isolated to establish primary tumor cell lines of the wild-type or *GFPT2* knockout phenotype. Cells will be cultures in tumorspheres with addition of TNF/TGFβ and analyzed for the induction of EMT using immunoblotting and QRT-PCR and for migratory and invasive phenotype using Boyden chamber assays. Furthermore subcutaneous injections into nude mice will be carried out and the formation of primary tumors and lung metastases will be analyzed as described above. We predict that *GFPT2* knockout mice will develop tumors with less metastatic phenotype as determined by decreased amount of bone, brain and liver metastases as compared to wild-type animals. Similarly primary lung tumor cells isolated from *GFPT2* knock-out mice will show decreased migration and invasion following induction of EMT with TNF/TGFβ in tumorsphere cultures. We predict that tumor cells derived from GFPT2 knockout mice will also show decreased lung metastases formation following subcutaneous injection into nude mice as compared to cells derived from wild-type animals. It is unclear whether *GFPT2* knockout would affect EMT. Our results using siRNA- and shRNA-mediated silencing of *GFPT2* show no significant effect on EMT. Similarly a lack of developmental defects in *GFPT2*

knockout mice could suggest that *GFPT2* is not required for EMT during gastrulation and embryogenesis (49). Alternatively K-Ras$^{LSL-G12D}$ mice could be crossed TP53$^{flox/flox}$ with *GFPT2* knockout mice to generate GFPT2$^{WT/WT}$/TP53$^{flox/flox}$/K-Ras$^{LSL-G12D}$, GFPT2$^{flox/WT}$/TP53$^{flox/flox}$/K-Ras$^{LSL-G12D}$ and GFPT2$^{flox/flox}$/TP53$^{flox/flox}$/K-Ras$^{LSL-G12D}$ mice in which K-Ras proto-oncogene, p53 tumor-suppressor and GFPT2 alleles will be deactivated using intra-nasally-delivered adenovirus expressing Cre recombinase (50). Animals will be monitored by CT/FDG-PET scan to determine the size and number of formed lung tumors as described above.

Determine the role of NF-κB, *GFPT2* and protein O-GlcNAcylation in the survival of *KRAS*-mutant NSCLC cells following MEK inhibition

Here we show that NF-κB pathway is induced in response to MEK inhibition in the *KRAS*-mutant NSCLC cell line A549 and that this NF-κB activation is required for the cell survival (Figure 1). This is consistent with previous reports indicating compensatory activation of NF-κB signaling in response to MEK inhibition in prostate cancer (33). Furthermore we show that *GFPT2* is induced in response to MEK inhibition with the similar expression kinetics as other NF-κB gene products upregulated following MEK inhibition (Figure 7 and 9). Concomitantly we observe an increase in the level of global protein O-GlcNAcylation in NSCLC following the treatment with MEK inhibitor (Figure 9). Protein O-GlcNAcylation is induced by a variety of stress stimuli

including heat shock, unfolded protein response and starvation to promote cell survival (15, 34-40). Previously our laboratory has shown that RelA/65 subunit of NF-κB is O-GlcNAcylated on threonine 305 which is required for p300-mediated acetylation of p65 on lysine 310, which is required to promote transcription (15). This observation is consistent with reports from other groups showing that O-GlcNAcylation of both RelA/p65 and IKK promotes NF-κB transcriptional activity (38-40). Here we present preliminary evidence that GFPT2 increases NF-κB activation thus establishing a positive-feedback loop where activated NF-κB increases flux through the HBP by upregulating *GFPT2* (Figure 10). Furthermore we indicate that *GFPT2* expression might have a role in the cell survival in response to MEK inhibition suggesting a possible benefit of combinatorial targeting MEK and HBP pathways in NSCLC (Figure 11).

We will pursue our initial observations to determine the role of NF-κB, *GFPT2* and protein O-GlcNAcylation in the survival of *KRAS*-mutant NSCLC cells following MEK inhibition. To accomplish this, we will determine the mechanism of NF-κB activation in response to treatment with MEK inhibitor. It has been reported that combinatorial inhibition of MEK and PI3K has proven more effective at inducing apoptosis in NSCLC cells than targeting either of the pathways alone (42-43). Consistent with these results we observe an induction of Akt phosphorylation following MEK inhibitor treatment in NSCLC A549 cells concomitant with NF-κB activation (Figure 7). To determine whether the induction of NF-κB following inhibition of MEK is mediated by PI3K pathway we will treat A549 and H358 NSCLC cells with MEK inhibitor and PI3K inhibitor (PI-103) alone

or in combination and we will assess activation of NF-κB pathway by immunoblotting for phosphorylated and total RelA/p65, IκB and IKK. QRT-PCR analysis will be carried out to measure changes in NF-κB gene expression of *TNFAIP3* and *BIRC3* (46). Since the combinatorial inhibition of MEK and PI3K has been shown to induce apoptosis in NSCLC, we may find the need to add caspase inhibitors (Z-DEVD-FMK) to prevent activation of apoptosis such that changes in NF-κB activity can be measured. We predict that inhibition of PI3K pathway will block MEK inhibitor-dependent activation of NF-κB.

Recently we identified *GFPT2* as a novel target of NF-κB in mesenchymal NSCLC cells. Given the concomitant induction of *GFPT2* and NF-κB pathway following treatment with MEK inhibitor with similar kinetics of expression as *GFPT2* and other known NF-κB targets, it is plausible to speculate that NF-κB is responsible for the induction of *GFPT2* in this context (Figure 7 and 9). We will seek to determine whether *GFPT2* is transcriptionally regulated by NF-κB following MEK inhibition. To accomplish this A549 and H358 cells will be infected with control GFP or SR-IκBα adenovirus followed by the treatment with DMSO control or the MEK inhibitor. Since the inhibition of NF-κB induced apoptosis in cells treated with MEK inhibitor, additional treatment with caspase inhibitor Z-DEVD-FMK will be administered to prevent the induction of cell death. The expression of *GFPT2* will be determined by QRT-PCR and immunoblotting. We predict that inhibition of NF-κB will block the induction of *GFPT2* and other NF-κB-regulated targets *TNFAIP3* and *BIRC3* by MEK inhibitor. Additionally we will determine whether NF-κB activation is required for the observed induction of

protein O-GlcNAcylation in NSCLC following MEK inhibition. To test this we will perform immunoblot analysis using O-GlcNAc-specific antibody on GFP control and SR-IκBα-expressing A549 cells treated with MEK inhibitor. Since NF-κB can potentially affect protein O-GlcNAcylation by transcriptional regulation of several metabolic proteins involved in the flux of HBP, including glucose transporter GLUT3, hexokinase 2 (HK2) and *GFPT2*, we predict that NF-κB silencing will result in decreased levels of global O-GlcNAcylation.

Next we will determine whether induction of *GFPT2* is required for MEK inhibitor-dependent elevation of protein O-GlcNAcylation. To accomplish that doxycycline-inducible *GFPT2* shRNA A549 and control cell lines will be pre-treated with doxycycline and DMSO or MEK inhibitor. The levels of global O-GlcNAcylation will be determined by immunoblot. Given that UDP-GlcNAc, an end-product of HBP, is a common precursor for the synthesis of variety of glycans in the cell, it is possible that, in addition to O-GlcNAcylation, levels of O- and N-glycosylation and proteoglycan might be affected by knockdown of *GFPT2*. To determine that lysates of *GFPT2* shRNA and control A549 cell lines will be analyzed by immunoblotting with PHA-L and DSL. Additionally immunofluorescence (IF) microscopy analysis with fluorescently labeled PHA-L, DSL and hyaluronan binding protein (HBP) will be performed. Given that neither GFPT1 isoform, nor OGT and OGA enzymes are affected by MEK inhibition it is plausible to speculate that GFPT2 is the main contributing enzyme responsible for the observed increase in O-GlcNAcylation. Therefore, we speculate that silencing of *GFPT2* in MEK-treated cells will result in a decrease in protein

O-GlcNAcylation and glycan content. To confirm the specificity of this phenotype, a rescue experiment with glucosamine supplementation and ectopic expression of wild-type and enzyme-dead *GFPT2* constructs will be performed. We expect that supplementation with glucosamine and ectopic expression of wild-type, but not enzyme-dead GFPT2 will result in a restoration of the levels of glycans present in MEK-treated control A549 cells.

Protein O-GlcNAcylation has been shown to be induced by a variety of stress stimuli to promote cell survival and inhibit apoptosis via sustaining NF-κB signaling (38-40). To test whether O-GlcNAcylation is required for cell survival following MEK inhibition, A549 cells will be transfected with siRNA against OGT, the main enzyme that adds O-GlcNAc modification onto target proteins, or control siRNA followed by treatment with MEK inhibitor (4). Cell viability will be determined by trypan blue staining, immunoblotting for cleaved caspase 3 and caspase 3 colorimetric enzyme assay (Genetex). Furthermore we will determine whether induction of *GFPT2* is required to prevent apoptosis following MEK inhibition. Our preliminary results indicate that knockdown of *GFPT2* results in a decreased cell survival in low glucose conditions as measured by trypan blue cell staining (Figure 11). We will determine whether this reduced cell viability is a result of an induction of apoptosis post-MEK inhibition. To confirm the specificity of the observed phenotype a rescue experiment using ectopic expression of the wild-type or enzyme-dead *GFPT2* constructs as well as glucosamine supplementation will be performed. We expect that *GFPT2* silencing will result in the induction of apoptosis in *GFPT2* shRNA A549 cell line following MEK

inhibition as determined by increased levels of caspase activity and cleaved caspase 3 product. Furthermore we predict that supplementation with glucosamine or ectopic expression of wild type but not domain-dead *GFPT2* will protect doxycycline pre-treated A549 *GFPT2* shRNA cells from MEK inhibitor-induced cell death.

To determine potential mechanism of the effect of *GFPT2* on the cell survival, we postulated that GFPT2 participates in the formation of the positive feedback-loop of NF-κB signaling via elevated flux through hexosamine biosynthesis pathway (HBP). In support of this hypothesis our preliminary data indicate that ectopic expression of GFPT2 is able to potentiate NF-κB signaling and transcriptional activity in HEK293T cells (Figure 10). To determine the mechanism of this effect, we will test whether ectopic expression of GFPT2 protein in HEK293T cells induces elevated O-GlcNAcylation of RelA/p65, using sWGA beads to pull-down total O-GlcNAcylated proteins followed by immunoblot analysis using p65-specific antibody. We predict that expression of GFPT2 will result in increased global protein O-GlcNAcylation as well as O-GlcNAcylation of specific targets such as RelA/p65. Next, we will determine whether MEK inhibition enhances O-GlcNAcylation of RelA/p65 in NSCLC cells and whether *GFPT2* expression is required in this process. To test this *GFPT2* shRNA and control A549 cell lines will be treated with MEK inhibitor and sWGA beads will be used for a pull-down assay followed by immunoblot analysis of the levels of bound RelA/p65. Eluates from sWGA extracts will be digested with trypsin and analyzed by mass spectrometry to identify additional O-GlcNAcylated targets.

We predict that treatment with MEK inhibitor will increase in levels of O-GlcNAcylated RelA/p65, consistent with global induction of O-GlcNAcylation. Furthermore, we expect to identify a list of O-GlcNAcylated targets potentially implicated in cell survival. Additionally, knockdown of *GFPT2* may result in decreased O-GlcNAcylation of RelA/p65 and this effect would be rescued by supplementation with glucosamine or expression of wild-type but not enzyme-dead *GFPT2* construct. Finally we will determine the effect of *GFPT2* knock-down on RelA/p65 transcriptional activity in NSCLC following MEK inhibition by performing electrophoretic mobility shifts assays (EMSA) for NF-κB, immunoblot analysis of phosphorylated components of NF-κB pathway as well QRT-PCR analysis of NF-κB regulated targets including *TNFAIP3* and *BIRC3* following the knockdown of *GFPT2* in the absence or presence of MEK inhibitor. We predict that *GFPT2* knockdown will result in a decreased transcriptional activity of NF-κB as determined by a reduced nuclear localization and DNA binding in EMSA assay, decreased phosphorylation of NF-κB pathway and dampened transcription of NF-κB target genes.

Together the proposed experiments described in the future directions will determine the importance of *GFPT2* in migration and invasion of mesenchymal NSCLC cells and will elucidate the relevance of *GFPT2* induction *in vivo* in lung cancer. Additionally, studies outlined in this section will characterize the role of *GFPT2* induction in response to MEK inhibition in NSCLC and will assess the potential benefit of combinatorial targeting of MEK and GFPT2 in lung cancers driven by Kras.

REFERENCES

1. Freeze HH, Elbein AD. Glycosylation precursors. 2nd ed. In: Varki A, Cummings RD, Esko JD, Freeze HH, Stanley P, Bertozzi CR, Hart GW, Etzler ME, editors. Source Essentials of Glycobiology, Chapter 4. Cold Spring Harbor, NY: Cold Spring Harbor Laboratory Press (2009). P. 47 – 61.

2. Iozzo RV, Sanderson RD. Proteoglycans in cancer biology, tumour microenvironment and angiogenesis. *J Cell Mol Med.* 2011 May; 15(5): 1013-1031. PMCID: PMC3633488.

3. Itano N, Kimata K. Altered hyaluronan biosynthesis in cancer progression. *Semin Cancer Biol.* 2008 Aug; 18(4): 268-274.

4. Stowell SR, Ju T, Cummings RD. Protein glycosylation in cancer. *Annu Rev Pathol.* 2015; 10: 473-510. PMCID: PMC4396820.

5. Ma Z, Vosseller K. O-GlcNAc in cancer biology. *Amino Acids.* 2013 Oct; 45(4): 719-733.

6. Lau KS, Dennis JW. N-glycans in cancer progression. *Glycobiology.* 2008 Oct; 18(10): 750-760.

7. Granovsky M, Fata J, Pawling J, Muller WJ, Khokha R, Dennis JW. Suppression of tumor growth and metastasis in Mgat5-deficient mice. *Nat Med.* 2000 Mar; 6(3): 306-312.

8. Ponting J, Howell A, Pye D, Kumar S. Prognostic relevance of serum hyaluronan levels in patients with breast cancer. *Int J Cancer.* 1992 Dec 2; 52(6): 873-876.

9. Li Z, Yi W. Regulation of cancer metabolism by O-GlcNAcylation. *Glycoconj J.* 2014 Apr; 31(3): 185-191.

10. Bonnans C, Chou J, Werb Z. Remodelling the extracellular matrix in development and disease. *Nat Rev Mol Cell Biol.* 2014 Dec; 15(12): 786-801. PMCID: PMC4316204.

11. Hood JD, Cheresh DA. Role of integrins in cell invasion and migration. *Nat Rev Cancer.* 2002 Feb; 2(2): 91-100.
12. Ponta H, Sherman L, Herrlich PA. CD44: From adhesion molecules to signalling regulators. *Nat Rev Mol Cell Biol.* 2003 Jan; 4(1): 33-45.

13. Huang X, Pan Q, Sun D, Chen W, Shen A, Huang M, Ding J, Geng M. O-GlcNAcylation of cofilin promotes breast cancer cell invasion. *J Biol Chem.* 2013 Dec 20; 288(51): 36418-36425. PMCID: PMC3868755.

14. Abdel Rahman AM, Ryczko M, Pawling J, Dennis JW. Probing the hexosamine biosynthetic pathway in human tumor cells by multitargeted tandem mass spectrometry. *ACS Chem Biol.* 2013 Sep 20; 8(9): 2053-2062.

15. Allison DF, Wamsley JJ, Kumar M, Li D, Gray LG, Hart GW, Jones DR, Mayo MW. Modification of RelA by O-linked N-acetylglucosamine links glucose metabolism to NF-kappaB acetylation and transcription.*Proc Natl Acad Sci U S A.* 2012 Oct 16; 109(42): 16888-16893. PMCID: PMC3479489.

16. Durand P, Golinelli-Pimpaneau B, Mouilleron S, Badet B, Badet-Denisot MA. Highlights of glucosamine-6P synthase catalysis. *Arch Biochem Biophys.* 2008 Jun 15; 474(2): 302-317.

17. Chevallet M, Diemer H, Van Dorssealer A, Villiers C, Rabilloud T. Toward a better analysis of secreted proteins: The example of the myeloid cells secretome. *Proteomics.* 2007 Jun; 7(11): 1757-1770. PMCID: PMC2386146.

18. Lim JM, Wollaston-Hayden EE, Teo CF, Hausman D, Wells L. Quantitative secretome and glycome of primary human adipocytes during insulin resistance. *Clin Proteomics.* 2014 May 12; 11(1): 20-0275-11-20. eCollection 2014. PMCID: PMC4055909.

19. Siiskonen H, Karna R, Hyttinen JM, Tammi RH, Tammi MI, Rilla K. Hyaluronan synthase 1 (HAS1) produces a cytokine-and glucose-inducible, CD44-dependent cell surface coat. *Exp Cell Res.* 2014 Jan 1; 320(1): 153-163.

20. Sasai K, Ikeda Y, Fujii T, Tsuda T, Taniguchi N. UDP-GlcNAc concentration is an important factor in the biosynthesis of beta1,6-branched oligosaccharides: Regulation based on the kinetic properties of N-acetylglucosaminyltransferase V. *Glycobiology.* 2002 Feb; 12(2): 119-127.

21. Shaul YD, Freinkman E, Comb WC, Cantor JR, Tam WL, Thiru P, Kim D, Kanarek N, Pacold ME, Chen WW, Bierie B, Possemato R, Reinhardt F, Weinberg RA, Yaffe MB, Sabatini DM. Dihydropyrimidine accumulation is required for the epithelial-mesenchymal transition. *Cell.* 2014 Aug 28; 158(5): 1094-1109. PMCID: PMC4250222.

22. Caswell PT, Vadrevu S, Norman JC. Integrins: Masters and slaves of endocytic transport. *Nat Rev Mol Cell Biol.* 2009 Dec; 10(12): 843-853.

23. http://www.proteinatlas.org/

24. Rubbi L, Titz B, Brown L, Galvan E, Komisopoulou E, Chen SS, Low T, Tahmasian M, Skaggs B, Muschen M, Pellegrini M, Graeber TG. Global phosphoproteomics reveals crosstalk between bcr-abl and negative feedback mechanisms controlling src signaling. *Sci Signal.* 2011 Mar 29; 4(166): ra18. PMCID: PMC4057100.

25. Wang Z, Gerstein M, Snyder M. RNA-seq: A revolutionary tool for transcriptomics. *Nat Rev Genet.* 2009 Jan; 10(1): 57-63. PMCID: PMC2949280.

26. Wamsley JJ, Kumar M, Allison DF, Clift SH, Holzknecht CM, Szymura SJ, Hoang SA, Xu X, Moskaluk CA, Jones DR, Bekiranov S, Mayo MW. Activin upregulation by NF-kappaB is required to maintain mesenchymal features of cancer stem-like cells in non-small cell lung cancer. *Cancer Res.* 2015 Jan 15; 75(2): 426-435. PMCID: PMC4297542.

27. Quail DF, Joyce JA. Microenvironmental regulation of tumor progression and metastasis. *Nat Med.* 2013 Nov; 19(11): 1423-1437. PMCID: PMC3954707.

28. Egeblad M, Ewald AJ, Askautrud HA, Truitt ML, Welm BE, Bainbridge E, Peeters G, Krummel MF, Werb Z. Visualizing stromal cell dynamics in different tumor microenvironments by spinning disk confocal microscopy. *Dis Model Mech.* 2008 Sep-Oct; 1(2-3): 155-67; discussion 165. PMCID: PMC2562195.

29. Chang Q, Su K, Baker JR, Yang X, Paterson AJ, Kudlow JE. Phosphorylation of human glutamine:Fructose-6-phosphate amidotransferase by cAMP-dependent protein kinase at serine 205 blocks the enzyme activity. *J Biol Chem.* 2000 Jul 21; 275(29): 21981-21987.

30. Broschat KO, Gorka C, Page JD, Martin-Berger CL, Davies MS, Huang Hc HC, Gulve EA, Salsgiver WJ, Kasten TP. Kinetic characterization of human glutamine-fructose-6-phosphate amidotransferase I: Potent feedback inhibition by glucosamine 6-phosphate. *J Biol Chem.* 2002 Apr 26; 277(17): 14764-14770.

31. Graack HR, Cinque U, Kress H. Functional regulation of glutamine:Fructose-6-phosphate aminotransferase 1 (GFAT1) of drosophila melanogaster in a UDP-N-acetylglucosamine and cAMP-dependent manner. *Biochem J.* 2001 Dec 1; 360(Pt 2): 401-412. PMCID: PMC1222241.

32. Hu Y, Riesland L, Paterson AJ, Kudlow JE. Phosphorylation of mouse glutamine-fructose-6-phosphate amidotransferase 2 (GFAT2) by cAMP-dependent protein kinase increases the enzyme activity. *J Biol Chem.* 2004 Jul 16; 279(29): 29988-29993.

33. Gioeli D, Wunderlich W, Sebolt-Leopold J, Bekiranov S, Wulfkuhle JD, Petricoin EF,3rd, Conaway M, Weber MJ. Compensatory pathways induced by MEK inhibition are effective drug targets for combination therapy against castration-resistant prostate cancer. *Mol Cancer Ther.* 2011 Sep; 10(9): 1581-1590. PMCID: PMC3315368.

34. Zachara NE, Molina H, Wong KY, Pandey A, Hart GW. The dynamic stress-induced "O-GlcNAc-ome" highlights functions for O-GlcNAc in regulating DNA damage/repair and other cellular pathways.*Amino Acids.* 2011 Mar; 40(3): 793-808. PMCID: PMC3329784.

35. Chatham JC, Not LG, Fulop N, Marchase RB. Hexosamine biosynthesis and protein O-glycosylation: The first line of defense against stress, ischemia, and trauma. *Shock.* 2008 Apr; 29(4): 431-440.

36. Zachara NE, O'Donnell N, Cheung WD, Mercer JJ, Marth JD, Hart GW. Dynamic O-GlcNAc modification of nucleocytoplasmic proteins in response to stress. A survival response of mammalian cells. *J Biol Chem.* 2004 Jul 16; 279(29): 30133-30142.

37. Kang JG, Park SY, Ji S, Jang I, Park S, Kim HS, Kim SM, Yook JI, Park YI, Roth J, Cho JW. O-GlcNAc protein modification in cancer cells increases in response to glucose deprivation through glycogen degradation. *J Biol Chem.* 2009 Dec 11; 284(50): 34777-34784. PMCID: PMC2787340.

38. Ma Z, Vocadlo DJ, Vosseller K. Hyper-O-GlcNAcylation is anti-apoptotic and maintains constitutive NF-kappaB activity in pancreatic cancer cells. *J Biol Chem.* 2013 May 24; 288(21): 15121-15130. PMCID: PMC3663532.

39. Kawauchi K, Araki K, Tobiume K, Tanaka N. Loss of p53 enhances catalytic activity of IKKbeta through O-linked beta-N-acetyl glucosamine modification. *Proc Natl Acad Sci U S A.* 2009 Mar 3; 106(9): 3431-3436. PMCID: PMC2651314.

40. Yang WH, Park SY, Nam HW, Kim do H, Kang JG, Kang ES, Kim YS, Lee HC, Kim KS, Cho JW. NFkappaB activation is associated with its O-GlcNAcylation state under hyperglycemic conditions. *Proc Natl Acad Sci U S A.* 2008 Nov 11; 105(45): 17345-17350. PMCID: PMC2582288.

41. Madrid LV, Wang CY, Guttridge DC, Schottelius AJ, Baldwin AS,Jr, Mayo MW. Akt suppresses apoptosis by stimulating the transactivation potential of the RelA/p65 subunit of NF-kappaB. *Mol Cell Biol.*2000 Mar; 20(5): 1626-1638. PMCID: PMC85346.

42. Sos ML, Fischer S, Ullrich R, Peifer M, Heuckmann JM, Koker M, Heynck S, Stuckrath I, Weiss J, Fischer F, Michel K, Goel A, Regales L, Politi KA, Perera S, Getlik M, Heukamp LC, Ansen S, Zander T, Beroukhim R, Kashkar H, Shokat KM, Sellers WR, Rauh D, Orr C, Hoeflich KP, Friedman L, Wong KK, Pao W, Thomas RK. Identifying genotype-dependent efficacy of single and combined PI3K- and MAPK-pathway inhibition in cancer. *Proc Natl Acad Sci U S A.* 2009 Oct 27; 106(43): 18351-18356. PMCID: PMC2757399.

43. Meng J, Dai B, Fang B, Bekele BN, Bornmann WG, Sun D, Peng Z, Herbst RS, Papadimitrakopoulou V, Minna JD, Peyton M, Roth JA. Combination treatment with MEK and AKT inhibitors is more effective than each drug alone in human non-small cell lung cancer in vitro and in vivo. *PLoS One.* 2010 Nov 29; 5(11): e14124. PMCID: PMC2993951.

44. Turke AB, Song Y, Costa C, Cook R, Arteaga CL, Asara JM, Engelman JA. MEK inhibition leads to PI3K/AKT activation by relieving a negative feedback on ERBB receptors. *Cancer Res.* 2012 Jul 1; 72(13): 3228-3237. PMCID: PMC3515079.

45. Yoon YK, Kim HP, Han SW, Oh do Y, Im SA, Bang YJ, Kim TY. KRAS mutant lung cancer cells are differentially responsive to MEK inhibitor due to AKT or STAT3 activation: Implication for combinatorial approach. *Mol Carcinog.* 2010 Apr; 49(4): 353-362.

46. http://www.bu.edu/nf-kb/gene-resources/target-genes/

47. http://www.mousephenotype.org/data/genes/MGI:1338883

48. Meuwissen R, Berns A. Mouse models for human lung cancer. *Genes Dev.* 2005 Mar 15; 19(6): 643-664.

49. Thiery JP, Acloque H, Huang RY, Nieto MA. Epithelial-mesenchymal transitions in development and disease. *Cell.* 2009 Nov 25; 139(5): 871-890.

50. DuPage M, Dooley AL, Jacks T. Conditional mouse lung cancer models using adenoviral or lentiviral delivery of cre recombinase. *Nat Protoc.* 2009; 4(7): 1064-1072. PMCID: PMC2757265.

A.

N-linked, O-linked glycosylation:

GALNT	2x (O-glycosylation)
MGAT4	2.8x (N-glycosylation)
MGAT4C	2x (N-glycosylation)
B4GALT1	10x (N-glycosylation)

Hyaluronan and glycosaminoglycans:

CHST2	14x (Keratan sulfate)
CSGALNACT1	4.5x (Heparan sulfate)
DSE	6.3x (Chondroitin sulfate)
XYLT1,2	13x (Heparan sulfate)
HS3ST3B1	44x (Heparan sulfate)
HAS3	3x (Hyaluronan)
HAS2	14x (Hyaluronan)

B.

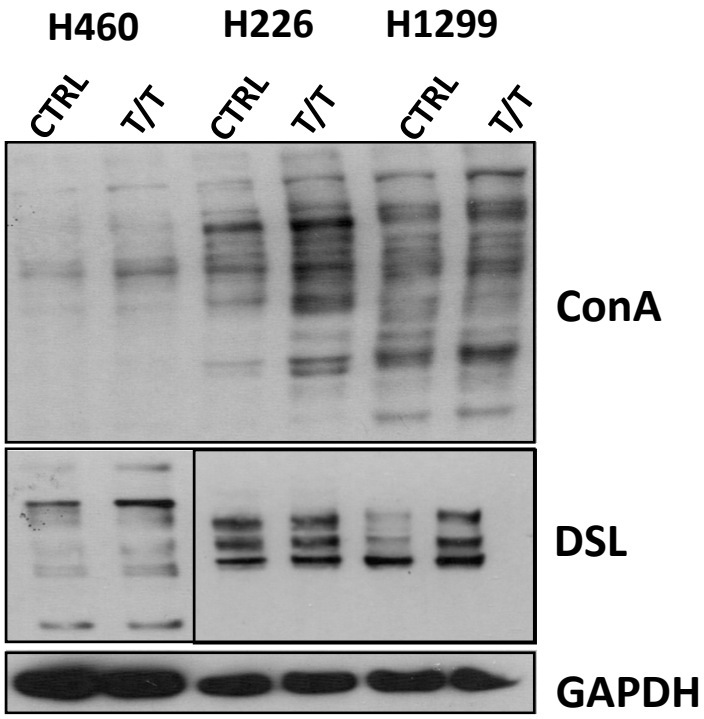

Figure 12. Mesenchymal NSCLC cells upregulate synthesis of multi-branched glycans. A. Table depicts a list of genes involved in N- and O-glycosylation and the synthesis of proteoglycans and hyaluronan up-regulated in mesenchymal A549 cells. Differentially regulated genes are presented as fold induction, compared to unstimulated cells. The type of glycan products generated by the enzyme noted are shown in parenthesis (26) **B.** NSCLC cell lines H460, H226 and H1299 were cultured in tumorsphere cultures alone (CTRL) or with the addition of TNF/TGFβ (T/T). Whole cell extract (WCE) were analyzed by immunoblotting using biotinylated lectins: 1) Concavalin A (ConA) recognize global N-glycosylation; and 2) Datura Stramonium Lectin (DSL) recognize multi-branched N-glycosylation. GAPDH levels were used as a loading control.

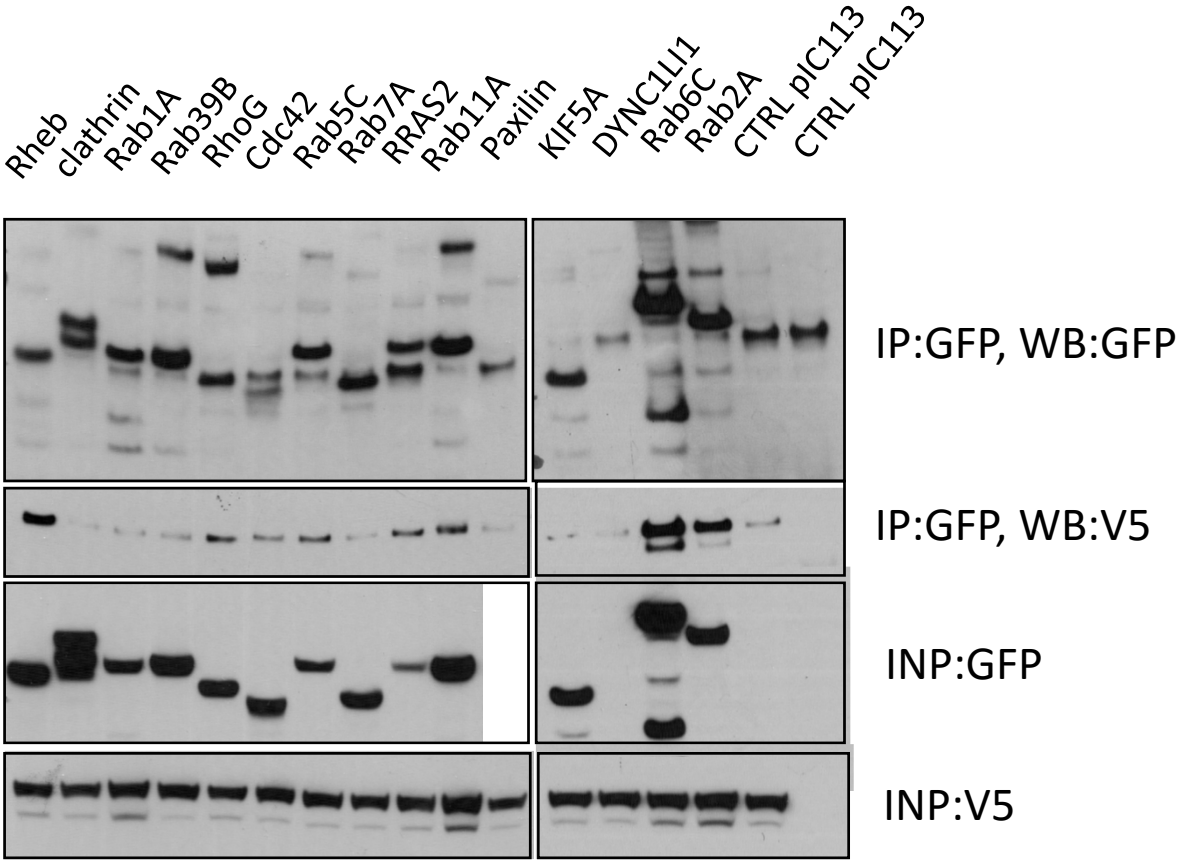
Rheb
clathrin
Rab1A
Rab39B
RhoG
Cdc42
Rab5C
Rab7A
RRAS2
Rab11A
Paxilin
KIF5A
DYNC1LI1
Rab6C
Rab2A
CTRL pIC113
CTRL pIC113
IP:GFP, WB:GFP
IP:GFP, WB:V5
INP:GFP
INP:V5

Figure 13. GFPT2 interacts with components of the migratory and endocytic machinery. HEK293T cells were transfected with V5-tagged GFPT2 in combination with GFP-tagged constructs encoding pro-migratory GTPases and components of endocytic pathway. HEK293T were lysed 24h post-transfection and immunoprecipitation using anti-GFP antibody was performed as described in materials and methods. Immunoblot analysis of pull-down samples and inputs was done using anti-GFP and anti-V5 antibodies.